

Age, Provenance and Metamorphic
Conditions of the Mercara Shear Zone,
Coorg Block, India

Thesis submitted in accordance with the requirements of the University of
Adelaide for an Honours Degree in Geology

William Harris Mansfield
November 2016



THE UNIVERSITY
of ADELAIDE

AGE, PROVENANCE AND METAMORPHIC CONDITIONS OF THE MERCARA SHEAR ZONE, COORG BLOCK, INDIA

RUNNING TITLE: MERCARA SHEAR ZONE METAMORPHISM

ABSTRACT

High pressure granulite metamorphism has never been recorded during the Mesoarchaeon. The Mercara shear zone in the Coorg Block, south west India plays host to kyanite-sillimanite-garnet-bearing felsic granulites that equilibrated at 11-13 kbar and 860 °C and 7.5-9 Kbar at 850-860 °C. LA-ICP-MS of U-Pb zircon and in-situ monazite geochronology reveal that the assemblages were first metamorphosed at ca. 3071 Ma, then again at ca. 676 ± 47 Ma. Pressure-temperature-time studies from the shearzone had not previously described conditions of this nature before, revealing how timing the suturing of the Coorg block will require extensive sampling methods. The conditions described however provide an insight into the thickened crust and low apparent thermal gradients existing during the stagnant-lid to first tectonism transitionary period. A period that usually only records high apparent thermal gradients and weakened crust. The ancient assemblage preserves regimes typical of a contractional orogenic events, implying crustal thicknesses of 35-40 km deep. Crustal thickening of this nature provides evidence for modern style tectonics operating during the Mesoarchaeon.

KEYWORDS

U-Pb geochronology, phase equilibria modelling, Archaean high pressure metamorphism, Neoproterozoic metamorphism, Mercara shearzone, Coorg block, India

Contents

Abstract.....	i
Keywords.....	i
List of Figures and Tables	2
Introduction	3
Geological Setting	5
Analytical Methods	8
U-Pb zircon geochronology	8
U-pb in-situ monazite geochronology	9
Mineral chemistry via electron microprobe	10
Bulk rock geochemistry using X-ray fluorescence.....	10
Petrography	10
Phase equilibria calculations.....	10
Observations and Results	12
Geochronology.....	12
Zircon U-Pb geochronology.....	12
Zircon Th-U VS $^{207}\text{Pb} / ^{206}\text{Pb}$ AGES.....	18
In-situ monazite U–Pb geochronology.....	20
Metamorphic Geology	24
Metamorphic petrology	24
Pressure/temperature-amount pseudosections.....	28
Pressure-temperature pseudosections.....	32
Mineral chemistry	34
Discussion.....	37
Age of metamorphism and Provenance of sedimentary photoliths	37
Pressure-Temperature-Time Evolution.....	38
Thermal Gradient and Tectonic Settings.....	39
Conclusions	43
Acknowledgments	44
References	45
Appendix A: Whole Rock Geochemisrty via XRF	50
Appendix B: Zircon standards.....	51
Appendix C: Zircon Analyses	65
Appendix D: Monazite standards	88

Appendix E: Monazite analyses 93
Appendix f: EXTENDED U-PB GEOCHRONOLOGY METHODS 98
Appendix g: Extended phase equilibria modelling methods 99

LIST OF FIGURES AND TABLES

Figure 1: Tectonic/geological map picturing the study area5
Figure 2: Images of zircons from samples I16-42, I16-64, I16-65 and I16-6612
Figure 3: U-Pb combined concordia diagrams displaying all data16
Figure 4: U-Pb combined concordia diagrams within a 10% concordance filter 16
Figure 5: Probability density plots for samples I16-42, I16-64, I16-65 and I16-66 17
Figure 6: Sample I16-42 zircon ²⁰⁶Pb/²³⁸U ages plotted against their concordancy 17
Figure 7: Th/U ratio vs 206Pb/238U ages for sample I16-42 18
Figure 8: Th/U ratio vs 206Pb/238U ages for sample I16-64 19
Figure 9: Th/U ratio vs 206Pb/238U ages for sample I16-65 19
Figure 10: Th/U ratio vs 207Pb/206Pb ages for sample I16-66 20
Figure 11: U-Pb Concordia diagrams for all monazite grains 22
Figure 12: U-Pb monazite geochronology within a 10% concordance filter 23
Figure 13: Photomicrographs of petrological relationships within all samples 25
Figure 14: P-Mo pseudosection for sample I16-65 29
Figure 15: P-Mo pseudosection for sample I16-42 30
Figure 16: T-Mh2O pseudosection for sample I16-65 31
Figure 17: Calculated P-T pseudosection for sample I16-42 33
Figure 18: Calculated P-T pseudosection for sample I16-65. 33
Figure 19: CL image of element composition transect of garnet porphyroblast34

INTRODUCTION

High pressure metamorphism is extremely rare in the first 2.5 billion years of Earth's history, (Brown, 2007). This is thought to be because typical Archaean crustal thicknesses of 45km would melt and delaminate at the base when contacting potential mantle temperatures of 1600°C, (Brown, 2014; Johnson et al., 2014). The oldest reported high pressure metamorphism is from southern India in the Kanja Malai Hills at ca. 2.5 Ga (Anderson et al., 2012). However, high pressure granulites have also been reported to occur in the Mercara shear zone (Santosh et al., 2015). Rocks in this region are of the oldest in India, (Santosh et al., 2015) and it is suspected that the high-pressure metamorphism may also be Mesoarchaeon (Amaldev et al., 2016). However in recent times the pressure–temperature (*P-T*) history of these rocks coupled with good age constraints has been lacking. The Mercara shear zone in south west India (Fig. 1), is a region of considerable controversy, with numerous researchers attempting to constrain the timings and conditions that lead to the suturing of the proposed exotic Coorg block, (Amaldev et al., 2016; Ishwar-Kumar et al., In Press; Ishwar-Kumar et al., 2013; Rekha et al., 2014; Santosh et al., 2015). The region is located between the Dharwar Craton in the north and the Nilgiri block to the south (Santosh et al., 2015). The Coorg block has been described as an exotic microcontinent welded to India at 1464 ± 94 Ma, based on U-Pb zircon lower intercepts, (Ishwar-Kumar et al., In Press; Santosh et al., 2015). The surrounding shear zones are thought to represent the suturing outline, with the Mercara shear zone yielding detrital zircon $^{207}\text{Pb}/^{206}\text{Pb}$ ages corresponding to the Mesoarchaeon and older (Ishwar-Kumar et al., In Press; Santosh et al., 2015). High pressure granulites and eclogites representing relatively low geothermal gradients similar to those found in Phanerozoic subduction zones, have been found back to the

Neoproterozoic, (Anderson et al., 2012; Brown, 2007; Collins et al., 2004). The absence of eclogites and high pressure granulites prior to 2500 Ma has been used to suggest that plate tectonics did not operate in the Archaean (Brown, 2007, 2014). However since the Mercara shear zone granulites are found to be both high pressure and Archaean, a reassessment of this hypothesis is required. This study presents data describing a full pressure–temperature–time (*P-T-t*) evolution of these rocks to determine whether they are in fact, low geothermal gradient, high pressure granulites and therefore indicative of crustal scale tectonic conditions (Kelsey & Hand, 2015). The interpreted geodynamics of low geothermal gradient, high pressure granulite metamorphism are commonly tied to long lived orogenic shortening (Brown, 2014; Kelsey & Hand, 2015).

Here, new field data, geochronology and the initial results of a metamorphic study are presented. Metamorphic phase diagrams, coupled with U-Pb zircon and in-situ monazite geochronology are used to define the earliest Mesoproterozoic high pressure granulite metamorphism. Providing an insight into Archaean crustal thickening and thermal regimes.

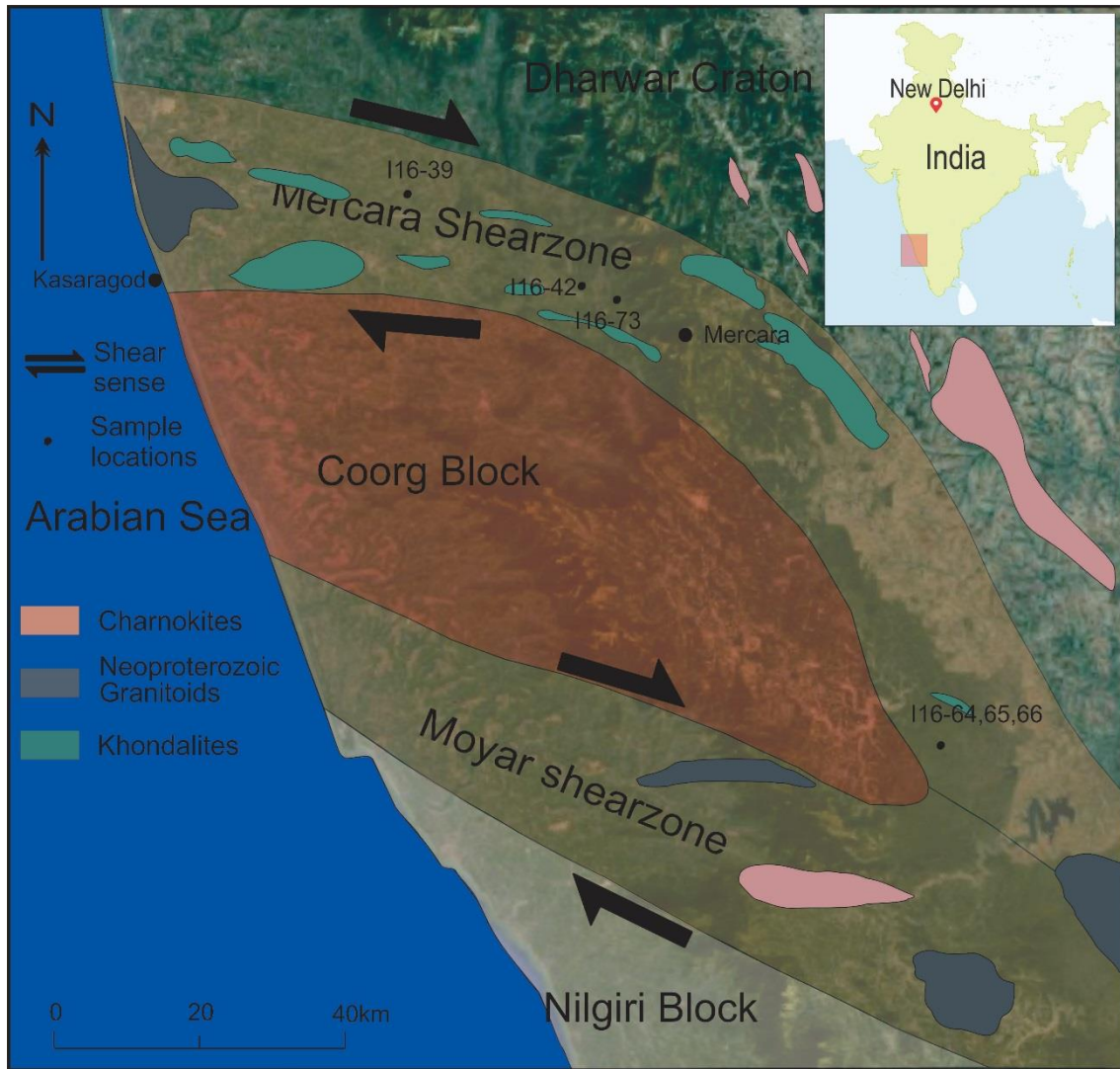


Figure 1: Tectonic/geological map picturing the study area highlighting the Coorg block and its bounding shear zones, the Mercara and Moyar.

GEOLOGICAL SETTING

MERCARA SHEAR ZONE:

The E-W trending Mercara shear zone binds the Coorg block to the Western Dharwar Craton. It is marked by a steep gravity gradient that has been interpreted as a reflection of under plated high density material in the lower crust (Sunil et al., 2010).

U-Pb zircon ages from pelitic gneisses in the Mercara shear zone are reported to range from 3249 to 3045 Ma (Ishwar-Kumar et al., In Press). $\epsilon_{\text{Hf}}(t)$ values from the same

zircons range from -18.9 to +4.2 with corresponding TDMc model ages varying from 4094 to 3314 Ma indicating that the detritus was recycled from ancient older crust (Ishwar-Kumar et al., In Press)

The shear zone is lithologically dominated by a suite of quartz-feldspathic and biotite rich gneisses, metamorphosed to granulite facies conditions. Khondalites are found intruded by Neoproterozoic aged suites of potassic syenites, anorthosites and Cretaceous aged gabbro-granophyre (Ishwar-Kumar et al., In Press; Santosh et al., 2015). The granulite metapelites have been interpreted to have formed in early Mesoproterozoic rifts followed by late Mesoproterozoic metamorphism (Santosh et al., 2015).

Based on mesoscopic structures and monazite age data, Rekha et al. (2014) suggested that the Mercara shear zone formed ca. 2300–2500 Ma. Meanwhile Ishwar-Kumar et al. (In Press) provides a metamorphic age of 1464 ± 94 Ma, MSWD = 2.9, based on U-Pb zircon lower intercepts.

COORG BLOCK:

The Coorg block is described as an exotic microcontinent welded to India at 1200 Ma, (Ishwar-Kumar et al., In Press; Santosh et al., 2015). Dominantly composed of granites, diorites, charnokites, TTG (Tonalite-Trondhjemite-Granodiorite) and felsic volcanic tuffs with lesser amounts of accreted oceanic remnants at block edges. Coeval mixing and mingling of mafic and felsic magmatism is evident, typical of an arc-setting, (A. J. R. White & Chappell, 1983). Trace and REE geochemistry confirm an arc-related signature from the Coorg block (Santosh et al., 2015). Juvenile magma sources appear throughout the block, contributing to crustal building via the partial recycling of basement rocks, these are dated back to 3800 Ma (Santosh et al., 2015). Coorg granulites have recorded

near-peak metamorphic conditions of 7 to 8.6 kbar at 720 to 760°C (Srikantappa et al., 1994). More recently a study based on the mineral chemistry of hornblende in charnockite reported P - T conditions of 6 kbar at 820–870 °C from the Coorg block granulites (Santosh et al., 2015).

MOYAR SHEAR ZONE:

The Moyar shear zone binds the Coorg block to the Nilgiri block trending E-W. Studies in the region have come to the following conclusions; 1.) Sm-Nd garnet whole rock analysis of mafic granulites in the shear zone yielded $^{207}\text{Pb}/^{206}\text{Pb}$ ages of $2355 \pm 22\text{Ma}$ (Samuel et al., 2014). 2.) Nd models for syntectonic intruded granites and tonalites provide ≤ 1.7 Ga crustal generation ages (Meißner et al., 2002). 3.) A Neoproterozoic gabbro-diorite-granite suite is interpreted to have been emplaced from $^{206}\text{Pb}/^{238}\text{U}$ ages ranging from 715 ± 4 to 832.5 ± 5 Ma. The timing of amalgamation of the Nilgiri block along the Moyar shear zone is not yet properly constrained. The shear zone then extends further east converging with the Salem-Attur shear zone.

ASSEMBLAGE PRESSURE/TEMPERATURE CONDITIONS:

A handful of pressure-temperature data for the Mercara shear zone are known. Devaraju (2004) describes staurolite, kyanite, and cordierite bearing pelites of the Mercara shear zone to have an estimated P - T stage varying from 550-750 °C at 4.5-8.6kbars, based on conventional thermobarometry. Leading to their conclusion of a middle to deep crustal residence of the pre-metamorphosed pelites. Ishwar-Kumar et al. (2013) finds metamorphic P - T conditions of $\sim 1000^\circ\text{C}$ at 15-20kbar, based on pressure, temperature calculations using Perple_X. Most recently Ishwar-Kumar et al. (In Press) found P - T conditions of 13 kbar at 825 °C. Indicating that the sediments would have been

subducted to a depth of about 40–50 km and were later exhumed, with a peak metamorphism range of 11–18 kbar, at 825–550 °C. Conditions were based on pressure, temperature calculations using *Perple_X*. While the timing of metamorphism was dated by zircon lower intercepts describing a 1464 ± 94 Ma suturing event (Ishwar-Kumar et al., In Press).

ANALYTICAL METHODS

Seventy four samples were collected from the Coorg block and surrounding regions from field work in January 2016, four were selected for geochronology and thermobarometric determination based on their assemblages, location and lithology.

U-Pb zircon geochronology

U-Pb age data were acquired from 4 samples of separated zircon grains. The samples were crushed and the zircons were separated from crushed material using standard sieving, panning, flotation and magnetic techniques. Zircons were then mounted by hand onto 2.5 cm-diameter epoxy disks and polished to expose the core of the grain. The grains were then imaged with a Gatan cathodoluminescence analyser, attached to a Phillips XL20 scanning electron microscope. U-Pb isotopic analysis was completed using a Laser Ablation Inductively Coupled Mass Spectrometer (LA-ICP-MS) at Adelaide Microscopy following the methods of (J. L. Payne et al., 2010). The instrument was a New Wave Research UP-213 laser with a spot-size of 30µm, a frequency of 5 Hz and an intensity of 65%. Isotopic data were attained with the Agilent 7500 series ICP-MS on eight masses: $^{206}\text{Pb}/^{238}\text{U}$; $^{207}\text{Pb}/^{235}\text{U}$; $^{207}\text{Pb}/^{206}\text{Pb}$; $^{208}\text{Pb}/^{232}\text{U}$. Mass discrimination was corrected for using zircon standard reference material GJ-1 with thermal ion mass spectrometry (TIMS) normalizing ages of $^{207}\text{Pb}/^{206}\text{Pb} = 608.3$ Ma, $^{206}\text{Pb}/^{238}\text{U} = 600.7$ Ma and

$^{207}\text{Pb}/^{235}\text{U} = 602.2 \text{ Ma}$ (Jackson et al., 2004). Data was corrected in the Iolite Version 3.0 (Van Achterbergh et al., 2001). Concordia diagrams and data analyses were produced with ISOPLOT 4.11 for Excel (Ludwig, 2009). Refer to appendix F for detailed methodology.

U-pb in-situ monazite geochronology

In-situ U-Pb monazite dating was completed from 4 thin section samples. The thin sections were then imaged with a Gatan cathodoluminescence analyser, attached to a Phillips XL20 scanning electron microscope (SEM). The grains were then analysed using the ASI M50 coupled with a 7700 ICP-MS at Adelaide Microscopy. Using Agilent 7500cs and NewWave UP213 Laser Ablation System. Samples underwent ablation within a He-ablation atmosphere of frequency 5 Hz, with a beam diameter of $9\mu\text{m}$ and a repetition rate of 4Hz. Total acquisition time for each analysis was 100 seconds, 30 seconds of background measurement, 10 seconds of closed shutter stabilisation and 40 seconds of ablation time. Measured isotopes of ^{204}Pb , ^{206}Pb , ^{207}Pb , and ^{238}U each had a dwell time of 10, 15, 30 and 15ms respectively.

Data reduction techniques were completed using Iolite 2.6, elemental fractionation, mass bias and downhole fractionation corrections were completed using the monazite standard MAde1 (TIMS) Normalisation data: $^{207}\text{Pb}/^{206}\text{Pb} = 491 \pm 2.7 \text{ Ma}$, $^{206}\text{Pb}/^{238}\text{U} = 518.37 \pm 0.99 \text{ Ma}$, $^{207}\text{Pb}/^{235}\text{U} = 513.13 \pm 0.19 \text{ Ma}$). Data accuracy was monitored using monazite standard 95-222 (ca 450Ma; (J. L. Payne et al., 2008). Throughout this study MAde1 provided weighted mean ages of $^{207}\text{Pb}/^{206}\text{Pb} = 425 \pm 23$, $^{206}\text{Pb}/^{238}\text{U} = 473.4 \pm 2.7$, $^{207}\text{Pb}/^{235}\text{U} = 471.0 \pm 4.5$, (n=20). Conventional concordia plots were generated using Isoplot 4.15 (Ludwig, 2008). Refer to appendix F for detailed methodology.

Mineral chemistry via electron microprobe

Mineral chemistry techniques followed are outlined in (Tucker et al., 2015). The chemical compositions of biotite, garnet, K-feldspar and plagioclase, were analysed to further constrain the P-T conditions using a CAMECA SX 5 microprobe. A beam current of 20 nA and an accelerating voltage of 20kV were used for all point analyses. A PAP correction was used for error reduction techniques. The method produced analyses for SiO₂, TiO₂, Cr₂O₃, Al₂O₃, FeO, MnO, MgO, CaO, Na₂O, K₂O, ZnO, Cl and F using Wavelength Dispersive Spectrometers (WDS).

Bulk rock geochemistry using X-ray fluorescence.

Whole-rock geochemical analyses for phase equilibria forward modelling were undertaken on 5 samples I16-39, I16-42, I16-64, I16-65, I16-66 using X-ray fluorescence (XRF) techniques at Bureau Veritas Minerals, Adelaide, South Australia. Major elements were analysed on glass beads having been cast using a 12:22 flux to form the bead, with I16-42 undergoing analysis using a 57:44 flux achieving greater fusion.

Petrography

Nineteen samples were cut and polished into thin sections 25mm x 76mm by Continental Instruments, India. Petrographic analysis was completed using an Olympus BH-2 optical microscope.

Phase equilibria calculations

Phase equilibria calculations were performed using *THERMOCALC* v. 3.40 software (Holland & Powell, 2011), in the model chemical system, MnNCKFMASHTOaxOam (MnO–Na₂O–CaO–K₂O–FeO–MgO–Al₂O₃–SiO₂–H₂O–TiO₂–O), acknowledging

that 'O' is a proxy for Fe_2O_3 , using the latest internally consistent thermodynamic data set Ds6. (Holland & Powell, 2011). Activity-composition (a-x) models used came from (Powell et al., 2014; R. W. White et al., 2014). Whole rock major element geochemical compositions obtained via XRF analysis were recalculated to molar oxide percent (appendix A) to use for modelling. Calculations in *THERMOCALC* are based on user specified stable mineral assemblages that then have their coordinates and area calculated exhaustively by line and point. Where lines and points represent the zero abundance of a single or two phases respectively. Starting a pseudosection relies on the calculation of a Gibbs energy minimisation at a set *P-T* condition to produce an initial stable assemblage. The pseudosection is then calculated around that initial starting assemblage by trial and error calculations in order to determine which phases appear or disappear according to pressure, temperature or composition. Throughout the calculation process the focal point of the calculations moves within the pseudosections P-T-X space ($X = \text{composition}$) requiring an update of the "starting guesses" (values for *THERMOCALC* to run its iterative least-squares calculation). Resulting in the user actively calculating every line and point to create a single diagram. P-Mo and P-M_{h2o} diagrams are used to more accurately constrain the abundances of H₂O and Fe₂O₃ (oxidation state) as the whole rock geochemical analysis produces uncertain results (Kelsey & Hand, 2015). Chosen amounts of H₂O and Fe₂O₃ are selected for the *P-T* modelling of samples as they correspond to the calculated stable assemblage of the interpreted peak metamorphic assemblage observed in the rocks. Refer to appendix G for detailed methodology.

OBSERVATIONS AND RESULTS

Geochronology

ZIRCON U-PB GEOCHRONOLOGY

Four samples were collected from the Mercara shear zone for U-Pb analyses.

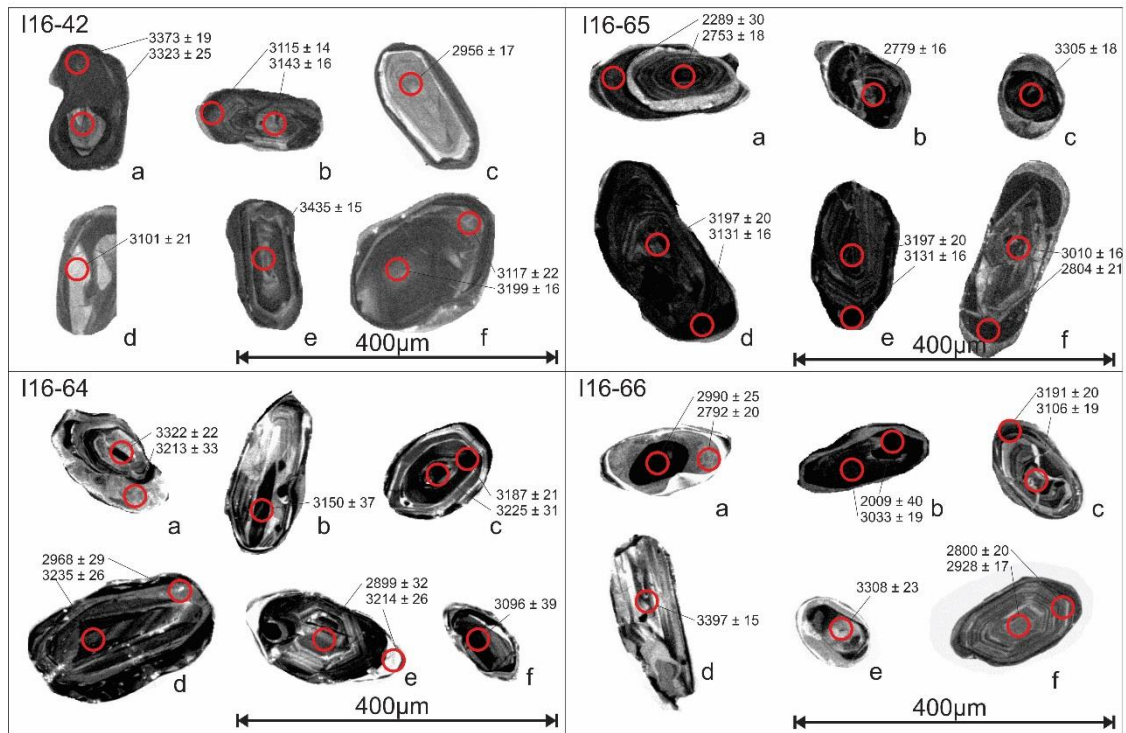


Figure 2: Images of zircons from samples I16-42, I16-64, I16-65 and I16-66 taken with the Gatan cathodoluminescence analyser, attached to a Phillips XL20 scanning electron microscope. Samples exhibit textural features and variable shapes and sizes.

Sample I16-42

A detailed cathodoluminescence study upon the zircons concluded that they ranged in length from 60µm to 250µm with the majority forming an aspect ratio of 2. Metamict and xenocrystic cores are evident (Fig. 2 a, b, d) some display irregular concentric zoning patterns (Fig. 2 c, e), with an euhedral grain shape. Metamorphic rims appear as a dominant texture within some grains. With almost all rims forming during the Archaean rather than the lower intercept Neoproterozoic ages. Despite this no significant relationship can be observed with differing Th/U ratios between rims and cores. Of the

concordant grains 183 out of 167 were of $\leq 10\%$ discordance yielding $^{207}\text{Pb}/^{206}\text{Pb}$ ages between 2800 Ma and 3500 Ma (Fig. 3). I16-42 shows a slight decrease in concordance with decreasing age prior to the old monazite age of 3071 ± 12 Ma (Fig.6), supporting the interpreted metamorphic age. However concordant zircons are found younger than this age, this may be due to an older lead loss event with subsequent shallower discordia lines or later zircon growth due to hydrothermal activity. A notable significance becomes apparent when the data is displayed on a probability density plot, (Fig. 5). Where the highest density of zircons analysed effectively clusters around 3071 Ma, implying a period of extensive zircon growth.

To remove uncertainty between metamorphic and detrital zircons, the relationship between the Th/U ratio and $^{207}\text{Pb}/^{238}\text{U}$ age is conducted. A decreasing trend with decreasing ages shows an increased presence in metamorphic zircons. The data shows a difference in apparent slope between interpreted trends before and after 3071 Ma, (Fig. 7).

Sample I16-64

A detailed cathodoluminescence study upon the zircons concluded that they ranged in length from $90\mu\text{m}$ to $270\mu\text{m}$, the majority forming an aspect ratio of 1.5. Metamict textures and xenocrystic cores are evident (Fig. 2 c, d and f) some displaying irregular concentric zoning patterns (Fig 2 a and e), with a euhedral to sub rounded grain shape. Metamorphic rims appear as a dominant texture within some grains, with almost all rims forming during the Archaean rather than the monazite dated metamorphic event during the Neoproterozoic. Suggesting the later metamorphic event dated to 676 ± 47 Ma leaves a dominant presence in all zircons, supported by the clearly decreasing trend apparent in the Th/U ratios when plotted against $^{207}\text{Pb}/^{238}\text{U}$ ages, (Fig. 8). A probability

density plot of the data (Fig. 5) describes the opposite to Sample I16-42, timing the metamorphic event to a period of little zircon growth. I16-64 provided 174 zircon grains, with 41 yielding results within 10% of concordance. These grains yielded $^{207}\text{Pb}/^{206}\text{Pb}$ ages describing two populations, one at ca. 3.1 Ga then at ca. 3.2 to 3.6 Ga, (Fig. 3).

Sample I16-65

A detailed cathodoluminescence study upon the zircons concluded that they ranged in length from 90 μm to 270 μm , the majority forming an aspect ratio of 1.5. Metamict textures and xenocrystic cores evident (Fig. 2 a, c, f) some displaying irregular concentric zoning patterns (Fig. 2 a, d, e), with an euhedral to sub rounded grain shape. Metamorphic rims appear as a dominant texture within some grains. With almost all rims forming during the Archaean rather than the monazite dated metamorphic event during the Neoproterozoic. Suggesting the later metamorphic event dated to 676 ± 47 Ma leaves a dominant presence in all zircons, supported by the clearly decreasing trend apparent in the Th/U ratios when plotted against $^{207}\text{Pb}/^{238}\text{U}$ ages, (Fig. 8). I16-65 provided 185 zircon grains with 46 yielding results within 10% of concordance. Analyses of $\leq 10\%$ discordant zircons yielded $^{207}\text{Pb}/^{206}\text{Pb}$ ages spreading from ca. 3.2 – 3.4 Ga, with a discordia line from 3.1 Ga to Neoproterozoic ages, (Fig. 3, 4).

Sample I16-66

A detailed cathodoluminescence study of the zircons concluded that they ranged in length from 70 μm to 240 μm , the majority forming an aspect ratio of 2. Metamict textures and xenocrystic cores evident (Fig. 2 a, d, e) some displaying irregular concentric zoning patterns (Fig. 2 b, e, f), with an euhedral to sub rounded grain shape. Metamorphic rims appear as a dominant texture within some grains. With almost all rims forming during the Archaean rather than the monazite dated metamorphic event during the Neoproterozoic. Suggesting the later metamorphic event dated to 676 ± 47 Ma leaves a

dominant presence in all zircons, supported by the clearly decreasing trend apparent in the Th/U ratios when plotted against $^{207}\text{Pb}/^{238}\text{U}$ ages, (Fig. 8). I16-66 provided 112 zircon grains with 63 yielding results of 10% concordance. 55 out of 63 of $\leq 10\%$ discordant zircon grains yielded a restricted $^{207}\text{Pb}/^{206}\text{Pb}$ population of zircons between 3.2 and 3.5 Ga, while all other have lost radiogenic Pb. More rims show discordant data suggesting that they formed by diffusional Pb loss during the Neoproterozoic metamorphism event (Fig. 3).

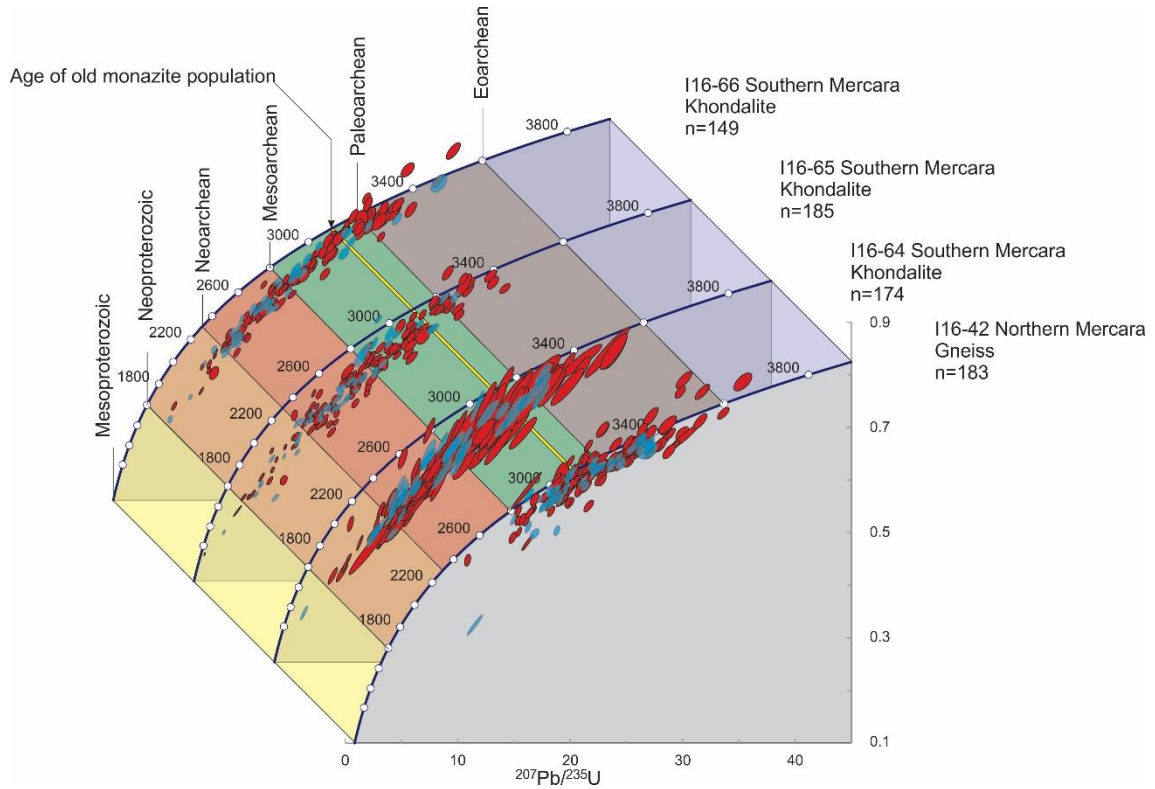


Figure 3: U-Pb combined concordia diagrams for zircon grains with a 2σ data point error ellipses. Individual data points are indicated as red ellipses (Cores) and blue ellipses (rims). A trend is apparent where the spreads of the data are getting more discordant as they get younger than 3.1 Ga, with the exception of I16-42.

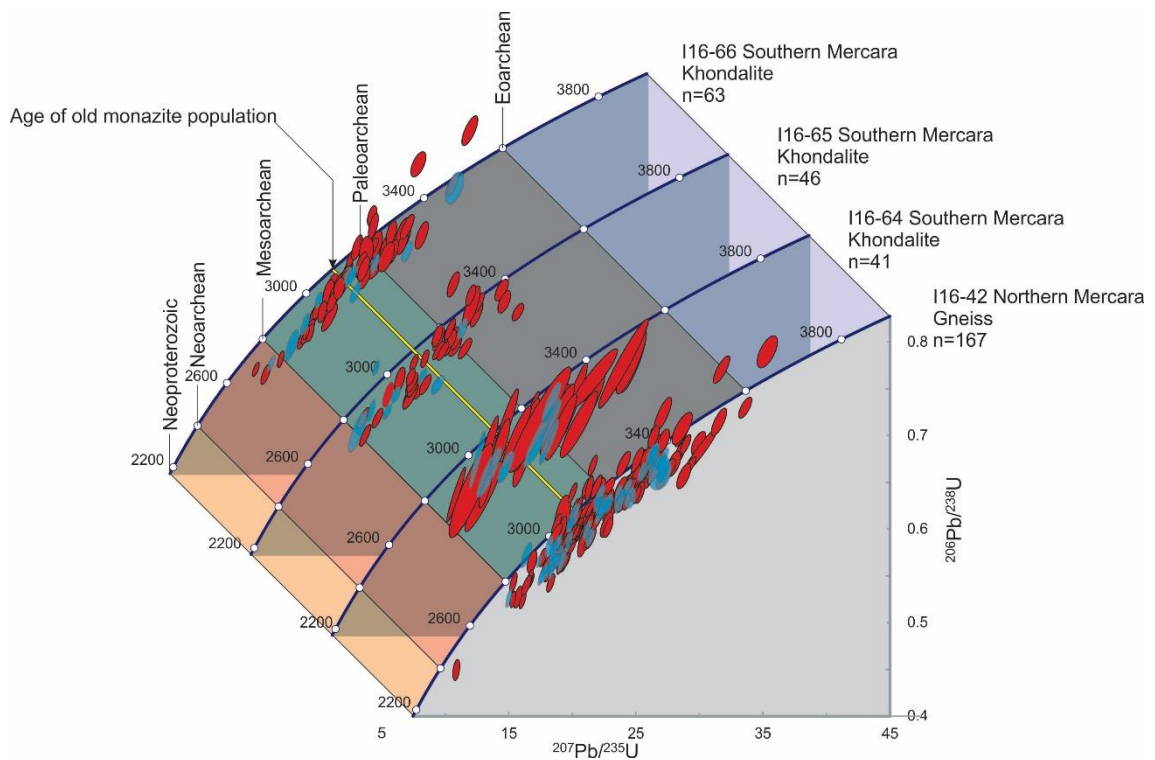


Figure 4: U-Pb combined concordia diagrams within a 10% concordance filter for zircon grains with a 2σ data point error ellipses. Individual data points are indicated as red ellipses (Cores) and blue ellipses (rims).

ellipses (rims). A trend is apparent where the spreads of the data are getting more discordant as they get younger than 3.1 Ga, with the exception of I16-42.

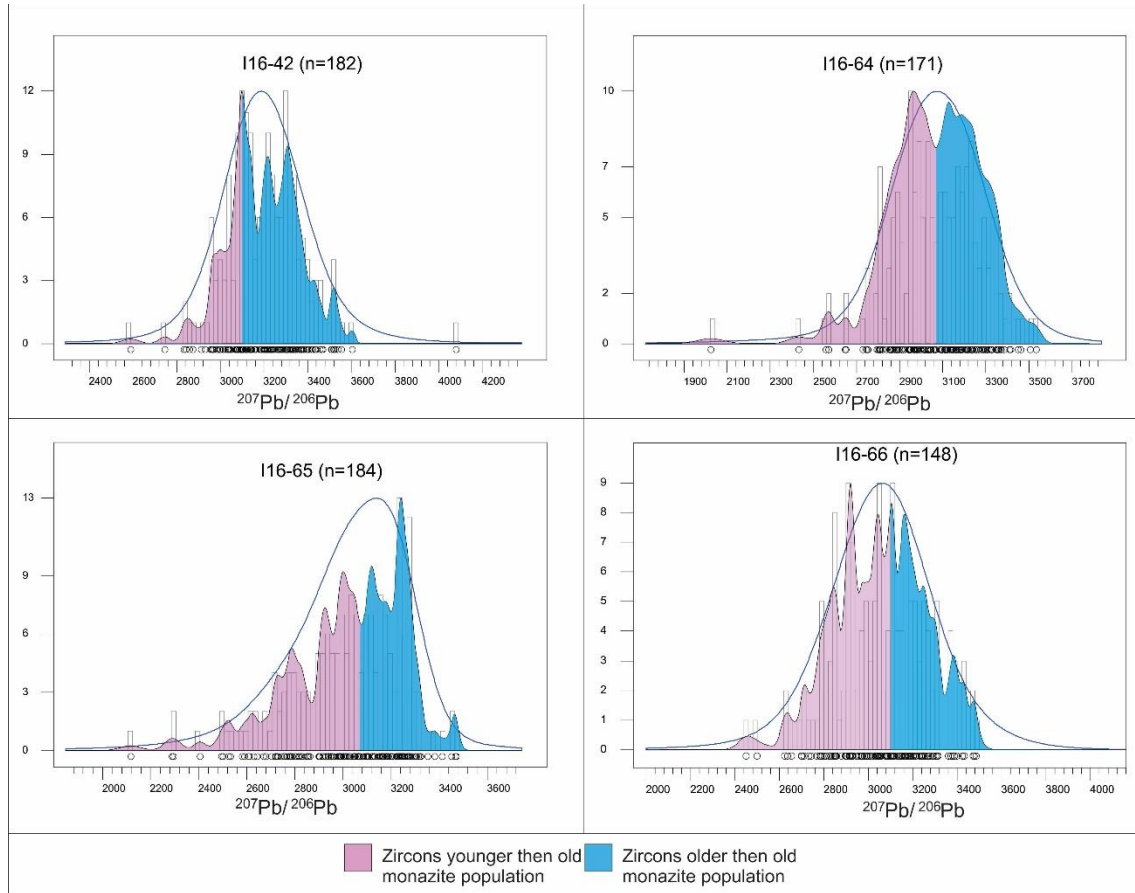


Figure 1: Probability density plots for samples I16-42, I16-64, I16-65 and I16-66, displaying all data. Where pink regions represent zircons younger than the old monazite population and blue regions represent zircons older than the old monazite population. Sample I16-64 provides an interpreted bimodal distribution almost centred by the monazite age, this may divide a detrital and metamorphic zircon

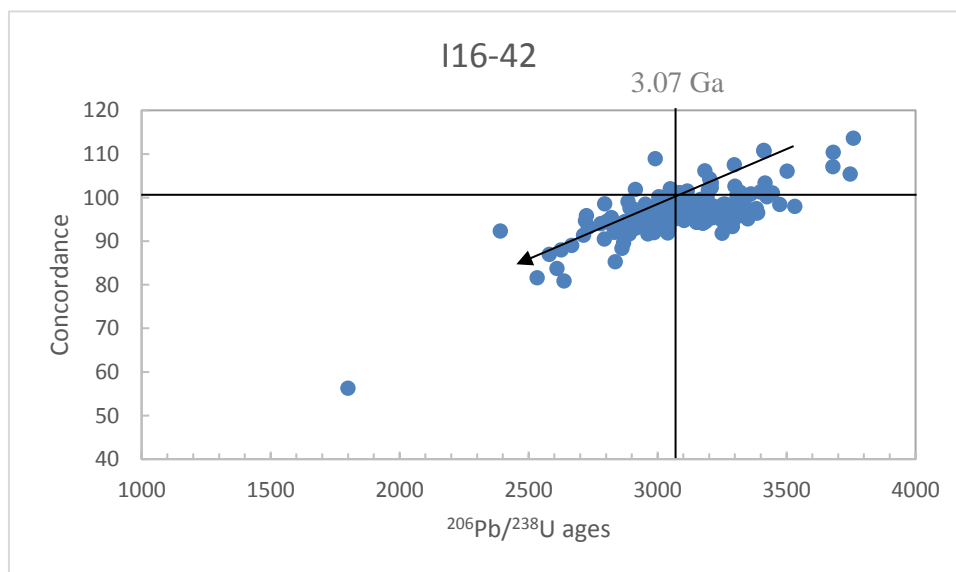


Figure 2: Sample I16-42 zircon $^{206}\text{Pb}/^{238}\text{U}$ ages plotted against their concordancy, producing a trend of decreasing concordancy with decreasing age. This trend suggests that the zircons with $^{206}\text{Pb}/^{238}\text{U}$ ages younger the 3071 Ma have lost small amounts of radiogenic Pb, illustrating that these near concordant ages are still younger than the time at which they grew.

ZIRCON TH-U VS $^{207}\text{Pb}/^{206}\text{Pb}$ AGES

An analysis upon the thorium-uranium ratios vs $^{206}\text{Pb}/^{238}\text{U}$ ages is used to determine if zircons present Th-U ratios <0.2 while also forming an decreasing trend with decreasing $^{206}\text{Pb}/^{238}\text{U}$ ages. This low value and decreasing trend is interpreted to be indicative of zircons undergoing metamorphic regrowth. (Möller et al., 2003; Wan et al., 2011). It is believed that during regrowth thorium is less compatible in the zircon structure than uranium and preferentially diffuses out of the crystal. Although in high grade rocks such as UHT granulites where anatectic melts are present the zircon will grow in a thorium rich environment as the thorium diffused from pre-existing zircons partitions into the melt phase. (Möller et al., 2003; Wan et al., 2011). This trend is apparent in figures 6, 7 and 8, for samples I16-42, I16-65 and I16-66 respectively.

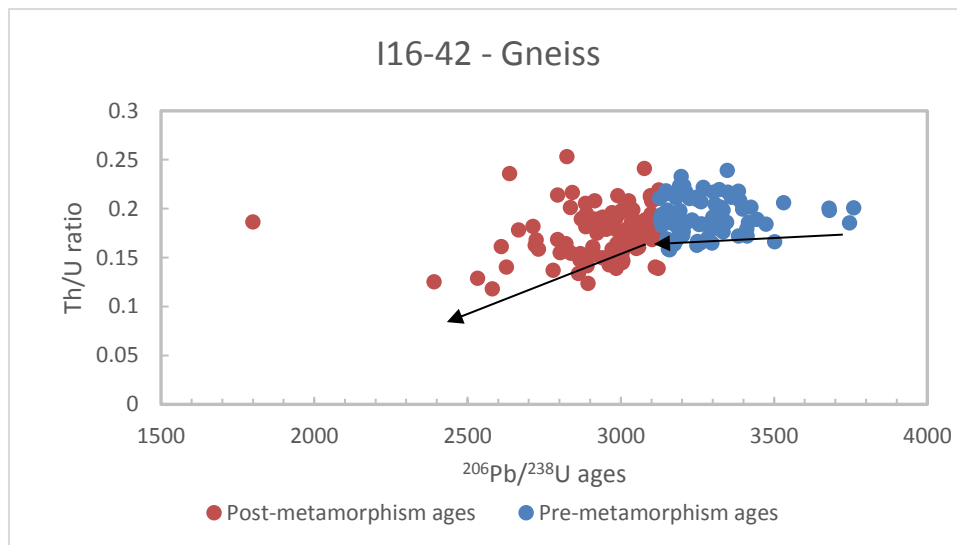


Figure 3: Th/U ratio vs $^{206}\text{Pb}/^{238}\text{U}$ ages for sample I16-42, two populations are shown here. The red dots represent zircon analyses from after the monazite determined metamorphism age, while the blue represent analyses from before the metamorphism age. Two slight trends become apparent, observable via the arrows. Post metamorphism ages fits a more decreasing trend while pre-metamorphism ages fit a more level trend.

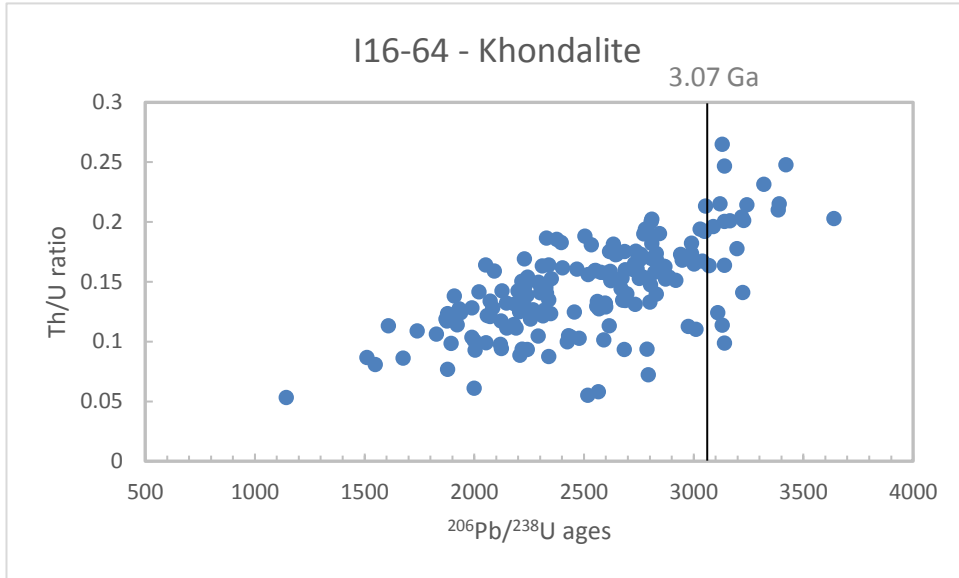


Figure 4: Th/U ratio vs $^{206}\text{Pb}/^{238}\text{U}$ ages for sample I16-64, an increasing trend is apparent with old $^{206}\text{Pb}/^{238}\text{U}$ ages and high Th/U values. This trend suggests that metamorphic zircon growth is apparent through all zircons, consistent with recording a second Neoproterozoic metamorphic event.

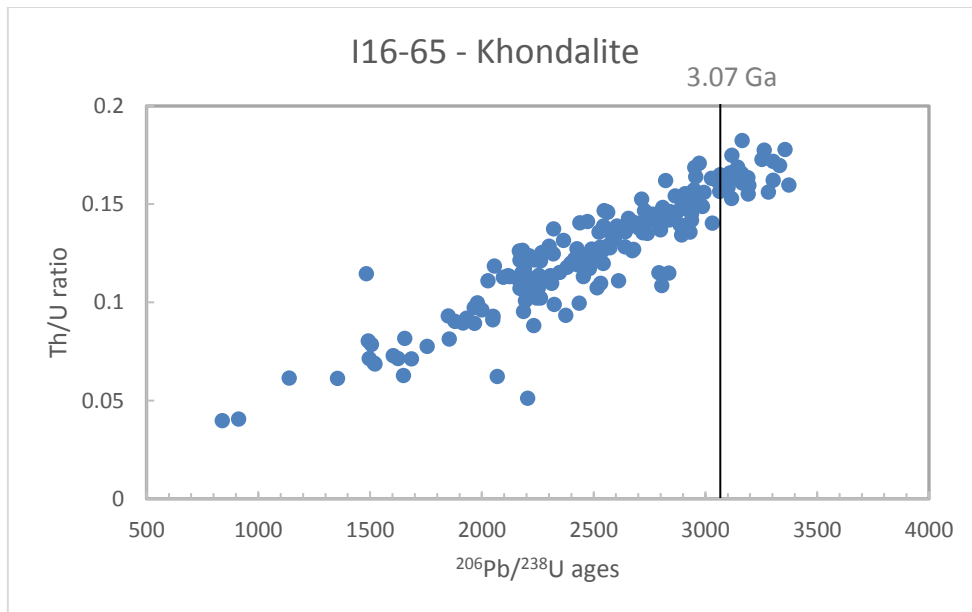


Figure 5: Th/U ratio vs $^{206}\text{Pb}/^{238}\text{U}$ ages for sample I16-65, an increasing trend is apparent with old $^{206}\text{Pb}/^{238}\text{U}$ ages and high Th/U values. This trend suggests that metamorphic zircon growth is apparent through all zircons, consistent with recording a second Neoproterozoic metamorphic event.

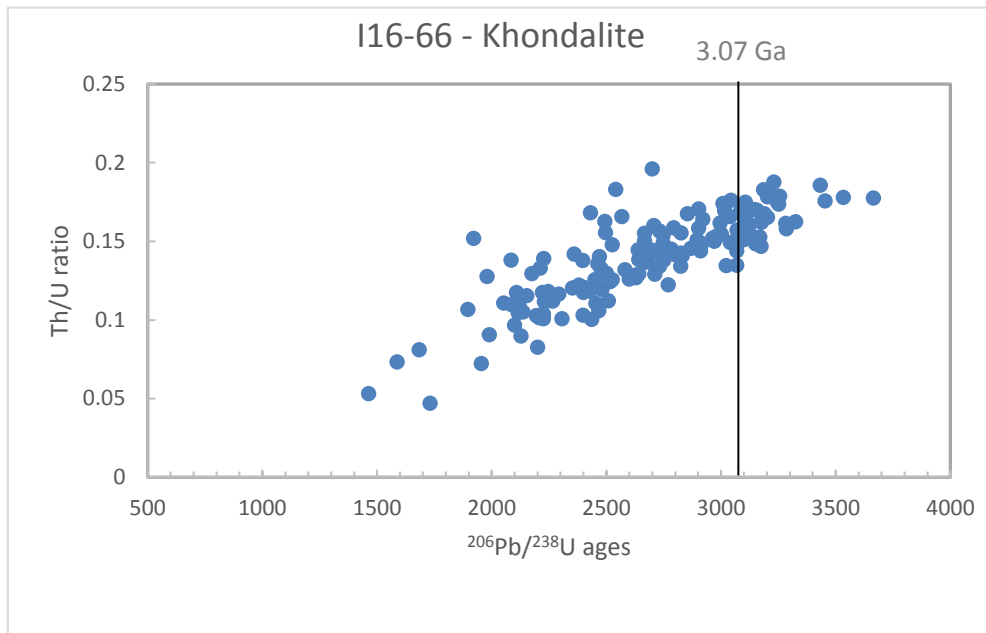


Figure 6: Th/U ratio vs ²⁰⁷Pb/²⁰⁶Pb ages for sample I16-66, an increasing trend is apparent with old ²⁰⁶Pb/²³⁸U ages and high Th/U values. This trend suggests that metamorphic zircon growth is apparent through all zircons, consistent with recording a second Neoproterozoic metamorphic event.

IN-SITU MONAZITE U-PB GEOCHRONOLOGY

In-situ U-Pb monazite geochronology was undertaken on samples I16-42, I16-64, I16-65 and I16-66 from the Mercara shear zone. Monazite is abundant within garnet aggregate bands, and uncommon throughout the matrix. Grain sizes range from 8-18 μ m, leaving some grains unsuitable for analysis. A total of 85 grains were successfully analysed across all samples, 43 from the northern Mercara, and 42 from the southern Mercara. The $\leq 10\%$ concordance data are displayed on concordia plots with ²⁰⁷Pb/²⁰⁶Pb weighted average plots (Fig. 12) and all data are shown on concordia plots in figure 11.

Sample I16-42

U-Pb analysis of sample I16-42 provided 49 individual monazite grains of which 35 provided an analysis of $\leq 10\%$ concordance. However a final plateau of 11 analyses were used in the trend analysis to reduce error, likewise ²⁰⁷Pb/²⁰⁶Pb ages were used to reduce uncertainty. The data appears to fall broadly on a discordia line, with an upper

intercept of 3078 ± 36 Ma and a poorly defined lower intercept of 1054 ± 150 Ma, with a very large MSWD of 16, (Fig. 11a). The associated weighted average reveals a $^{207}\text{Pb}/^{206}\text{Pb}$ age of 3024 ± 25 Ma with an MSWD of 11.4 (Fig. 12b red). However focussing on the plateau of the oldest 11 analyses a line calculation is conducted providing an upper intercept value of 3126 ± 41 Ma and a MSWD of 3.4 (Fig. 12a). The same data provides a $^{207}\text{Pb}/^{206}\text{Pb}$ weighted mean age of 3071 ± 12 Ma, (MSWD =1.4), (Fig. 12b green). This is interpreted to represent the age of monazite growth during the metamorphic event.

Sample I16-64

U-Pb analysis of sample I16-64 provided 8 individual monazite grains of which 1 provided an analysis of $\leq 10\%$ concordance, producing a $^{206}\text{Pb}/^{238}\text{U}$ value of 735 ± 35 Ma (Fig. 12c).

Sample I16-65

U-Pb analysis of sample I16-65 provided 5 individual monazite grains of which all provided an analysis of $\leq 10\%$ concordance (Fig 12c). Using all data provides an upper intercept of 3092 ± 30 Ma with and MSWD of 1.7 (Fig. 11c). The $^{207}\text{Pb}/^{206}\text{Pb}$ data are spread from 650 Ma to 760 Ma (Fig. 12d), with a $^{207}\text{Pb}/^{206}\text{Pb}$ weighted average of 722 ± 25 Ma and an MSWD of 1.5 (Fig. 12d). $^{207}\text{Pb}/^{206}\text{Pb}$ ages were used to reduce uncertainty when modelling the data.

Sample I16-66

U-Pb analysis of sample I16-66 provided 37 individual monazite grains of which 16 provided analyses within $\leq 10\%$ of concordance (Fig. 12e). Using all data provides an upper intercept of 3082 ± 44 Ma with and MSWD of 3.3 (Fig. 11c). The $^{207}\text{Pb}/^{206}\text{Pb}$ data are spread from 700 Ma to 860 Ma (Fig. 12f), with a $^{207}\text{Pb}/^{206}\text{Pb}$ weighted average of 683 ± 46 Ma and an MSWD of 1 (Fig. 12f). $^{207}\text{Pb}/^{206}\text{Pb}$ ages were used to reduce uncertainty when modelling the data.

Samples I16-65 and I16-66

These two samples were combined due to their correlation of results and outcrop proximity of several metres. Providing a total of 45 individual monazite grains of which 21 were $\leq 10\%$ concordance (Fig. 12g). The $^{207}\text{Pb}/^{206}\text{Pb}$ data is spread from 650 Ma to 860 Ma (Fig. 12h), with a $^{207}\text{Pb}/^{206}\text{Pb}$ weighted average of 676 ± 47 Ma and an MSWD of 1.2 (Fig. 12h). $^{207}\text{Pb}/^{206}\text{Pb}$ ages were used to reduce uncertainty when modelling the data.

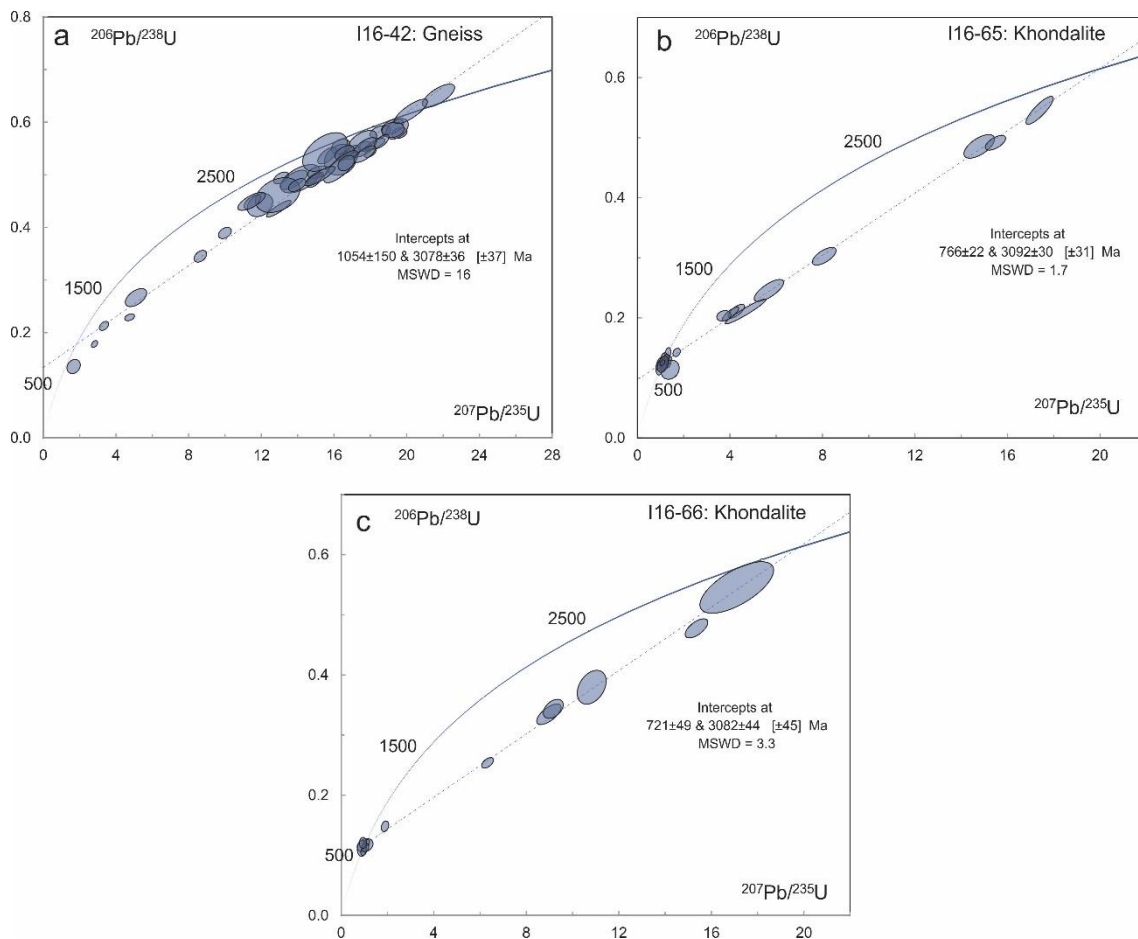


Figure 7: U-Pb Concordia diagrams for all monazite grains with 2σ data point error ellipses. Samples correspond to a) Mercara gneiss (I16-42), b) Mercara khondalite (I16-65) and c) Mercara khondalite (I16-66).

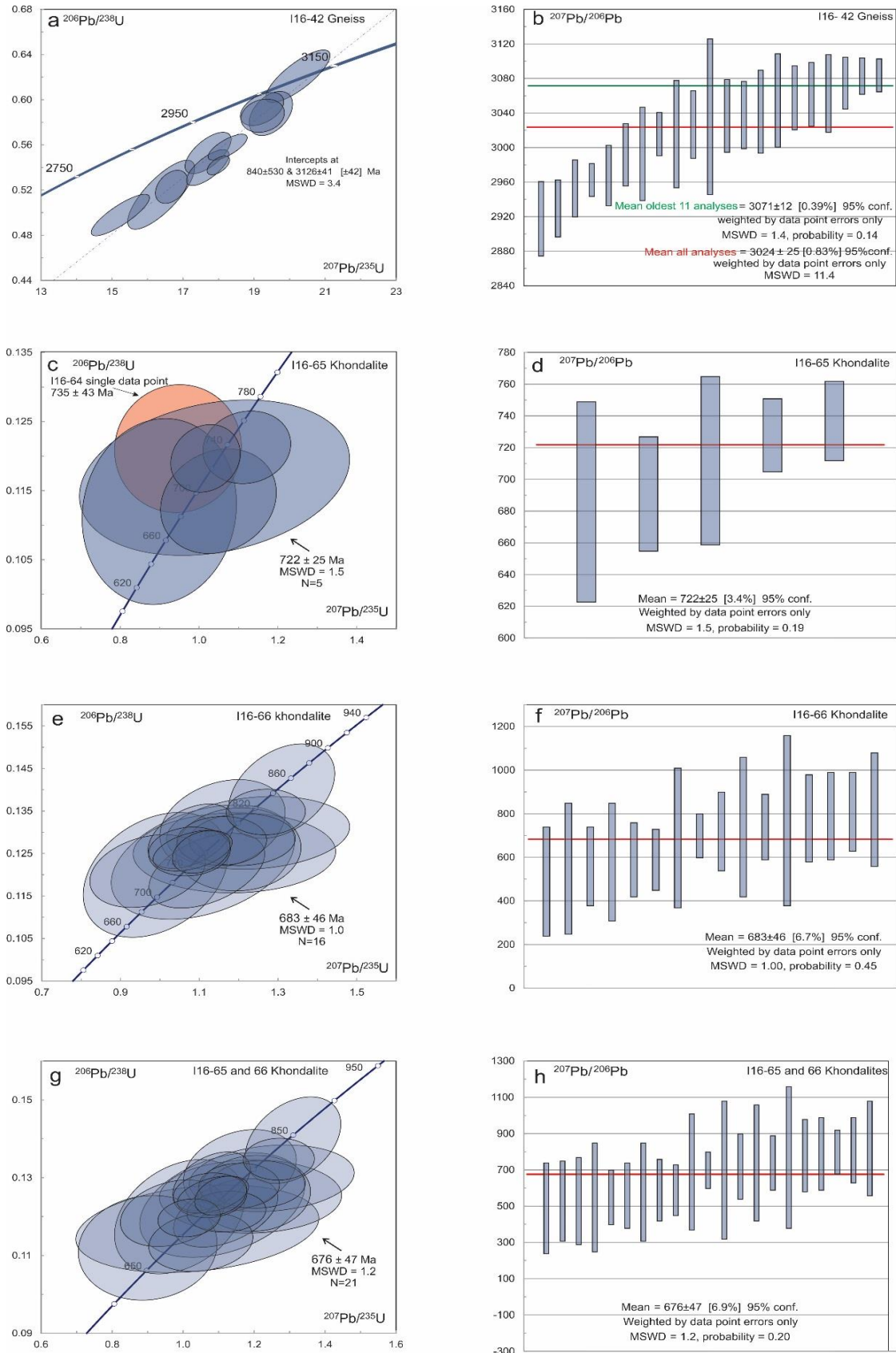


Figure 8: U-Pb monazite geochronology within a 10% concordance filter for samples I16-42 (a and b), I16-65 (c and d), I16-66 (e and f) and combined data for samples I16-65 and I16-66 (g and h).

Metamorphic Geology

METAMORPHIC PETROLOGY

A detailed petrographic analysis was undertaken upon samples from the Mercara region, a gneiss and 3 samples from the khondalite quarry. Peak and retrograde mineral assemblages have been interpreted upon the basis of micro textural context and grain size.

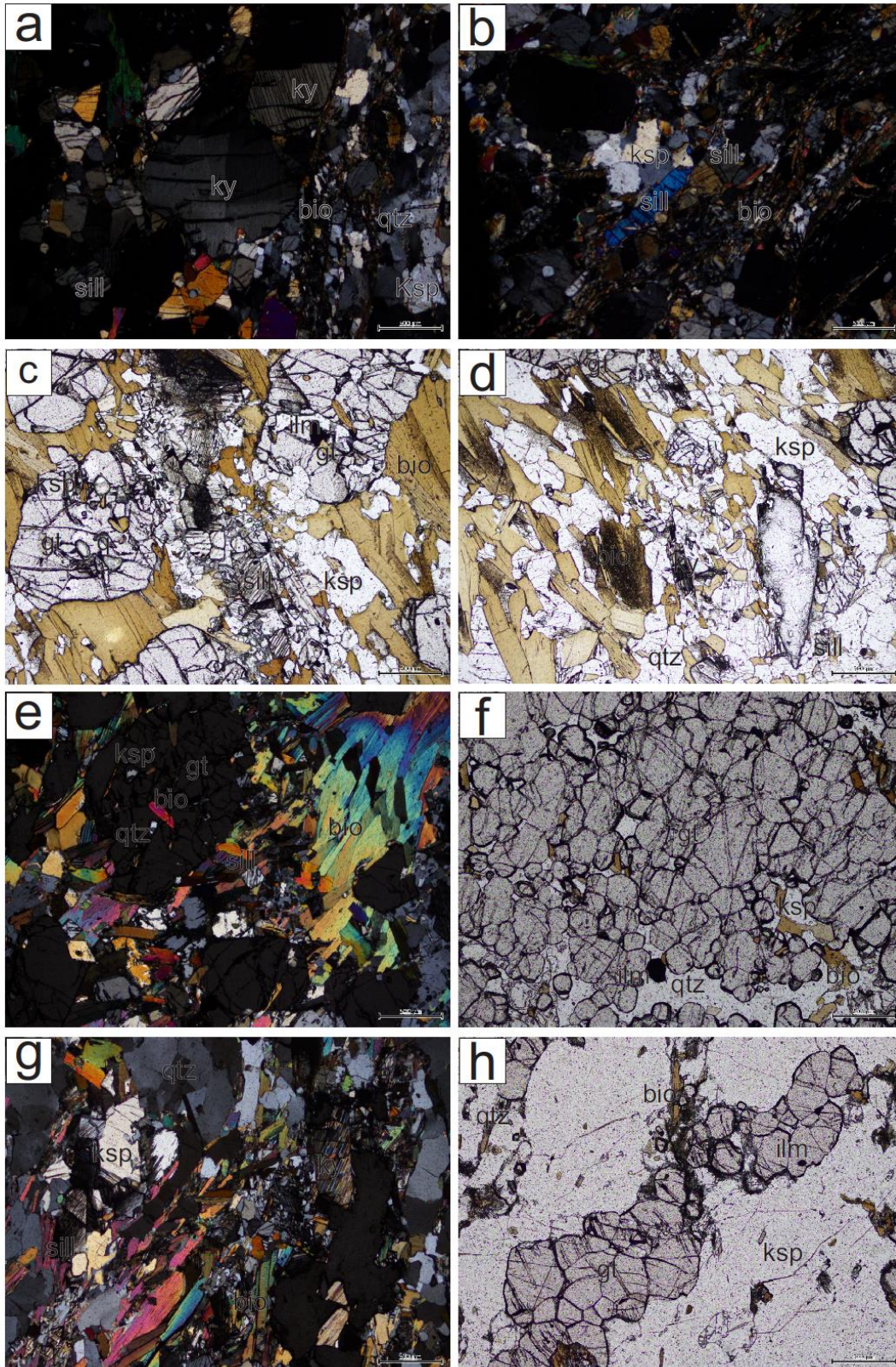


Figure 9: Photomicrographs of petrological relationships within the Mercara gneiss and khondalite. a) I16-42 (Mercara gneiss) showing twinned coarse kyanite with an almost 90° cleavage angle while Sillimanite is seen as an inclusion in garnet. b) I16-42 (Mercara gneiss) showing a very fine fabric defined by biotite, sillimanite can be seen displaying twinning perpendicular to its cleavage. c) I16-

64 (Mercara khondalite) showing poikoblastic porphyroblasts of garnet, with inclusions of Ilmenite, quartz and K-feldspar. d) I16-64 (Mercara khondalite) showing a very coarse fabric defined by biotite and sillimanite. Kyanite is seen in contact with quartz, K-feldspar and biotite. e) I16-65 (Mercara khondalite) showing poikoblastic porphyroblasts of garnet with inclusions of biotite, quartz and K-feldspar, mildly wrapped around by a medium grained biotite and sillimanite fabric. f) I16-65 (Mercara khondalite) showing a wide garnet aggregate, with inclusions between the garnet grains of Ilmenite, K-feldspar and biotite. g) I16-66 (Mercara khondalite) showing kyanite with 2 cleavages preserved near 90° occurring in contact with quartz and biotite adjacent a very weak fabric consisting of biotite and sillimanite. h) I16-66 (Mercara khondalite) showing a garnet aggregate with inclusions of ilmenite, contacting biotite and K-feldspar.

I16 42: Mercara gneiss

Collected from very large (4m) roadside boulders, presenting partially melted leucosomes and psammite layering. The sample contains quartz, K-feldspar, garnet, kyanite, sillimanite, biotite, rutile, ilmenite with minor plagioclase. A very fine fabric is observed (0.05-0.1mm) containing biotite and sillimanite, (Fig. 13b). Garnet is seen more commonly as very coarse (1-15mm) poikoblastic porphyroblasts. Containing inclusions of biotite, quartz, sillimanite and kyanite. The kyanite is also observed to be medium grained (0.5-1mm), contacting K-feldspar, quartz, garnet and sillimanite (Fig. 13a). Kyanite is seen to preserve twinning parallel to cleavage, as well as oblique extinction (Fig. 13a). Kyanite uncommonly will contain inclusions of K-feldspar and quartz. Sillimanite is seen preserve twinning perpendicular to cleavage (Fig. 13b), parallel extinction while also containing inclusions of quartz. A moderate foliation can be observed affecting both the fabric and coarse minerals, nodular equigranular medium grained (0.2-0.5mm) quartz and K-feldspar makes up the coarse grained portions.

Sample I16-64:

Collected from the Mercara shear zone khondalite quarry, along with I16-65 and I16-66. The sample contains quartz K-feldspar, plagioclase, garnet, biotite, sillimanite, kyanite with minor ilmenite, rutile. A modest foliation forming fabric of dominantly fine grained (0.1-0.4) biotite with some minor sillimanite presence is observed to wrap around larger grains (0.5-1.5) of garnet, cross-section sillimanite, kyanite and K-feldspar (Fig.

13c). Biotite is seen in straw brown elongate grains of 0.5 to 1.5mm. Garnet is observed in poikoblastic porphyroblasts, containing inclusions of plagioclase, quartz, biotite and k-feldspar, (Fig. 13d). A coarse grained elongate equigranular matrix is observed, composed of quartz, K-feldspar, plagioclase, garnet aggregates and minor biotite seen as a secondary mineral filling gaps between minerals, much like (I16-65, Fig. 13f). The coarse grained assemblage appears to follow a trend, where all grains are aligned along their long side. The peak metamorphic assemblage is garnet – plagioclase – K-feldspar – quartz – ilmenite – rutile \pm sillimanite.

Sample I16-65:

The sample contains quartz, garnet, biotite, cordierite, feldspar, plagioclase sillimanite and kyanite with minor rutile and ilmenite. An intermittent pervasive fabric of fine grained (0.1-0.7mm) biotite and sillimanite wraps around larger grains (0.1-1mm) of quartz, garnet, K-feldspar and coarse sillimanite grains (Fig. 13e). Sillimanite is observed in contact with quartz and biotite. Biotite is seen in straw brown elongate grains of 0.2 to 1.5mm. Kyanite occurs in the matrix in small blocky elongate grains of 0.3 to 0.8mm, in contact with biotite and quartz. Coarse grained garnet aggregates do not occur through the matrix, but as their own thin section spanning aggregates 10-100mm across, containing inclusions of biotite, quartz and feldspar (Fig. 13f). Between the grains within the aggregate is commonly quartz, magnetite, rutile and biotite (Fig 13f). Cordierite, quartz and garnet can also be seen in moderately poikoblastic porphyroblasts (1.5 to 3.5mm), containing biotite, quartz, feldspar and radioactive minerals particularly in cordierite. The peak metamorphic assemblage is garnet – quartz – plagioclase – feldspar – sillimanite – rutile – ilmenite.

Sample I16-66:

Regular similarities are observed between samples I16-64 and I16-66. The sample contains quartz, K-feldspar, plagioclase, garnet, biotite, sillimanite, kyanite with minor ilmenite and rutile. A weak foliation is observed of medium grained (0.3-1mm) biotite with minor sillimanite is seen to partially wrap around larger grains (0.8-1.5mm) of garnet, kyanite, quartz, K-feldspar and coarse sillimanite, (Fig. 13g). Coarse grained poikoblastic garnet porphyroblasts are observed with inclusions of K-feldspar, quartz, biotite. Some inclusions of K-feldspar contained their own inclusions of quartz and biotite. A equigranular crystalline matrix of coarse grained quartz, K-feldspar, plagioclase and large (10-40mm) garnet aggregated are observed, (Fig. 13h) biotite and ilmenite and rutile are observed between the larger grains. (Fig. 13h) The peak metamorphic assemblage is quartz, garnet, K-feldspar, plagioclase, biotite, sillimanite \pm ilmenite and rutile.

PRESSURE/TEMPERATURE-AMOUNT PSEUDOSECTIONS

A $P-M_o$ (Fig. 14, 15) and a $T-M_{H_2O}$ (Fig. 16) pseudosection were calculated to determine appropriate Fe_2O_3 ('O') and H_2O contents for P-T modelling of samples. I16-42 did not require a $T-M_{H_2O}$ pseudosection as its initial H_2O content was already low. Subsequently a value based on the loss of ignition data from the XRF analysis takes its place, this value is used in the subsequent $P-T$ pseudosection.

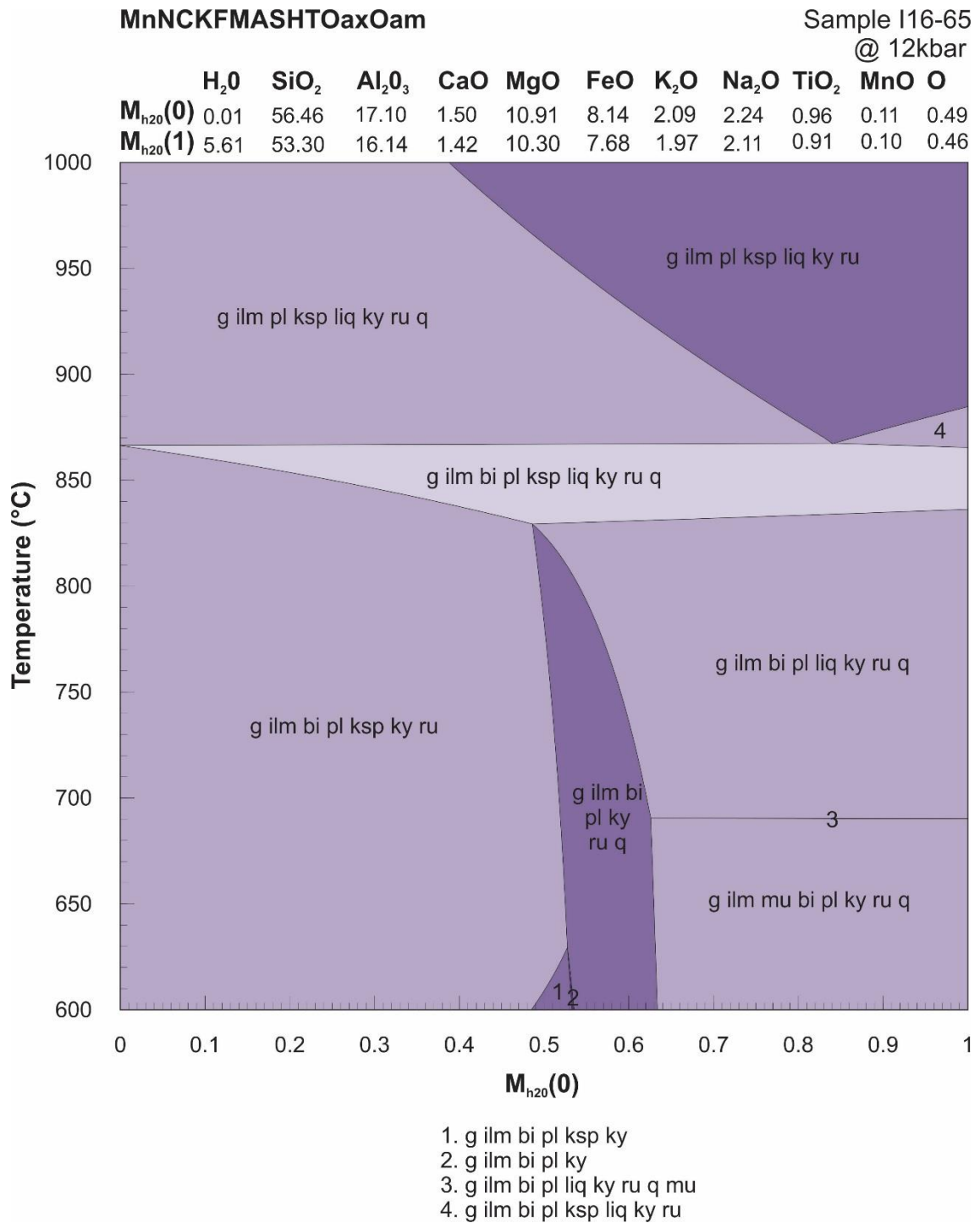
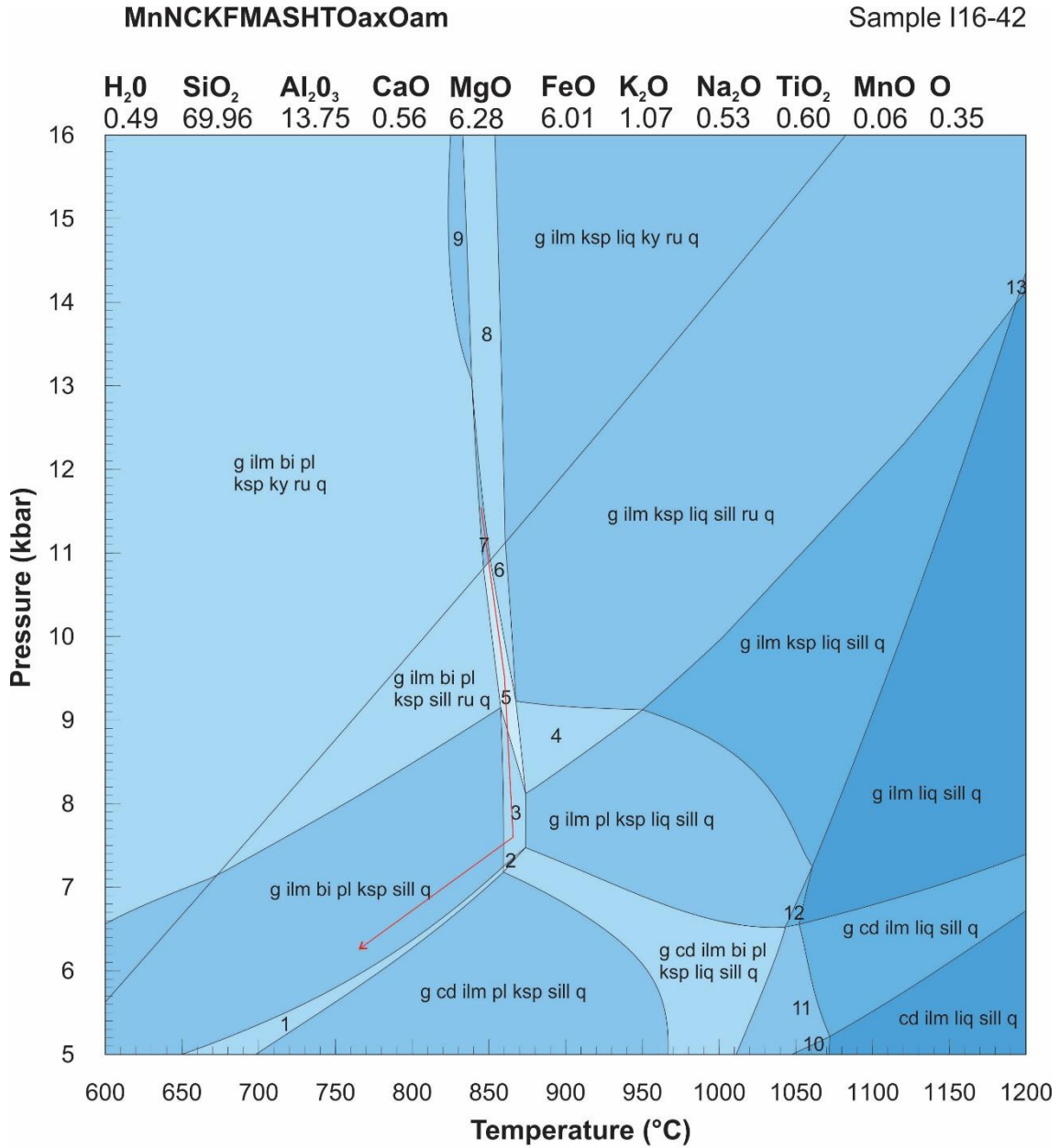


Figure 12: T-Mh₂O pseudosection for sample I16-65 from the Mercara shear zone. Above the diagram expressed as mole percent are the bulk composition used for modelling the diagram. No value for h₂O can be selected from this pseudosection, as the peak field traverses the pseudosection from 0 to 1. Subsequently a value based on the loss of ignition data from the XRF analysis takes its place, this value is used the subsequent P-T pseudosection.

Pressure-temperature pseudosections

P-T pseudosections were calculated for a single sample from the Mercara shear zone. With the aim of interpreting a *P-T* path and thermal gradient for rocks in the Mercara shear zone.



- | | |
|----------------------------------|-----------------------------|
| 1. g cd ilm bi pl ksp sill q | 8. g ilm bi ksp liq ky ru q |
| 2. g cd ilm bi pl ksp liq sill q | 9. g ilm bi pl ksp ky ru q |
| 3. g ilm bi pl ksp liq sill q | 10. cd ilm ksp liq sill q |
| 4. g ilm pl ksp liq sill ru q | 11. g cd ilm ksp liq sill q |
| 5. g ilm bi pl ksp liq sill ru q | 12. g ilm ksp liq sill q |
| 6. g ilm bi ksp liq sill ru q | 13. g ilm liq sill ru q |
| 7. g ilm bi pl ksp liq ky ru q | |

Figure 13: Calculated P-T pseudosection for sample I16-42 from the Mercara shear zone. Atop the diagram expressed as Mole percent are the bulk composition used for modelling the diagram. The peak field is denoted as 7, comprising of the composition, garnet, biotite, ilmenite, plagioclase, K-feldspar, kyanite, rutile and quartz. With conditions of 11-13 kbar at 860 °C.

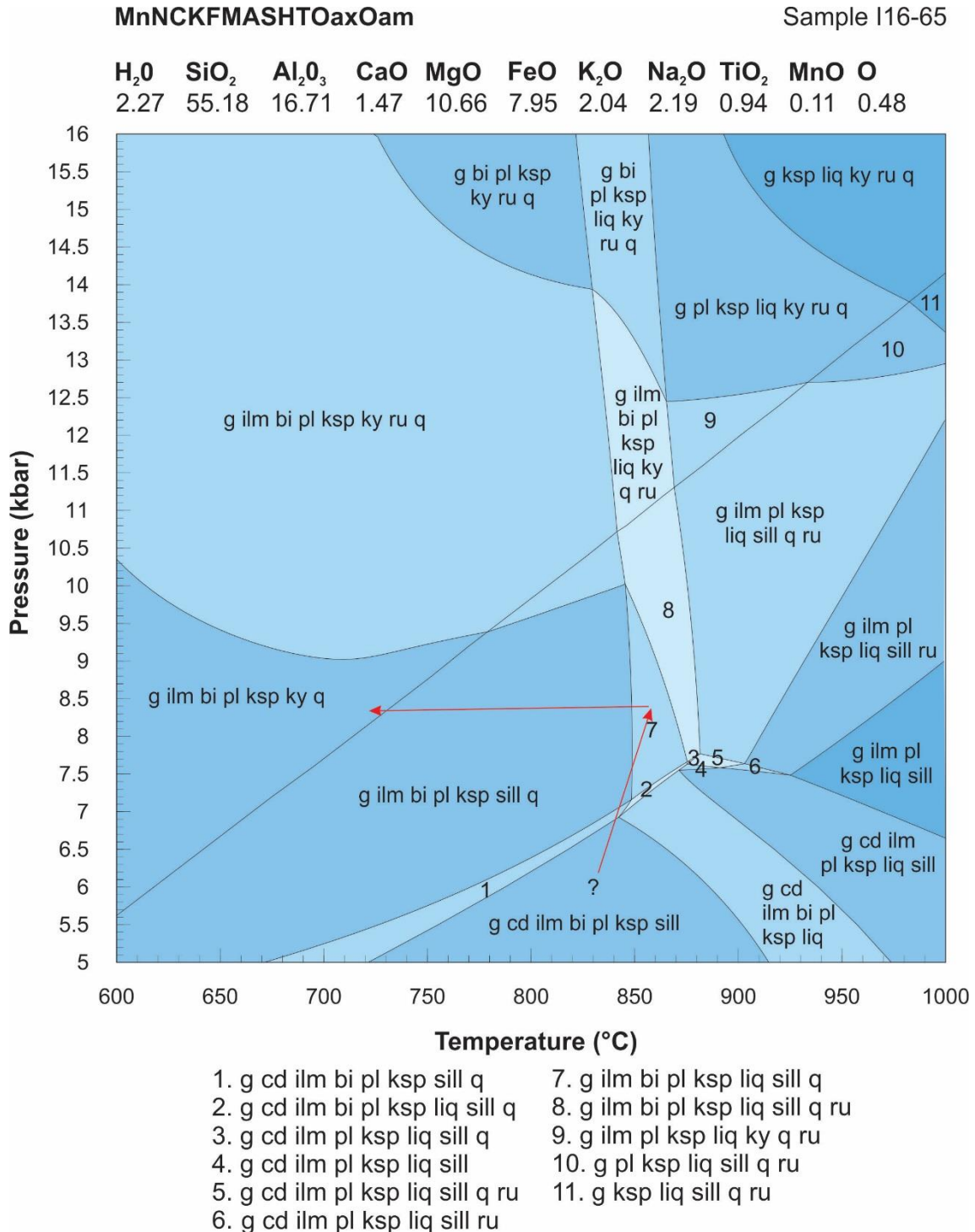


Figure 14: Calculated P-T pseudosection for sample I16-65 from the Mercara shear zone. Above the diagram expressed as Mole percent are the bulk composition used for modelling the diagram. The peak field is denoted with a 7, comprising of the composition, garnet, ilmenite, biotite, plagioclase, K-feldspar, liquid, sillimanite and quartz. With conditions of 7.5-9 Kbar at 850-860 °C.

MINERAL

CHEMISTRY

Electron microprobe analysis was completed upon the silicate minerals in samples I16-42 and I16-65. K-feldspar, plagioclase, biotite and garnet were analysed for their relative elemental abundance. This data was then used to further constrain P-T conditions via the implementation of compositional variable contours upon pseudosections. Compositional transects were completed upon garnets in both samples providing trends that show decreasing Mg from core to rim and increasing Mn from core to rim. See table 1 and 2.

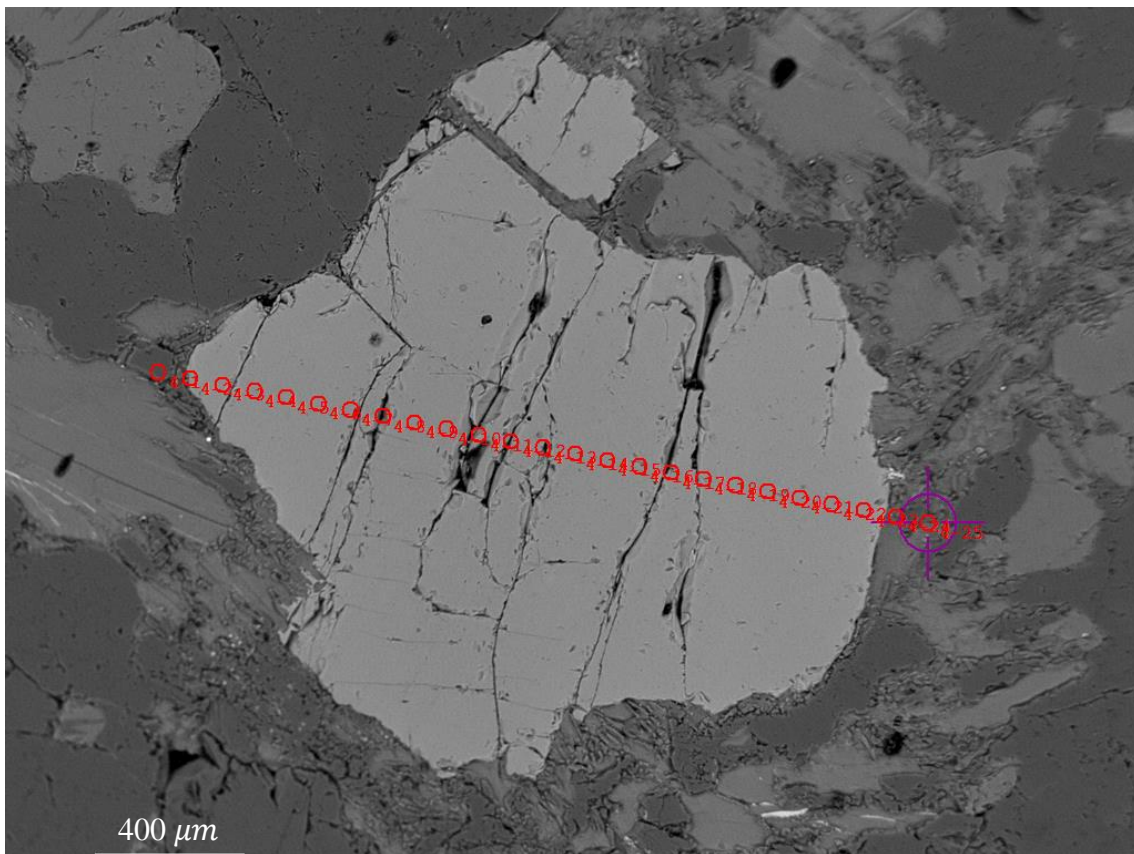


Figure 15: Microprobe image of element composition transect of garnet porphyroblast in sample I16-42. Camera error can be noted where probe spots (red) can be seen outside the fringe of the grain, yet the spots were taken upon the actual grain. Transect end-member cation values are seen in Table 1.

Mineral	K-Feldspar	Plagioclase	Biotite	Garnet rim	Garnet core
Sample	I16-42	I16-42	I16-42	I16-42	I16-42
SiO2	64.9089	61.5729	38.2285	38.315075	38.83683333
TiO2	0.05902	0	3.0665	0.010438	0.030271
Al2O3	18.4221	23.2315	16.3248	22.161125	22.41515
Cr2O3	0	0	0.211218	0.08689725	0.106737833
FeO	0.011635	0	6.53386	26.41345	24.45456667
MnO	0	0	0.010934	0.34065675	0.2832555
MgO	0.001245	0	20.6939	11.310825	12.26191667
ZnO	0.037307	0.013819	0.074936	0.00817075	0.0174555
CaO	0.039723	4.24142	0.042987	1.029081	0.915969
Na2O	1.0277	9.28994	0.080589	0.02807175	0.073220667
K2O	14.8465	0.221961	9.61654	0.004147	0.038318667
Cl	0.003041	0.006234	0.020616	0.005127	0.057011
F	0	0	0.920554	0.03390475	0.029895833
Total	99.36	98.58	95.43	99.73	99.50
End member variation					
Albite	0.095	0.789			
Anorthite	0.002	0.199			
Sanidine	0.903	0.012			
Almandine				0.548	0.512
Pyrope				0.418	0.458
Grossular				0.027	0.025
Spessartine				0.007	0.006
Xmg			0.850		

Table 1: Single mineral main oxide elemental abundance values for sample I16-42, minerals analysed K-feldspar, plagioclase, biotite, garnet core and garnet rim averages.

Mineral	Plagioclase	Biotite	Garnet rim	Garnet core
Sample	I16-65	I16-65	I16-65	I16-65
SiO ₂	67.2251	64.6363	39.2351	38.9550667
TiO ₂	0.016521	0.011939	0.007265	0.001084
Al ₂ O ₃	20.1591	21.9448	22.094	21.8980333
Cr ₂ O ₃	0	0	0.131193667	0.15326133
FeO	0.058731	0.085633	25.9786	26.1835667
MnO	0	0	0.651811667	0.65672467
MgO	0	0.042624	11.18826667	11.0998333
ZnO	0.01335	0.022294	0.017393667	0.01928867
CaO	1.06062	2.8391	0.666432	0.601412
Na ₂ O	11.2621	10.1801	0.020570333	0.01047167
K ₂ O	0.118001	0.092396	0.001469	0
Cl	0.00479	0.003405	0.003498667	0.008028
F	0	0	0.007547333	0.04994133
Total	99.92	99.86	100.00	99.61
End member variation				
Albite	0.944			
Anorthite	0.049			
Sanidine	0.007			
Almandine			0.548	0.552
Pyrope			0.420	0.417
Grossular			0.018	0.016
Spessartine			0.014	0.014
Xmg		0.470		

Table 2: Single mineral main oxide elemental abundance values for sample I16-65, minerals analysed, plagioclase, biotite, garnet core and garnet rim averages.

DISCUSSION

The aim of this study is to unravel the provenance and metamorphic history of the Coorg block and the Mercara shear zone, focussing on the metamorphic architecture and timings of metamorphism. Providing an insight into the regions tectonic evolution and furthermore tectonic implications during the Mesoarchean.

Age of metamorphism and Provenance of sedimentary protoliths

The U-Pb zircon ages recorded were classified as metamorphic and detrital, some displaying evidence of metamorphic overgrowth and metamictisation (Fig. 2) (Corfu et al., 2003). The U-Pb zircon results for khondalite samples I16-64, I16-65 and I16-66 describe Archean aged cores and rims, yet rims are seen further down the discordia line suffering radiogenic Pb loss (Fig. 3). I16-42 records an interesting distribution of ages with evidence supporting the monazite dated metamorphic event at 3.07 Ga, as the highest density of zircon ages is clustered at 3.1 Ga, see (Fig. 5). U-Pb zircons do provide compelling results that confirm the majority of concordant zircons lie between 3.1 Ga and 3.4 Ga. Coupled with a $^{207}\text{Pb}/^{206}\text{Pb}$ monazite weighted average age timed to 3.07 Ma, the interpretation that original detrital zircons are only seen before 3.07 Ga. Endorsing the interpretation of a Mesoarchean to Paleoarchean protolith from the Western Dharwar Craton peninsular gneiss (Peucat et al., 2013; Santosh et al., 2015). This is also the interpreted protolith for the Coorg block charnokites and metasedimentary rocks, (Peucat et al., 2013; Santosh et al., 2015). I16-42 records a metamorphism timing from $^{207}\text{Pb}/^{206}\text{Pb}$ monazite data of 3.07 Ga.

Pressure-Temperature-Time Evolution

Mineralogical and petrographic distinctions observed within thin section combined with compositional variations within garnet, biotite, plagioclase and K-feldspar provide information that can further describe and constrain the metamorphic conditions of the rocks in the northern and southern Mercara. In the southern Mercara khondalite sample I16-65, the peak assemblage estimates temperatures of 850-870°C at 7.5-9 kbar. The field outcrop suggested the *P-T* conditions had reached the solidus, as leucosomes were present. Petrographically cordierite is seen contacting peak assemblage minerals garnet, sillimanite, quartz and K-feldspar, while also containing inclusions of biotite. Suggesting that the rock briefly passed through the cordierite stability field during the prograde, yet exited the field before reaching its peak stability. Cordierite is not seen contacting biotite or sillimanite and does not form any part of the retrograde fabric.

Petrographically kyanite is only seen contacting biotite and sillimanite in weakly formed fabrics. It is observed to form in the outer sections of the fabric upon regularly contacting sillimanite. Which suggests the rock passed over the kyanite-sillimanite stability boundary during retrogression, leading to an interpretation of a near isobaric cooling process from 850°C to 600°C occurring at a faster rate than depressurisation. Leading to the interpretation of an anti-clockwise *P-T* path, (Fig. 16).

In the northern Mercara shear zone, Mercara gneiss sample I16-42 provides peak conditions of 860°C at 11-13kbar. *P-T* conditions had reached the solidus as leucosomes were present in the sample. Petrographically, sillimanite is seen as inclusions inside garnet, while also being a major fabric forming mineral in conjunction with biotite. Leading to the interpretation of sillimanite being stable during the prograde and

retrograde. Kyanite is observed contacting peak assemblage minerals, K-feldspar, plagioclase, quartz and garnet, with medium grain sizes, suggesting peak conditions allowed for the stable growth of kyanite. The dominant appearance of biotite in the fabric directs a retrogressive path at near-isothermal conditions from 11-13 kbar to 7kbar. Wholly leading to the interpretation of a clock-wise P - T path as seen in (Fig. 15).

U-Pb age data from monazites within the Mercara khondalites plot concordantly, I16-65 provides a $^{207}\text{Pb}/^{206}\text{Pb}$ weighted average value of 722 ± 25 Ma with an MSWD of 1.5. When combined with I16-66 they produce a $^{207}\text{Pb}/^{206}\text{Pb}$ weighted average of 676 ± 47 Ma with an MSWD of 1.2 (Fig. 9). This age is interpreted to reflect the timing of near peak metamorphic conditions, as monazites have been shown to grow in metapelites from 525°C (Corrie & Kohn, 2008; Wing et al., 2003). U-Pb age monazite data from Mercara gneiss sample (I16-42) preserves a weighted average age of 3071 ± 12 Ma, (MSWD =1.4), (Fig. 11b green). Suggesting that the metamorphism in the southern Mercara shear zone occurred at a much younger Neoproterozoic era, with traces from the Mesoarchean metamorphism evident. Meanwhile the northern Mercara shear zone had results suggesting a metamorphism event occurring during the early Mesoarchean, with a much less significant Neoproterozoic overprint.

Thermal Gradient and Tectonic Settings

The interpreted peak P - T conditions experienced by the Mercara gneiss and khondalite samples provide distinctly opposing results, making it hard to describe the Mercara shear zone as evidence of a single suturing event. The Mercara shear zone is commonly described as the domain in which evidence for the Coorg blocks amalgamation to the

Western Dharwar is contained (Ishwar-Kumar et al., In Press; Ishwar-Kumar et al., 2013; Rekha et al., 2014; Santosh et al., 2015). Variable suturing ages have been tested, 750 Ma (Ishwar-Kumar et al., 2013), 1.2 Ga (Ishwar-Kumar et al., In Press; Santosh et al., 2015) and 2.5 Ga (Rekha et al., 2014). The domain is most recently described as a 1.2 Ga collisional event, following ocean closure with a clockwise *P-T* path and associated major, trace and REE signatures representing arc magmatic rocks. This leads to the interpretation of the Coorg block as an exotic microcontinent containing subduction related magmatism (Ishwar-Kumar et al., In Press; Ishwar-Kumar et al., 2013; Santosh et al., 2015). This study provides evidence according to a $^{207}\text{Pb}/^{206}\text{Pb}$ weighted average value in the southern Mercara shear zone for a 722 ± 25 Ma metamorphic event with an anti-clockwise *P-T* path. THERMOCALC calculations describe peak *P-T* conditions of 850-870°C at 7.5-9 kbar with near-isobaric cooling from 850-600°C, possibly describing a long lived metamorphic event (Kelsey & Hand, 2015). An apparent thermal gradient describes Barrovian conditions of 95.5 – 114.6°C/kbar interpreted as regional evidence for an extensional environment (Brown, 2007, 2014; Kelsey & Hand, 2015), associated with nearby granite and gabbro intrusions (Deeju et al.; Santosh et al., 2014). The intrusions are described as middle Neoproterozoic intraplate magmatism occurring in response to decompression melting of the mantle, melting of the crust and magma mixing (Deeju et al.; Santosh et al., 2014). Dated with a $^{206}\text{Pb}/^{238}\text{U}$ weighted mean range from 715 ± 4 to 832.5 ± 5 Ma. This is interpreted as the timing of emplacement, considered to be coeval with the peak metamorphism of the southern Mercara khondalites. A similar setting is described on the west coast of India in the Dharmapuri rift zone (Renjith et al., 2016), as well as in the younger environment in the Hidaka metamorphic belt, Japan.

Where near-isobaric granulite cooling conditions are linked to mafic magma under-accretion and lithospheric thinning, (A. I. S. Kemp et al., 2007).

Meanwhile P - T - t evolution in the northern Mercara provides evidence for a metamorphic event occurring at a $^{207}\text{Pb}/^{206}\text{Pb}$ weighted average value of 3017 ± 12 Ma. THERMOCALC calculations describe peak P - T conditions of 860°C at 11-13kbar with an apparent thermal gradient describing Barrovian conditions of $71.66 - 78.18^\circ\text{C}/\text{kbar}$. The event describes a clock-wise P - T path with near iso-thermal retrogression conditions. Indicative of the characteristics of a convergent setting, similarly comparable to that postulated by (Amaldev et al., 2016). Clockwise P - T paths are commonly associated with convergent tectonic settings, (Brown, 2007; Kukkonen & Lauri, 2009; Sizova et al., 2014). This challenges the current thought of Mesoarchaeon tectonic regimes of Brown (2014). Associated nearby metagabbro magmatism is thought have experience coeval emplacement with the peak metamorphism of I16-42, recording a metamorphic event from igneous zircon rims with a $^{207}\text{Pb}/^{206}\text{Pb}$ weighted mean age of 3021 ± 57 Ma (MSWD = 2.4), and a core weighted mean $^{207}\text{Pb}/^{206}\text{Pb}$ age of 3229 ± 80 Ma (MSWD = 4.0) (Amaldev et al., 2016). Yet the study only provides conventional thermobarometric techniques for constraining P - T conditions. Such conditions provide metapelite gneiss peak conditions in the range of 5.5 kbar at 600°C to 10 kbar at 800°C , and metagabbro peak conditions of 10 kbar at 700°C to 12 kbar at 900°C . Similar to the results found in this study of 860°C at 11-13kbar, with a common petrographic based interpretation of a clock-wise P - T path.

This latter metamorphic event dated to 3071 ± 12 Ma, has been interpreted to describe conditions not before seen during the Mesoarchaeon. This provides evidence for a

contractional tectonic environment with peak pressures of 11-13kbar followed by rapid exhumation defined by an isothermal retrogressive P - T path. These conditions are not expected with stagnant lid convection theory (Brown, 2014; Kemp et al., 2010; Reese et al., 1998). The theory describes conditions where an immobile lithosphere (stagnant lid) sits above a convective layer. The convection is reported to periodically bring up bursts of new melt, recycling and replenishing the lid as a result of asthenospheric mantle overturn. Supported by 2D geodynamic modelling, (Brown, 2014; Griffin et al., 2014; Johnson et al., 2014; Kemp et al., 2010; Sizova et al., 2014).

Numerical modelling studies have suggested that the transition from a stagnant lid regime to the beginning of plate tectonics is marked by Rayleigh-Taylor instabilities becoming inefficient as a declining mantle potential temperature reaches 1550-1500°C, (Brown, 2014; Herzberg et al., 2010; Johnson et al., 2014; Sizova et al., 2014). The transition to steep slab subduction then occurred during the late Archaean to early Paleoproterozoic, (Brown, 2014). Data sets from this period present intense magmatism, perhaps reflecting continued mantle overturns, (Griffin et al., 2014). These postulated mantle overturns possibly describe the dynamics of early crustal growth, first postulated by (Naeraa et al., 2012). Stating that large volumes of highly depleted buoyant sub-continental lithospheric mantle (SCLM), provide “life rafts” to preserve newly formed crust. However in a crustal system indicated to support greater mantle heat flow and increased radiogenic crustal heat production. The Archean lithosphere may still have been too weak to support any significant crustal thickening (Rey & Houseman, 2006; Sizova, 2010; Sizova et al., 2014). In contrast to this the high- P rocks recorded here provide a rare insight into the presence of continental crustal thicknesses of up to 40km thick during the early Mesoarchean. Such

levels of crustal thickening imply conditions consistent with early plate tectonics, conditions not yet previously recorded from rocks of such antiquity.

CONCLUSIONS

Integrated U-Pb geochronological data and forward modelled phase diagrams in this study present a first insight into the conditions preserved in the Mesoarchean metamorphic rocks found in the Mercara shear zone, Coorg block, India.

- Mesoarchaean to Paleoproterozoic protolith from the Western Dharwar Craton peninsular gneiss/Coorg block.
- Two metamorphic events recorded by U-Pb monazites, southern Mercara samples record event at 676 ± 47 Ma. Northern Mercara samples records event at 3071 ± 12 Ma.
- Conditions of Neoproterozoic metamorphism interpreted to be an anti-clockwise *P-T* path, with peak metamorphism at 7.5-9 Kbar at 850-860 °C. representing a crustal scale extensional tectonic environment.
- Conditions of early Mesoarchean metamorphism interpreted to be a clock-wise *P-T* path with peak metamorphism at 11-13 Kbar at 860°C, consistent with a convergent setting. Conditions have not been previously reported from rocks of this antiquity.

ACKNOWLEDGMENTS

A big thank you goes out to my supervisors Alan Collins and David Kelsey, for their dedication of time and guidance throughout the year. M. Santosh and E. Shaji are thanked for their hospitality, logistical support and guidance through fieldwork. Laura Morrissey, Naomi Tucker and Brandon Alessio are also thanked for their continued support with THERMOCALC. Sheree Armistead is thanked for her support in the field and the office. Ben Wade, Aoife McFadden and Adelaide microscopy are thanked for their assistance and troubleshooting support with all instruments. Finally a big thanks to Katie and everyone in 211, for all the help and humour that made this year go so fast.

REFERENCES

- Amaldev, T., Santosh, M., Tang, L., Baiju, K. R., Tsunogae, T., & Satyanarayanan, M. (2016). Mesoarchean convergent margin processes and crustal evolution: Petrologic, geochemical and zircon U–Pb and Lu–Hf data from the Mercara Suture Zone, southern India. *Gondwana Research*, 37, 182-204. doi: <http://dx.doi.org/10.1016/j.gr.2016.05.017>
- Anderson, J. R., Kelsey, J. L. P. D. E., Collins, M. H. A. S., & Santosh, M. (2012). High-pressure granulites at the dawn of the Proterozoic. *Geological society of America*, V. 40(no. 5), pp 431-434.
- Brown, M. (2007). Metamorphism, Plate Tectonics, and the Supercontinent Cycle. *Earth Science Frontiers*, 14(1), 1-18. doi: [http://dx.doi.org/10.1016/S1872-5791\(07\)60001-3](http://dx.doi.org/10.1016/S1872-5791(07)60001-3)
- Brown, M. (2014). The contribution of metamorphic petrology to understanding lithosphere evolution and geodynamics. *Geoscience Frontiers*, 5(4), 553-569. doi: <http://dx.doi.org/10.1016/j.gsf.2014.02.005>
- Collins, A. S., Reddy, S. M., Buchan, C., & Mruma, A. (2004). Temporal constraints on Palaeoproterozoic eclogite formation and exhumation (Usagaran Orogen, Tanzania). *Earth and Planetary Science Letters*, 224, 175-192.
- Corfu, F., Hanchar, J. M., Hoskin, P. W. O., & Kinny, P. (2003). Atlas of Zircon Textures. *Reviews in Mineralogy and Geochemistry*, 53(1), 469.
- Corrie, S. L., & Kohn, M. J. (2008). Trace-element distributions in silicates during prograde metamorphic reactions: implications for monazite formation. *Journal of Metamorphic Geology*, 26(4), 451-464. doi: 10.1111/j.1525-1314.2008.00769.x
- Deeju, T. R., Santosh, M., Yang, Q.-Y., Pradeepkumar, A. P., & Shaji, E. Mid-Neoproterozoic intraplate magmatism in the northern margin of the Southern Granulite Terrane, India: Constraints from geochemistry, zircon U-Pb geochronology and Lu-Hf isotopes. *Journal of Asian Earth Sciences*. doi: <http://dx.doi.org/10.1016/j.jseaes.2016.06.016>
- Devaraju, J. J., A. S. . (2004). Metamorphic history of staurolite-kyanite-garnet-cordierite-bearing pelites of Mangalore-Mercara lineament, South India. *JOURNAL OF THE GEOLOGICAL SOCIETY OF INDIA*, 63(5), 555-561.
- Griffin, W. L., Belousova, E. A., O'Neill, C., O'Reilly, S. Y., Malkovets, V., Pearson, N. J., . . . Wilde, S. A. (2014). The world turns over: Hadean–Archean crust–mantle evolution. *Lithos*, 189, 2-15. doi: <http://dx.doi.org/10.1016/j.lithos.2013.08.018>
- Herzberg, C., Condie, K., & Korenaga, J. (2010). Thermal history of the Earth and its petrological expression. *Earth and Planetary Science Letters*, 292(1–2), 79-88. doi: <http://dx.doi.org/10.1016/j.epsl.2010.01.022>
- Holland, T. J. B., & Powell, R. (2011). An improved and extended internally consistent thermodynamic dataset for phases of petrological interest, involving a new equation of state for solids. *Journal of Metamorphic Geology*, 29(3), 333-383. doi: 10.1111/j.1525-1314.2010.00923.x
- Ishwar-Kumar, C., Santosh, M., Wilde, S. A., Tsunogae, T., Itaya, T., Windley, B. F., & Sajeew, K. (In Press). Mesoproterozoic suturing of Archean crustal blocks in

- western peninsular India: Implications for India–Madagascar correlations. *Lithos*. doi: <http://dx.doi.org/10.1016/j.lithos.2016.01.016>
- Ishwar-Kumar, C., Windley, B. F., Horie, K., Kato, T., Hokada, T., Itaya, T., . . . Sajeew, K. (2013). A Rodinian suture in western India: New insights on India–Madagascar correlations. *Precambrian Research*, 236, 227–251. doi: <http://dx.doi.org/10.1016/j.precamres.2013.07.023>
- Jackson, S. E., Pearson, N. J., Griffin, W. L., & Belousova, E. A. (2004). The application of laser ablation-inductively coupled plasma-mass spectrometry to in situ U–Pb zircon geochronology. *Chemical Geology*, 211(1–2), 47–69. doi: <http://dx.doi.org/10.1016/j.chemgeo.2004.06.017>
- Johnson, T. E., Brown, M., Kaus, B. J. P., & VanTongeren, J. A. (2014). Delamination and recycling of Archaean crust caused by gravitational instabilities. *Nature Geosci*, 7(1), 47–52. doi: 10.1038/ngeo2019
<http://www.nature.com/ngeo/journal/v7/n1/abs/ngeo2019.html#supplementary-information>
- Kelsey, D. E., & Hand, M. (2015). On ultrahigh temperature crustal metamorphism: Phase equilibria, trace element thermometry, bulk composition, heat sources, timescales and tectonic settings. *Geoscience Frontiers*, 6(3), 311–356. doi: <http://dx.doi.org/10.1016/j.gsf.2014.09.006>
- Kemp, Wilde, S. A., Hawkesworth, C. J., Coath, C. D., Nemchin, A., Pidgeon, R. T., . . . DuFrane, S. A. (2010). Hadean crustal evolution revisited: New constraints from Pb–Hf isotope systematics of the Jack Hills zircons. *Earth and Planetary Science Letters*, 296(1–2), 45–56. doi: <http://dx.doi.org/10.1016/j.epsl.2010.04.043>
- Kemp, A. I. S., Shimura, T., Hawkesworth, C. J., & EIMF. (2007). Linking granulites, silicic magmatism, and crustal growth in arcs: Ion microprobe (zircon) U–Pb ages from the Hidaka metamorphic belt, Japan. *Geology*, 35(9), 807–810. doi: 10.1130/g23586a.1
- Kukkonen, I. T., & Lauri, L. S. (2009). Modelling the thermal evolution of a collisional Precambrian orogen: High heat production migmatitic granites of southern Finland. *Precambrian Research*, 168(3–4), 233–246. doi: <http://dx.doi.org/10.1016/j.precamres.2008.10.004>
- Ludwig, K. R. (2009). Isoplot 3.0.
- Meißner, B., Deters, P., Srikantappa, C., & Köhler, H. (2002). Geochronological evolution of the Moyar, Bhavani and Palghat shear zones of southern India: implications for east Gondwana correlations. *Precambrian Research*, 114(1–2), 149–175. doi: [http://dx.doi.org/10.1016/S0301-9268\(01\)00222-4](http://dx.doi.org/10.1016/S0301-9268(01)00222-4)
- Möller, A., O’Brien, P. J., Kennedy, A., & Kröner, A. (2003). Linking growth episodes of zircon and metamorphic textures to zircon chemistry: an example from the ultrahigh-temperature granulites of Rogaland (SW Norway). *Geological Society, London, Special Publications*, 220(1), 65–81. doi: 10.1144/gsl.sp.2003.220.01.04
- Naeraa, T., Schersten, A., Rosing, M. T., Kemp, A. I. S., Hoffmann, J. E., Kokfelt, T. F., & Whitehouse, M. J. (2012). Hafnium isotope evidence for a transition in the dynamics of continental growth 3.2[thinsp]Gyr ago. *Nature*, 485(7400), 627–630. doi:

- <http://www.nature.com/nature/journal/v485/n7400/abs/nature11140.html#supplementary-information>
- Payne, J. e. a. (2010). Pitfalls of classifying ancient magmatic suites with tectonic discrimination diagrams: An example from the Paleoproterozoic Tunkillia Suite, southern Australia. *Precambrian Research*, 177(3–4), 227-240. doi: <http://dx.doi.org/10.1016/j.precamres.2009.12.005>
- Payne, J. L., Ferris, G., Barovich, K. M., & Hand, M. (2010). Pitfalls of classifying ancient magmatic suites with tectonic discrimination diagrams: An example from the Paleoproterozoic Tunkillia Suite, southern Australia. *Precambrian Research*, 177(3–4), 227-240. doi: <http://dx.doi.org/10.1016/j.precamres.2009.12.005>
- Payne, J. L., Hand, M., Barovich, K. M., & Wade, B. P. (2008). Temporal constraints on the timing of high-grade metamorphism in the northern Gawler Craton: implications for assembly of the Australian Proterozoic. *Australian Journal of Earth Sciences*, 55(5), 623-640. doi: 10.1080/08120090801982595
- Peucat, J.-J., Jayananda, M., Chardon, D., Capdevila, R., Fanning, C. M., & Paquette, J.-L. (2013). The lower crust of the Dharwar Craton, Southern India: Patchwork of Archean granulitic domains. *Precambrian Research*, 227, 4-28. doi: <http://dx.doi.org/10.1016/j.precamres.2012.06.009>
- Powell, R., & Holland, T. J. B. (1988). An internally consistent dataset with uncertainties and correlations: 3. Applications to geobarometry, worked examples and a computer program. *Journal of Metamorphic Geology*, 6(2), 173-204. doi: 10.1111/j.1525-1314.1988.tb00415.x
- Powell, R., White, R. W., Green, E. C. R., Holland, T. J. B., & Diener, J. F. A. (2014). On parameterizing thermodynamic descriptions of minerals for petrological calculations. *Journal of Metamorphic Geology*, 32(3), 245-260. doi: 10.1111/jmg.12070
- Reese, C. C., Solomatov, V. S., & Moresi, L. N. (1998). Heat transport efficiency for stagnant lid convection with dislocation viscosity: Application to Mars and Venus. *Journal of Geophysical Research: Planets*, 103(E6), 13643-13657. doi: 10.1029/98JE01047
- Rekha, S., Bhattacharya, A., & Chatterjee, N. (2014). Tectonic restoration of the Precambrian crystalline rocks along the west coast of India: Correlation with eastern Madagascar in East Gondwana. *Precambrian Research*, 252, 191-208. doi: 10.1016/j.precamres.2014.07.013
- Renjith, M. L., Santosh, M., Li, T., Satyanarayanan, M., Korakoppa, M. M., Tsunogae, T., . . . Nirmal Charan, S. (2016). Zircon U–Pb age, Lu–Hf isotope, mineral chemistry and geochemistry of Sundamalai peralkaline pluton from the Salem Block, southern India: Implications for Cryogenian adakite-like magmatism in an aborted-rift. *Journal of Asian Earth Sciences*, 115, 321-344. doi: <http://dx.doi.org/10.1016/j.jseaes.2015.10.001>
- Rey, P. F., & Houseman, G. (2006). Lithospheric scale gravitational flow: the impact of body forces on orogenic processes from Archaean to Phanerozoic. *Geological Society, London, Special Publications*, 253(1), 153-167. doi: 10.1144/gsl.sp.2006.253.01.08
- Samuel, V. O., Santosh, M., Liu, S., Wang, W., & Sajeev, K. (2014). Neoproterozoic continental growth through arc magmatism in the Nilgiri Block, southern

- India. *Precambrian Research*, 245, 146-173. doi:
<http://dx.doi.org/10.1016/j.precamres.2014.02.002>
- Santosh, M., Yang, Q.-Y., Ram Mohan, M., Tsunogae, T., Shaji, E., & Satyanarayanan, M. (2014). Cryogenian alkaline magmatism in the Southern Granulite Terrane, India: Petrology, geochemistry, zircon U–Pb ages and Lu–Hf isotopes. *Lithos*, 208–209, 430-445. doi:
<http://dx.doi.org/10.1016/j.lithos.2014.09.016>
- Santosh, M., Yang, Q.-Y., Shaji, E., Tsunogae, T., Mohan, M. R., & Satyanarayanan, M. (2015). An exotic Mesozoic microcontinent: The Coorg Block, southern India. *Gondwana Research*, 27(1), 165-195. doi:
<http://dx.doi.org/10.1016/j.gr.2013.10.005>
- Sizova, E. (2010). Subduction styles in the Precambrian: Insight from numerical experiments. *Lithos*, 116(3–4), 209-229. doi:
<http://dx.doi.org/10.1016/j.lithos.2009.05.028>
- Sizova, E., Gerya, T., & Brown, M. (2014). Contrasting styles of Phanerozoic and Precambrian continental collision. *Gondwana Research*, 25(2), 522-545. doi:
<http://dx.doi.org/10.1016/j.gr.2012.12.011>
- Srikantappa, C., Venugopal, L., Devaraju, J., & Basavalingu, B. (1994). P-T conditions of metamorphism and fluid inclusion characteristics of the Coorg granulites, Karnataka. *Journal - Geological Society of India*, 44(5), 495-504.
- Sunil, P. S., Radhakrishna, M., Kurian, P. J., Murty, B. V. S., Subrahmanyam, C., Nambiar, C. G., . . . Mohan, S. K. (2010). Crustal structure of the western part of the Southern Granulite Terrain of Indian Peninsular Shield derived from gravity data. *Journal of Asian Earth Sciences*, 39(6), 551-564. doi:
<http://dx.doi.org/10.1016/j.jseaes.2010.04.028>
- Tucker, N. M., Hand, M., Kelsey, D. E., & Dutch, R. A. (2015). A duality of timescales: Short-lived ultrahigh temperature metamorphism preserving a long-lived monazite growth history in the Grenvillian Musgrave–Albany–Fraser Orogen. *Precambrian Research*, 264, 204-234. doi:
<http://dx.doi.org/10.1016/j.precamres.2015.04.015>
- Van Acherterbergh, E., Ryan, C., Jackson, S., & Griffin, W. (2001). Data reduction software for LA-ICP-MS. *Laser-Ablation-ICPMS in the earth sciences—principles and applications. Miner Assoc Can (short course series)*, 29, 239-243.
- Wan, Y., Liu, D., Dong, C., Liu, S., Wang, S., & Yang, E. (2011). U–Th–Pb behavior of zircons under high-grade metamorphic conditions: A case study of zircon dating of meta-diorite near Qixia, eastern Shandong. *Geoscience Frontiers*, 2(2), 137-146. doi: <http://dx.doi.org/10.1016/j.gsf.2011.02.004>
- White, A. J. R., & Chappell, B. W. (1983). Granitoid types and their distribution in the Lachlan Fold Belt, southeastern Australia. *Geological Society of America Memoirs*, 159, 21-34. doi: 10.1130/MEM159-p21
- White, R. W., Powell, R., Holland, T. J. B., Johnson, T. E., & Green, E. C. R. (2014). New mineral activity–composition relations for thermodynamic calculations in metapelitic systems. *Journal of Metamorphic Geology*, 32(3), 261-286. doi: 10.1111/jmg.12071
- Wing, B. A., Ferry, J. M., & Harrison, T. M. (2003). Prograde destruction and formation of monazite and allanite during contact and regional

metamorphism of pelites: petrology and geochronology. *Contributions to Mineralogy and Petrology*, 145(2), 228-250. doi: 10.1007/s00410-003-0446-1

APPENDIX A: WHOLE ROCK GEOCHEMISTRY VIA XRF

WHOLE ROCK GEOCHEMICAL ANALYSES

SAMPLE	I16-42	I16-64	I16-65	I16-66	I16-73	I16-74
Major elements (wt%)						
Fe ₂ O ₃	5.1	8.18	6.64	5.55	11.89	0.61
SiO ₂	63.83	56.59	49.62	66.11	49.33	75.16
Al ₂ O ₃	21.3	18.8	25.5	15.7	13.8	14
CaO	0.48	1.01	1.24	0.26	9.68	1.1
MgO	3.85	6.43	6.43	6	6.17	0.13
MnO	0.07	0.18	0.11	0.08	0.2	<0.01
P	0.005	0.004	0.002	0.004	0.037	0.01
S	0.004	0.149	0.218	0.013	0.076	<0.001
K ₂ O	1.54	2.32	2.88	1.47	0.27	3.65
Na ₂ O	0.5	1.49	2.03	0.77	1.56	2.31
TiO ₂	0.74	0.81	1.13	0.82	1.18	0.06
Ba	0.026	0.047	0.066	0.033	0.015	0.076
total	97.445	96.01	95.866	96.81	94.208	97.106
LOI	0.21	0.47	0.56	0.51	1.46	1.78

APPENDIX B: ZIRCON STANDARDS

Analysis	Pb ²⁰⁷ /Pb ²⁰⁶	1σ	Pb ²⁰⁶ /U ²³⁸	1σ	Pb ²⁰⁷ /U ²³⁸	1σ	Pb ²⁰⁸ /Th ²³²	1σ	% Conc	Pb ²⁰⁷ /U ²³⁵	1σ	Pb ²⁰⁶ /U ²³⁸	1σ	Pb ²⁰⁸ /Th ²³²	1σ	Pb ²⁰⁷ /Pb ²⁰⁶	1σ
GJ Zircon standard																	
I16-42																	
Z_GJ1_0	0.062	0.0025	0.1768	0.0033	1.527	0.06	0.058	0.007	173.2	933	24	1048	18	1110	140	605	84
Z_GJ1_1	0.063	0.0024	0.1482	0.0028	1.305	0.04	0.056	0.008	136.3	841	19	890	16	1100	150	653	79
Z_GJ1_2	0.06	0.0025	0.1074	0.0021	0.892	0.03	0.043	0.006	124.6	642	18	659	12	840	120	529	87
Z_GJ1_3	0.061	0.0024	0.0993	0.0021	0.837	0.03	0.041	0.006	107.2	614	17	610	12	820	120	569	83
Z_GJ1_5	0.063	0.0024	0.0957	0.0018	0.834	0.03	0.041	0.005	90.77	613	15	590	10	800	100	650	79
Z_GJ1_6	0.065	0.0026	0.0922	0.0019	0.831	0.03	0.044	0.006	79.33	608	17	568	11	850	110	716	84
Z_GJ1_7	0.06	0.0024	0.0945	0.0019	0.789	0.03	0.035	0.005	110	586	18	582	11	700	110	529	84
Z_GJ1_8	0.059	0.0022	0.0943	0.0019	0.78	0.03	0.003	0.006	117.6	581	17	580	11	50	120	493	79
Z_GJ1_9	0.062	0.0023	0.0931	0.002	0.794	0.03	-0.03	0.006	94.71	591	16	573	12	-720	120	605	81
Z_GJ1_10	0.059	0.0023	0.0913	0.0019	0.755	0.03	0.031	0.005	109.5	566	16	563	11	600	97	514	82
Z_GJ1_11	0.062	0.0024	0.0968	0.0022	0.838	0.03	-0.09	0.012	96.91	611	18	595	13	-2010	260	614	83
Z_GJ1_12	0.06	0.0025	0.0972	0.0022	0.801	0.03	-0.21	0.014	112.6	591	17	597	13	-4940	370	530	86
Z_GJ1_13	0.057	0.0026	0.0953	0.002	0.748	0.03	0.031	0.005	142.6	560	18	586	12	610	100	411	92
Z_GJ1_14	0.046	0.0027	0.0941	0.0021	0.607	0.04	0.029	0.005	1930	472	22	579	13	570	100	30	100
Z_GJ1_15	0.06	0.0025	0.0959	0.002	0.791	0.03	0.035	0.006	112.6	588	18	590	12	680	110	524	85
Z_GJ1_16	0.061	0.0025	0.0933	0.002	0.79	0.03	0.039	0.005	98.8	587	17	575	12	756	98	582	85
Z_GJ1_17	0.06	0.0024	0.096	0.0024	0.773	0.03	0.034	0.006	109.3	576	16	590	14	650	110	540	83
Z_GJ1_18	0.061	0.0027	0.091	0.002	0.771	0.03	0.039	0.006	99.64	574	18	561	12	770	110	563	91
Z_GJ1_19	0.062	0.0025	0.0941	0.0021	0.813	0.03	0.046	0.007	95.54	597	18	579	13	900	130	606	88
Z_GJ1_20	0.058	0.0026	0.0938	0.002	0.754	0.03	0.036	0.005	126	564	19	577	12	700	100	458	93
Z_GJ1_21	0.059	0.0026	0.0937	0.0025	0.751	0.03	0.028	0.006	114	565	19	578	15	550	110	507	95
Z_GJ1_22	0.062	0.0027	0.0917	0.002	0.78	0.03	0.034	0.005	97.25	579	19	565	12	670	100	581	89
Z_GJ1_23	0.062	0.0028	0.0905	0.0021	0.788	0.03	0.035	0.005	94.1	584	18	558	12	662	94	593	90
Z_GJ1_24	0.059	0.0025	0.0963	0.0021	0.771	0.03	-0.14	0.012	121.2	574	17	594	13	-3190	290	490	90
Z_GJ1_25	0.057	0.0026	0.0926	0.0021	0.729	0.03	0.033	0.005	138	551	19	570	13	640	100	413	95

William Mansfield
Metamorphic evolution of the Mercara Shear Zone

Z_GJ1_26	0.064	0.0025	0.0898	0.0019	0.8	0.03	0.033	0.005	82.44	593	17	554	11	643	93	672	82
Z_GJ1_27	0.059	0.0024	0.0987	0.0021	0.815	0.03	0.037	0.006	116.5	599	17	606	12	720	120	520	83
Z_GJ1_28	0.061	0.0025	0.1014	0.0024	0.846	0.03	0.04	0.006	111.3	619	17	622	14	780	110	559	86
Z_GJ1_29	0.061	0.0028	0.0967	0.0022	0.816	0.04	0.041	0.006	107	598	20	594	13	800	110	555	92
Z_GJ1_30	0.059	0.0024	0.0955	0.0021	0.784	0.03	0.043	0.007	115.7	582	17	588	12	840	130	508	84
Z_GJ1_31	0.062	0.0026	0.0937	0.002	0.806	0.03	0.032	0.005	96.65	596	19	577	12	630	100	597	88
Z_GJ1_32	0.06	0.0024	0.0918	0.0022	0.773	0.03	0.037	0.005	100.9	577	18	567	13	723	91	562	90
Z_GJ1_33	0.059	0.0025	0.0943	0.0021	0.758	0.03	0.031	0.005	119.3	567	17	580	12	608	99	486	88
Z_GJ1_34	0.061	0.0025	0.0925	0.0021	0.781	0.03	0.037	0.005	98.45	580	17	570	12	720	100	579	87
Z_GJ1_35	0.059	0.0025	0.1074	0.0022	0.886	0.03	0.052	0.007	124	642	19	657	13	1010	120	530	90
Z_GJ1_36	0.061	0.0027	0.1093	0.0027	0.926	0.04	0.038	0.006	111.7	660	20	668	16	740	110	598	92
Z_GJ1_37	0.062	0.0025	0.1026	0.002	0.9	0.04	0.031	0.005	99.84	647	19	629	12	617	93	630	86
Z_GJ1_38	0.064	0.0029	0.1016	0.0023	0.896	0.04	0.036	0.006	94.39	642	19	623	14	700	110	660	87
Z_GJ1_39	0.061	0.0028	0.0977	0.0023	0.823	0.03	0.039	0.006	107	605	19	600	14	760	110	561	94
Z_GJ1_40	0.061	0.0029	0.0964	0.0023	0.804	0.03	0.039	0.005	109.4	596	20	593	13	780	110	542	97
Z_GJ1_41	0.061	0.0025	0.0979	0.0017	0.824	0.03	0.032	0.005	106.7	605	17	603	11	628	97	565	86
Z_GJ1_42	0.061	0.0025	0.0953	0.0021	0.791	0.03	0.038	0.005	105.2	588	17	586	12	750	100	557	85
Z_GJ1_43	0.062	0.0025	0.1059	0.0022	0.915	0.04	0.033	0.005	108.2	654	20	650	13	650	100	601	85
Z_GJ1_44	0.062	0.0027	0.106	0.0025	0.914	0.04	0.027	0.005	105.7	656	20	649	15	549	98	614	93
Z_GJ1_45	0.061	0.0024	0.1017	0.0022	0.853	0.03	0.033	0.005	108.7	627	18	624	13	648	92	574	83
Z_GJ1_46	0.064	0.0028	0.0985	0.0021	0.865	0.03	0.035	0.005	89.63	631	19	605	12	690	100	675	94
Z_GJ1_47	0.062	0.0028	0.0995	0.0022	0.849	0.03	0.037	0.005	102.2	618	18	611	13	733	95	598	92
Z_GJ1_48	0.06	0.0024	0.0958	0.0021	0.81	0.03	0.033	0.005	103.3	599	17	589	12	640	100	570	86
Z_GJ1_49	0.059	0.0027	0.0959	0.0024	0.781	0.03	0.034	0.006	115.5	581	20	589	14	660	110	510	96
Z_GJ1_50	0.06	0.0027	0.0977	0.0021	0.815	0.03	0.031	0.005	110.7	603	19	601	12	630	100	543	93
Z_GJ1_51	0.062	0.0026	0.1055	0.0025	0.907	0.04	0.035	0.005	105.9	651	20	646	14	680	100	610	85
Z_GJ1_52	0.063	0.0029	0.1104	0.0025	0.939	0.04	0.025	0.005	108.3	667	20	675	15	495	88	623	93
Z_GJ1_53	0.059	0.0026	0.1035	0.0025	0.845	0.03	0.037	0.005	128.6	615	19	634	15	710	100	493	90
Z_GJ1_54	0.063	0.0028	0.0985	0.0023	0.854	0.03	0.028	0.005	93.8	625	19	605	14	560	100	645	95
Z_GJ1_55	0.061	0.0026	0.0986	0.0024	0.814	0.03	0.031	0.005	109.8	604	17	605	14	612	91	551	89

William Mansfield
Metamorphic evolution of the Mercara Shear Zone

Z_GJ1_56	0.06	0.0025	0.0988	0.0023	0.828	0.03	-0.14	0.012	110.4	606	18	607	14	-3160	280	550	88
Z_GJ1_57	0.064	0.0031	0.0993	0.002	0.883	0.04	-0.27	0.019	93.13	635	20	610	12	-6770	550	655	94
Z_GJ1_58	0.064	0.0029	0.0991	0.0019	0.878	0.04	0.035	0.005	93.84	633	19	609	11	676	94	649	96
Z_GJ1_59	0.061	0.0022	0.1017	0.0022	0.858	0.03	0.027	0.004	106.3	626	16	624	13	540	85	587	76
Z_GJ1_60	0.061	0.0023	0.1055	0.0022	0.867	0.03	0.025	0.004	114.1	628	17	646	13	495	81	566	81
Z_GJ1_61	0.062	0.0024	0.098	0.0021	0.833	0.03	0.032	0.005	100.7	610	17	602	12	627	89	598	84
Z_GJ1_62	0.06	0.0023	0.0928	0.0023	0.767	0.03	0.03	0.005	104.4	578	15	572	13	588	92	548	80
Z_GJ1_63	0.062	0.0026	0.0943	0.0021	0.805	0.03	0.025	0.004	97.64	594	17	580	13	482	84	594	89
Z_GJ1_64	0.062	0.0027	0.0948	0.0022	0.809	0.04	0.033	0.005	100.9	594	20	583	13	643	88	578	91
Z_GJ1_65	0.059	0.003	0.0936	0.0021	0.747	0.03	0.031	0.006	125.2	562	18	576	12	600	110	460	100
Z_GJ1_66	0.041	0.0023	0.0925	0.0022	0.529	0.03	0.029	0.004	-365	426	20	570	13	573	84	-156	93
Z_GJ1_67	0.061	0.0025	0.1013	0.0022	0.854	0.03	0.038	0.006	104.5	625	17	622	13	740	110	595	86
Z_GJ1_68	0.061	0.0024	0.1024	0.0023	0.864	0.03	0.037	0.005	108.7	627	17	628	14	734	95	578	82
Z_GJ1_69	0.061	0.0024	0.0987	0.002	0.826	0.03	0.035	0.005	104.7	612	17	606	12	695	94	579	79
Z_GJ1_70	0.06	0.0024	0.0959	0.0023	0.795	0.03	0.028	0.005	108.9	588	17	590	13	545	87	542	86
Z_GJ1_71	0.059	0.0023	0.0942	0.0022	0.774	0.03	0.027	0.005	109.2	579	15	580	13	531	88	531	80
Z_GJ1_72	0.062	0.0023	0.0952	0.0021	0.814	0.03	0.029	0.004	95.9	599	16	585	13	574	86	610	80
Z_GJ1_73	0.063	0.003	0.0967	0.0024	0.836	0.04	0.046	0.006	95.35	609	20	594	14	890	110	623	99
Z_GJ1_74	0.063	0.0028	0.0953	0.002	0.825	0.03	0.039	0.006	93.76	606	19	586	12	760	110	625	92
Z_GJ1_75	0.061	0.0026	0.0988	0.002	0.83	0.03	0.035	0.005	107.4	609	19	607	12	680	100	565	91
Z_GJ1_76	0.062	0.0027	0.1039	0.0025	0.889	0.03	0.038	0.006	104.6	640	18	636	14	730	110	608	89
Z_GJ1_77	0.061	0.0025	0.0986	0.0023	0.829	0.03	0.028	0.005	105.4	606	18	605	13	542	87	574	90
Z_GJ1_78	0.058	0.0027	0.0959	0.0022	0.766	0.04	0.026	0.005	129.4	569	20	590	13	504	88	456	98
Z_GJ1_79	0.062	0.0025	0.0943	0.0022	0.812	0.03	0.027	0.004	95.71	597	18	580	13	527	84	606	87
II6-64																	
Z_GJ1_0	0.062	0.0022	0.1016	0.003	0.924	0.03	0.094	0.02	93.27	663	17	624	18	1800	360	669	75
Z_GJ1_1	0.061	0.0019	0.1016	0.0031	0.892	0.03	0.063	0.012	101.8	647	17	624	18	1230	230	613	68
Z_GJ1_2	0.063	0.0021	0.098	0.0033	0.91	0.05	0.055	0.014	85.88	655	26	602	19	1080	260	701	69
Z_GJ1_3	0.062	0.0027	0.0972	0.0034	0.852	0.03	0.044	0.007	90.88	625	17	598	20	870	140	658	90
Z_GJ1_4	0.06	0.0019	0.0984	0.0028	0.847	0.03	0.04	0.007	99.34	622	16	605	17	780	130	609	69

William Mansfield
Metamorphic evolution of the Mercara Shear Zone

Z_GJ1_5	0.062	0.0025	0.0973	0.0023	0.854	0.04	0.042	0.006	92.57	625	20	598	14	820	120	646	88
Z_GJ1_6	0.06	0.0026	0.0974	0.0028	0.826	0.04	0.037	0.006	102	609	23	599	16	730	120	587	95
Z_GJ1_7	0.061	0.0024	0.0934	0.0029	0.774	0.03	0.023	0.004	90.71	588	22	576	17	455	69	635	81
Z_GJ1_8	0.062	0.0024	0.0971	0.0033	0.817	0.04	0.026	0.005	91.01	605	21	597	19	510	100	656	83
Z_GJ1_9	0.06	0.0024	0.0979	0.0025	0.784	0.03	0.026	0.006	100.5	592	17	602	15	520	120	599	88
Z_GJ1_10	0.057	0.0021	0.0977	0.0035	0.789	0.04	0.038	0.006	125.5	590	19	600	21	750	110	478	82
Z_GJ1_11	0.048	0.0022	0.0973	0.0027	0.661	0.03	0.034	0.005	398.7	514	19	598	16	667	94	150	110
Z_GJ1_12	0.06	0.0022	0.0977	0.0038	0.803	0.04	0.035	0.006	104.2	597	21	601	22	690	120	577	85
Z_GJ1_13	0.062	0.0023	0.0962	0.0036	0.809	0.03	0.028	0.005	91.64	601	17	592	21	561	96	646	81
Z_GJ1_14	0.061	0.0022	0.0964	0.0033	0.836	0.03	0.045	0.007	95.49	616	17	593	20	880	130	621	80
Z_GJ1_15	0.062	0.0027	0.098	0.0034	0.834	0.04	0.031	0.004	91.23	615	21	603	20	624	80	661	93
Z_GJ1_16	0.062	0.0029	0.0981	0.0045	0.829	0.04	0.031	0.005	91.36	612	20	603	26	623	99	660	110
Z_GJ1_17	0.061	0.0028	0.0983	0.0042	0.809	0.04	0.027	0.005	97.42	600	25	604	24	534	96	620	100
Z_GJ1_18	0.061	0.0026	0.0957	0.0035	0.755	0.03	0.025	0.004	94.54	570	18	589	21	499	79	623	89
Z_GJ1_19	0.061	0.0027	0.0948	0.0043	0.741	0.04	0.025	0.005	95.11	561	22	584	25	501	95	614	99
Z_GJ1_20	0.061	0.0021	0.0969	0.0044	0.735	0.03	0.022	0.005	93.71	558	18	596	26	439	98	636	87
Z_GJ1_21	0.062	0.0027	0.0987	0.0029	0.864	0.03	0.035	0.007	90.19	631	18	607	17	690	130	673	84
Z_GJ1_22	0.06	0.0024	0.0993	0.0036	0.842	0.03	0.038	0.007	97.44	619	18	610	21	740	130	626	97
Z_GJ1_23	0.063	0.003	0.0972	0.0039	0.847	0.04	0.032	0.008	86.67	628	24	598	23	630	150	690	97
Z_GJ1_24	0.061	0.0026	0.096	0.0034	0.847	0.05	0.044	0.008	94.11	629	29	591	20	860	160	628	92
Z_GJ1_25	0.062	0.0023	0.0972	0.0051	0.862	0.05	0.039	0.008	90.47	637	31	598	30	770	150	661	79
Z_GJ1_26	0.06	0.0027	0.0971	0.0038	0.811	0.04	0.039	0.01	104.7	601	23	597	23	770	200	570	95
Z_GJ1_27	0.061	0.0038	0.0971	0.0038	0.824	0.05	0.033	0.006	99.5	608	28	597	22	640	120	600	130
Z_GJ1_28	0.061	0.0026	0.0966	0.0052	0.799	0.04	0.029	0.006	95.5	595	21	594	30	570	120	622	93
Z_GJ1_29	0.06	0.0029	0.1045	0.0049	0.835	0.03	0.027	0.006	112.3	615	18	640	29	530	120	570	100
Z_GJ1_30	0.062	0.0025	0.1016	0.0041	0.84	0.04	0.031	0.006	94.69	618	21	624	24	610	120	659	80
Z_GJ1_31	0.061	0.0026	0.1012	0.0044	0.813	0.03	0.029	0.006	98.57	603	18	621	26	570	110	630	100
Z_GJ1_32	0.062	0.003	0.1007	0.0039	0.823	0.04	0.022	0.003	95.08	608	22	618	23	435	65	650	100
Z_GJ1_33	0.061	0.0027	0.0983	0.0044	0.778	0.04	0.031	0.006	98.85	582	21	604	26	610	110	611	93
Z_GJ1_34	0.061	0.0033	0.1003	0.0033	0.739	0.03	0.024	0.004	102.7	567	22	616	19	471	69	600	110

William Mansfield
Metamorphic evolution of the Mercara Shear Zone

Z_GJ1_35	0.061	0.0033	0.1012	0.0034	0.738	0.04	0.019	0.004	101.8	560	22	621	20	375	85	610	110
Z_GJ1_36	0.06	0.0026	0.1018	0.0043	0.71	0.03	0.023	0.004	110.2	544	19	625	25	462	80	567	99
Z_GJ1_37	0.061	0.0032	0.0959	0.0052	0.848	0.06	0.036	0.007	95.16	621	30	590	31	720	130	620	110
Z_GJ1_38	0.061	0.0025	0.0972	0.0032	0.85	0.04	0.037	0.009	96.61	623	22	598	19	730	170	619	86
Z_GJ1_39	0.062	0.0028	0.0995	0.0035	0.88	0.04	0.035	0.008	92.58	639	23	611	21	690	150	660	93
Z_GJ1_40	0.06	0.0039	0.1	0.0044	0.848	0.06	0.034	0.006	107.7	620	33	614	26	670	120	570	140
Z_GJ1_41	0.06	0.0024	0.1005	0.004	0.835	0.03	0.036	0.006	101.3	616	17	617	24	700	120	609	97
Z_GJ1_42	0.06	0.0032	0.0998	0.0047	0.795	0.04	0.028	0.005	105.7	592	24	613	27	565	98	580	110
Z_GJ1_43	0.06	0.0026	0.0987	0.0045	0.883	0.05	0.048	0.01	101	641	24	606	26	940	190	600	110
Z_GJ1_44	0.061	0.0023	0.0987	0.0055	0.891	0.06	0.045	0.009	95.58	644	29	606	32	880	170	634	90
Z_GJ1_45	0.062	0.0029	0.0976	0.0039	0.856	0.04	0.034	0.006	92.02	626	21	600	23	660	130	652	99
Z_GJ1_46	0.051	0.0032	0.098	0.0049	0.726	0.04	0.046	0.008	261.7	553	22	602	29	910	140	230	130
Z_GJ1_47	0.044	0.0033	0.0966	0.0047	0.624	0.06	0.044	0.01	-743	488	35	594	27	860	190	-80	140
Z_GJ1_48	0.061	0.0023	0.098	0.0043	0.869	0.04	0.045	0.007	95.71	641	28	602	25	880	140	629	95
Z_GJ1_49	0.062	0.0026	0.0986	0.0052	0.912	0.06	0.043	0.013	92.1	655	29	606	30	840	240	658	90
Z_GJ1_50	0.063	0.0024	0.0979	0.0053	0.848	0.05	0.035	0.007	88.51	630	34	601	31	680	130	679	82
Z_GJ1_51	0.06	0.0032	0.0981	0.0044	0.804	0.04	0.023	0.004	105.8	605	28	603	26	453	81	570	120
Z_GJ1_52	0.061	0.0028	0.0962	0.0046	0.797	0.05	0.029	0.006	93.97	593	28	592	27	580	110	630	110
Z_GJ1_53	0.061	0.0028	0.0976	0.004	0.834	0.03	0.036	0.005	95.39	615	15	600	24	710	100	629	94
Z_GJ1_54	0.063	0.0029	0.0979	0.0032	0.865	0.04	0.034	0.005	88.4	638	24	602	19	673	94	681	96
Z_GJ1_55	0.06	0.0033	0.0965	0.0043	0.806	0.04	0.03	0.006	102.4	598	22	594	25	600	120	580	110
Z_GJ1_56	0.061	0.0027	0.0953	0.0042	0.797	0.03	0.028	0.011	95.44	594	19	586	25	560	200	614	96
Z_GJ1_57	0.059	0.0025	0.0956	0.0051	0.77	0.04	0.031	0.005	105.2	578	22	588	30	612	87	559	90
Z_GJ1_58	0.063	0.0038	0.098	0.0042	0.909	0.04	0.049	0.006	88.53	662	28	602	24	970	120	680	130
Z_GJ1_59	0.059	0.0027	0.0954	0.0035	0.848	0.05	0.044	0.005	104.8	621	25	587	20	870	100	560	110
Z_GJ1_60	0.062	0.0032	0.096	0.0035	0.881	0.05	0.04	0.007	90.92	639	24	591	21	790	140	650	110
Z_GJ1_61	0.061	0.0024	0.0985	0.004	0.845	0.05	0.038	0.007	95.28	619	27	606	23	740	140	636	86
Z_GJ1_62	0.06	0.0028	0.0989	0.0044	0.828	0.04	0.027	0.005	97.9	611	21	607	26	534	89	620	110
Z_GJ1_63	0.062	0.003	0.0958	0.0043	0.823	0.05	0.028	0.006	90.77	607	25	590	25	550	110	650	100
Z_GJ1_64	0.059	0.0025	0.0972	0.0047	0.797	0.05	0.026	0.005	104.7	592	29	597	28	521	95	570	100

William Mansfield
Metamorphic evolution of the Mercara Shear Zone

Z_GJ1_65	0.062	0.003	0.0964	0.004	0.813	0.04	0.026	0.005	89.85	602	25	593	23	523	92	660	100
I16-65																	
Z_GJ1_0	0.062	0.0025	0.1768	0.0033	1.527	0.06	0.058	0.007	173.2	933	24	1048	18	1110	140	605	84
Z_GJ1_1	0.063	0.0024	0.1482	0.0028	1.305	0.04	0.056	0.008	136.3	841	19	890	16	1100	150	653	79
Z_GJ1_2	0.063	0.0029	0.1104	0.0025	0.939	0.04	0.025	0.005	108.3	667	20	675	15	495	88	623	93
Z_GJ1_3	0.061	0.0027	0.1093	0.0027	0.926	0.04	0.038	0.006	111.7	660	20	668	16	740	110	598	92
Z_GJ1_5	0.059	0.0025	0.1074	0.0022	0.886	0.03	0.052	0.007	124	642	19	657	13	1010	120	530	90
Z_GJ1_6	0.06	0.0025	0.1074	0.0021	0.892	0.03	0.043	0.006	124.6	642	18	659	12	840	120	529	87
Z_GJ1_7	0.062	0.0027	0.106	0.0025	0.914	0.04	0.027	0.005	105.7	656	20	649	15	549	98	614	93
Z_GJ1_8	0.062	0.0025	0.1059	0.0022	0.915	0.04	0.033	0.005	108.2	654	20	650	13	650	100	601	85
Z_GJ1_9	0.061	0.0023	0.1055	0.0022	0.867	0.03	0.025	0.004	114.1	628	17	646	13	495	81	566	81
Z_GJ1_10	0.062	0.0026	0.1055	0.0025	0.907	0.04	0.035	0.005	105.9	651	20	646	14	680	100	610	85
Z_GJ1_11	0.062	0.0027	0.1039	0.0025	0.889	0.03	0.038	0.006	104.6	640	18	636	14	730	110	608	89
Z_GJ1_12	0.059	0.0026	0.1035	0.0025	0.845	0.03	0.037	0.005	128.6	615	19	634	15	710	100	493	90
Z_GJ1_13	0.062	0.0025	0.1026	0.002	0.9	0.04	0.031	0.005	99.84	647	19	629	12	617	93	630	86
Z_GJ1_14	0.061	0.0024	0.1024	0.0023	0.864	0.03	0.037	0.005	108.7	627	17	628	14	734	95	578	82
Z_GJ1_15	0.061	0.0024	0.1017	0.0022	0.853	0.03	0.033	0.005	108.7	627	18	624	13	648	92	574	83
Z_GJ1_16	0.061	0.0022	0.1017	0.0022	0.858	0.03	0.027	0.004	106.3	626	16	624	13	540	85	587	76
Z_GJ1_17	0.064	0.0029	0.1016	0.0023	0.896	0.04	0.036	0.006	94.39	642	19	623	14	700	110	660	87
Z_GJ1_18	0.061	0.0025	0.1014	0.0024	0.846	0.03	0.04	0.006	111.3	619	17	622	14	780	110	559	86
Z_GJ1_19	0.061	0.0025	0.1013	0.0022	0.854	0.03	0.038	0.006	104.5	625	17	622	13	740	110	595	86
Z_GJ1_20	0.062	0.0028	0.0995	0.0022	0.849	0.03	0.037	0.005	102.2	618	18	611	13	733	95	598	92
Z_GJ1_21	0.061	0.0024	0.0993	0.0021	0.837	0.03	0.041	0.006	107.2	614	17	610	12	820	120	569	83
Z_GJ1_22	0.064	0.0031	0.0993	0.002	0.883	0.04	-0.27	0.019	93.13	635	20	610	12	-6770	550	655	94
Z_GJ1_23	0.064	0.0029	0.0991	0.0019	0.878	0.04	0.035	0.005	93.84	633	19	609	11	676	94	649	96
Z_GJ1_24	0.06	0.0025	0.0988	0.0023	0.828	0.03	-0.14	0.012	110.4	606	18	607	14	-3160	280	550	88
Z_GJ1_25	0.061	0.0026	0.0988	0.002	0.83	0.03	0.035	0.005	107.4	609	19	607	12	680	100	565	91
Z_GJ1_26	0.059	0.0024	0.0987	0.0021	0.815	0.03	0.037	0.006	116.5	599	17	606	12	720	120	520	83
Z_GJ1_27	0.061	0.0024	0.0987	0.002	0.826	0.03	0.035	0.005	104.7	612	17	606	12	695	94	579	79
Z_GJ1_28	0.061	0.0026	0.0986	0.0024	0.814	0.03	0.031	0.005	109.8	604	17	605	14	612	91	551	89

William Mansfield
Metamorphic evolution of the Mercara Shear Zone

Z_GJ1_29	0.061	0.0025	0.0986	0.0023	0.829	0.03	0.028	0.005	105.4	606	18	605	13	542	87	574	90
Z_GJ1_30	0.063	0.0028	0.0985	0.0023	0.854	0.03	0.028	0.005	93.8	625	19	605	14	560	100	645	95
Z_GJ1_31	0.064	0.0028	0.0985	0.0021	0.865	0.03	0.035	0.005	89.63	631	19	605	12	690	100	675	94
Z_GJ1_32	0.062	0.0024	0.098	0.0021	0.833	0.03	0.032	0.005	100.7	610	17	602	12	627	89	598	84
Z_GJ1_33	0.061	0.0025	0.0979	0.0017	0.824	0.03	0.032	0.005	106.7	605	17	603	11	628	97	565	86
Z_GJ1_34	0.06	0.0027	0.0977	0.0021	0.815	0.03	0.031	0.005	110.7	603	19	601	12	630	100	543	93
Z_GJ1_35	0.061	0.0028	0.0977	0.0023	0.823	0.03	0.039	0.006	107	605	19	600	14	760	110	561	94
Z_GJ1_36	0.06	0.0025	0.0972	0.0022	0.801	0.03	-0.21	0.014	112.6	591	17	597	13	-4940	370	530	86
Z_GJ1_37	0.062	0.0024	0.0968	0.0022	0.838	0.03	-0.09	0.012	96.91	611	18	595	13	-2010	260	614	83
Z_GJ1_38	0.061	0.0028	0.0967	0.0022	0.816	0.04	0.041	0.006	107	598	20	594	13	800	110	555	92
Z_GJ1_39	0.063	0.003	0.0967	0.0024	0.836	0.04	0.046	0.006	95.35	609	20	594	14	890	110	623	99
Z_GJ1_40	0.061	0.0029	0.0964	0.0023	0.804	0.03	0.039	0.005	109.4	596	20	593	13	780	110	542	97
Z_GJ1_41	0.059	0.0025	0.0963	0.0021	0.771	0.03	-0.14	0.012	121.2	574	17	594	13	-3190	290	490	90
Z_GJ1_42	0.06	0.0024	0.096	0.0024	0.773	0.03	0.034	0.006	109.3	576	16	590	14	650	110	540	83
Z_GJ1_43	0.058	0.0027	0.0959	0.0022	0.766	0.04	0.026	0.005	129.4	569	20	590	13	504	88	456	98
Z_GJ1_44	0.059	0.0027	0.0959	0.0024	0.781	0.03	0.034	0.006	115.5	581	20	589	14	660	110	510	96
Z_GJ1_45	0.06	0.0025	0.0959	0.002	0.791	0.03	0.035	0.006	112.6	588	18	590	12	680	110	524	85
Z_GJ1_46	0.06	0.0024	0.0959	0.0023	0.795	0.03	0.028	0.005	108.9	588	17	590	13	545	87	542	86
Z_GJ1_47	0.06	0.0024	0.0958	0.0021	0.81	0.03	0.033	0.005	103.3	599	17	589	12	640	100	570	86
Z_GJ1_48	0.063	0.0024	0.0957	0.0018	0.834	0.03	0.041	0.005	90.77	613	15	590	10	800	100	650	79
Z_GJ1_49	0.059	0.0024	0.0955	0.0021	0.784	0.03	0.043	0.007	115.7	582	17	588	12	840	130	508	84
Z_GJ1_50	0.057	0.0026	0.0953	0.002	0.748	0.03	0.031	0.005	142.6	560	18	586	12	610	100	411	92
Z_GJ1_51	0.061	0.0025	0.0953	0.0021	0.791	0.03	0.038	0.005	105.2	588	17	586	12	750	100	557	85
Z_GJ1_52	0.063	0.0028	0.0953	0.002	0.825	0.03	0.039	0.006	93.76	606	19	586	12	760	110	625	92
Z_GJ1_53	0.062	0.0023	0.0952	0.0021	0.814	0.03	0.029	0.004	95.9	599	16	585	13	574	86	610	80
Z_GJ1_54	0.062	0.0027	0.0948	0.0022	0.809	0.04	0.033	0.005	100.9	594	20	583	13	643	88	578	91
Z_GJ1_55	0.06	0.0024	0.0945	0.0019	0.789	0.03	0.035	0.005	110	586	18	582	11	700	110	529	84
Z_GJ1_56	0.059	0.0022	0.0943	0.0019	0.78	0.03	0.003	0.006	117.6	581	17	580	11	50	120	493	79
Z_GJ1_57	0.059	0.0025	0.0943	0.0021	0.758	0.03	0.031	0.005	119.3	567	17	580	12	608	99	486	88
Z_GJ1_58	0.062	0.0026	0.0943	0.0021	0.805	0.03	0.025	0.004	97.64	594	17	580	13	482	84	594	89

William Mansfield
Metamorphic evolution of the Mercara Shear Zone

Z_GJ1_59	0.062	0.0025	0.0943	0.0022	0.812	0.03	0.027	0.004	95.71	597	18	580	13	527	84	606	87
Z_GJ1_60	0.059	0.0023	0.0942	0.0022	0.774	0.03	0.027	0.005	109.2	579	15	580	13	531	88	531	80
Z_GJ1_61	0.046	0.0027	0.0941	0.0021	0.607	0.04	0.029	0.005	1930	472	22	579	13	570	100	30	100
Z_GJ1_62	0.062	0.0025	0.0941	0.0021	0.813	0.03	0.046	0.007	95.54	597	18	579	13	900	130	606	88
Z_GJ1_63	0.058	0.0026	0.0938	0.002	0.754	0.03	0.036	0.005	126	564	19	577	12	700	100	458	93
Z_GJ1_64	0.059	0.0026	0.0937	0.0025	0.751	0.03	0.028	0.006	114	565	19	578	15	550	110	507	95
Z_GJ1_65	0.062	0.0026	0.0937	0.002	0.806	0.03	0.032	0.005	96.65	596	19	577	12	630	100	597	88
Z_GJ1_66	0.059	0.003	0.0936	0.0021	0.747	0.03	0.031	0.006	125.2	562	18	576	12	600	110	460	100
Z_GJ1_67	0.061	0.0025	0.0933	0.002	0.79	0.03	0.039	0.005	98.8	587	17	575	12	756	98	582	85
Z_GJ1_68	0.062	0.0023	0.0931	0.002	0.794	0.03	-0.03	0.006	94.71	591	16	573	12	-720	120	605	81
Z_GJ1_69	0.06	0.0023	0.0928	0.0023	0.767	0.03	0.03	0.005	104.4	578	15	572	13	588	92	548	80
Z_GJ1_70	0.057	0.0026	0.0926	0.0021	0.729	0.03	0.033	0.005	138	551	19	570	13	640	100	413	95
Z_GJ1_71	0.041	0.0023	0.0925	0.0022	0.529	0.03	0.029	0.004	-365	426	20	570	13	573	84	-156	93
Z_GJ1_72	0.061	0.0025	0.0925	0.0021	0.781	0.03	0.037	0.005	98.45	580	17	570	12	720	100	579	87
Z_GJ1_73	0.065	0.0026	0.0922	0.0019	0.831	0.03	0.044	0.006	79.33	608	17	568	11	850	110	716	84
Z_GJ1_74	0.06	0.0024	0.0918	0.0022	0.773	0.03	0.037	0.005	100.9	577	18	567	13	723	91	562	90
I16-66																	
Z_GJ1_0	0.058	0.0026	0.0984	0.0022	0.79	0.03	0.026	0.005	128.5	586	19	604	13	505	89	470	91
Z_GJ1_1	0.059	0.0023	0.0995	0.0021	0.817	0.03	0.029	0.004	114	603	17	611	12	574	86	536	84
Z_GJ1_2	0.062	0.0026	0.0985	0.0021	0.834	0.03	0.034	0.005	101.2	610	17	605	12	658	92	598	87
Z_GJ1_3	0.06	0.0022	0.0984	0.002	0.819	0.03	0.034	0.005	108.4	603	16	605	12	671	88	558	77
Z_GJ1_4	0.064	0.0026	0.096	0.0018	0.845	0.04	0.032	0.004	92.2	615	19	591	10	656	86	641	87
Z_GJ1_5	0.061	0.0028	0.0958	0.0023	0.803	0.03	0.03	0.005	105.7	593	17	589	13	585	92	557	92
Z_GJ1_6	0.059	0.0025	0.0993	0.002	0.797	0.03	0.035	0.005	121.3	590	16	610	12	700	100	503	84
Z_GJ1_7	0.059	0.0025	0.0979	0.0023	0.794	0.03	0.028	0.004	118.1	590	18	601	13	559	84	509	87
Z_GJ1_8	0.059	0.0024	0.0943	0.0021	0.771	0.03	0.03	0.005	110.5	575	17	581	12	577	97	526	87
Z_GJ1_9	0.063	0.0027	0.0931	0.0021	0.809	0.03	0.027	0.004	88.46	597	19	575	12	538	85	650	92
Z_GJ1_10	0.059	0.0027	0.1005	0.0023	0.812	0.03	0.028	0.004	125.9	597	18	617	13	551	85	490	89
Z_GJ1_11	0.062	0.0026	0.0982	0.0022	0.827	0.03	0.03	0.005	101.9	610	18	603	13	599	96	592	89
Z_GJ1_12	0.061	0.0024	0.0972	0.0021	0.824	0.03	0.035	0.005	103.1	603	18	597	12	688	91	579	85

William Mansfield
Metamorphic evolution of the Mercara Shear Zone

Z_GJ1_13	0.06	0.0025	0.1009	0.002	0.831	0.03	0.03	0.004	117.7	610	15	619	12	582	80	526	84
Z_GJ1_14	0.06	0.0022	0.1008	0.0021	0.834	0.03	0.029	0.004	112.8	611	16	619	12	579	86	549	78
Z_GJ1_15	0.06	0.0027	0.0968	0.0021	0.796	0.03	0.028	0.004	118.1	587	19	595	12	556	79	504	92
Z_GJ1_16	0.06	0.0026	0.101	0.0023	0.825	0.03	0.029	0.004	120.2	606	19	620	14	576	85	516	91
Z_GJ1_17	0.06	0.0026	0.0988	0.0021	0.815	0.04	0.027	0.004	116.1	598	19	607	12	523	86	523	90
Z_GJ1_18	0.06	0.0025	0.0985	0.0019	0.819	0.03	0.028	0.004	108	601	17	605	11	544	80	560	88
Z_GJ1_19	0.061	0.0024	0.0987	0.0023	0.819	0.03	0.027	0.005	107.1	604	17	606	13	535	87	566	83
Z_GJ1_20	0.063	0.0026	0.0983	0.0022	0.848	0.03	0.036	0.005	97.26	620	18	604	13	700	100	621	89
Z_GJ1_21	0.059	0.0023	0.0991	0.0021	0.818	0.03	0.031	0.005	117.1	601	17	610	12	607	88	521	83
Z_GJ1_22	0.061	0.0026	0.0956	0.0021	0.806	0.03	0.033	0.005	100.3	598	19	588	12	650	94	586	94
Z_GJ1_23	0.061	0.0024	0.0976	0.0021	0.828	0.03	0.032	0.005	102.9	608	18	600	13	632	89	583	85
Z_GJ1_24	0.061	0.0026	0.0949	0.0021	0.799	0.03	0.028	0.005	102.5	591	19	584	13	558	93	570	89
Z_GJ1_25	0.057	0.0025	0.1015	0.0023	0.802	0.03	0.033	0.006	143.9	591	18	623	13	650	110	433	90
Z_GJ1_26	0.061	0.0026	0.0994	0.0022	0.835	0.03	0.027	0.005	103.6	615	18	612	13	526	90	591	86
Z_GJ1_27	0.059	0.0024	0.0999	0.0022	0.818	0.03	0.03	0.005	121.6	600	18	613	13	585	87	504	83
Z_GJ1_28	0.06	0.0025	0.0981	0.0022	0.816	0.03	0.03	0.005	109.6	599	18	603	13	590	93	550	87
Z_GJ1_29	0.061	0.0026	0.099	0.002	0.84	0.04	0.027	0.004	106.1	611	19	608	12	537	86	573	90
Z_GJ1_30	0.061	0.0027	0.0965	0.0021	0.809	0.03	0.027	0.004	105.5	596	18	594	12	549	80	563	93
Z_GJ1_31	0.06	0.0026	0.0954	0.0023	0.784	0.03	0.025	0.004	110.3	581	18	587	14	497	81	532	92
Z_GJ1_32	0.065	0.0024	0.0953	0.0018	0.862	0.03	0.061	0.006	80.63	630	17	587	11	1180	120	728	78
Z_GJ1_33	0.058	0.0026	0.1025	0.0021	0.818	0.03	0.026	0.004	133.5	600	19	629	12	502	82	471	92
Z_GJ1_34	0.06	0.0026	0.097	0.0021	0.797	0.03	0.061	0.007	113.9	590	19	597	12	1200	130	524	91
Z_GJ1_35	0.06	0.0026	0.0926	0.0022	0.754	0.03	0.046	0.006	112.2	566	19	570	13	890	110	508	91
Z_GJ1_36	0.062	0.0029	0.1021	0.0027	0.854	0.03	0.047	0.006	104.9	622	19	626	16	910	110	597	92
Z_GJ1_37	0.064	0.0026	0.1002	0.0024	0.868	0.03	0.051	0.006	94.04	630	19	615	14	1010	110	654	88
Z_GJ1_38	0.065	0.0029	0.0991	0.0021	0.872	0.04	0.055	0.005	91.73	632	20	610	12	1060	100	665	92
Z_GJ1_39	0.062	0.0025	0.0946	0.0019	0.81	0.03	0.044	0.005	95.41	599	17	582	11	859	98	610	81
Z_GJ1_40	0.061	0.0024	0.0945	0.0021	0.784	0.03	0.027	0.004	97.16	590	17	582	12	523	82	599	84
Z_GJ1_41	0.06	0.0026	0.0981	0.0021	0.814	0.03	0.029	0.004	113.3	600	19	604	12	566	85	533	91
Z_GJ1_42	0.059	0.0024	0.098	0.0023	0.797	0.03	0.029	0.005	123.3	591	18	604	14	564	90	490	87

William Mansfield
Metamorphic evolution of the Mercara Shear Zone

Z_GJ1_43	0.061	0.0027	0.0989	0.0023	0.824	0.03	0.025	0.004	108.4	606	19	607	14	500	80	560	91
Z_GJ1_44	0.061	0.0025	0.0955	0.0019	0.798	0.03	0.029	0.004	102.8	593	17	588	11	570	81	572	83
Z_GJ1_45	0.06	0.0026	0.1007	0.0022	0.816	0.03	0.028	0.004	121.7	599	19	618	13	549	80	508	88
Z_GJ1_46	0.062	0.0026	0.0968	0.0022	0.831	0.03	0.031	0.005	98.35	607	18	595	13	608	93	605	90
Z_GJ1_47	0.062	0.0026	0.0949	0.002	0.805	0.03	0.026	0.004	100.3	593	19	584	12	523	80	582	88
Z_GJ1_48	0.059	0.0026	0.0967	0.0023	0.78	0.03	0.027	0.004	125.8	579	19	594	13	535	78	472	89
Z_GJ1_49	0.058	0.0028	0.0975	0.0021	0.773	0.03	0.03	0.005	135.5	574	19	599	12	581	87	442	95
Z_GJ1_50	0.06	0.0027	0.0954	0.0022	0.791	0.03	0.029	0.005	109.1	587	18	587	13	570	88	538	93
Z_GJ1_51	0.061	0.0026	0.0969	0.002	0.819	0.03	0.029	0.005	103.3	602	19	596	12	563	87	577	91
Z_GJ1_52	0.061	0.0023	0.1021	0.0024	0.858	0.03	0.023	0.004	110.2	623	17	626	14	463	70	568	79
Z_GJ1_53	0.057	0.0025	0.1035	0.0023	0.817	0.03	0.027	0.004	146	604	18	638	14	540	73	437	90
Z_GJ1_54	0.06	0.0024	0.0995	0.0024	0.816	0.03	0.028	0.004	113.1	605	21	611	14	545	85	540	89
Z_GJ1_55	0.062	0.0027	0.098	0.0022	0.832	0.03	0.04	0.005	101.7	609	18	602	13	780	100	592	90
Z_GJ1_56	0.058	0.0025	0.0979	0.0022	0.784	0.03	0.03	0.005	128.6	582	19	602	13	594	88	468	90
Plesovice In-house Zircon standard																	
I16-42																	
ples1.D	0.068	0.0026	0.05247	0.0009	0.495	0.02	0.039	0.002	39.81	408	12	329.6	5	769	43	828	80
ples2.D	0.064	0.0019	0.05174	0.0009	0.464	0.02	0.033	0.002	46.38	385	10	325.1	5	644	39	701	66
ples3.D	0.057	0.0018	0.04996	0.0008	0.397	0.01	0.021	0.001	70.77	337.6	9.2	314.2	5	423	25	444	71
ples4.D	0.062	0.0022	0.0517	0.0009	0.441	0.02	0.028	0.002	52.81	368	11	324.8	6	549	41	615	74
ples5.D	0.081	0.0025	0.05279	0.001	0.593	0.02	0.061	0.004	27.72	472	11	331.5	6	1187	73	1196	62
ples6.D	0.083	0.0037	0.05181	0.0009	0.604	0.03	0.067	0.005	27.81	474	17	325.6	6	1300	100	1171	84
ples7.D	0.114	0.0049	0.0551	0.0011	0.87	0.04	0.101	0.007	19.38	632	22	345.3	7	1930	120	1782	82
ples8.D	0.065	0.0026	0.0536	0.001	0.479	0.02	0.025	0.002	47.49	394	14	336.7	6	496	39	709	83
ples9.D	0.053	0.0018	0.05097	0.0009	0.373	0.01	0.02	0.001	112	320.2	9.3	320.3	6	390	26	286	69
ples10.D	0.056	0.0019	0.04938	0.0008	0.381	0.01	0.019	0.001	75.19	325.9	9	311.3	5	374	27	414	73
ples11.D	0.056	0.0016	0.05033	0.0009	0.392	0.01	0.011	0.001	77.93	334.2	8.3	316.4	6	217	25	406	62
ples12.D	0.068	0.0031	0.0526	0.0011	0.491	0.02	0.034	0.002	40.45	401	15	330.1	7	670	47	816	90
ples13.D	0.081	0.0026	0.05419	0.001	0.612	0.02	0.056	0.003	28.72	482	11	340.1	6	1097	53	1184	65
ples14.D	0.055	0.0018	0.0519	0.0009	0.392	0.01	0.019	0.001	88.35	335.4	9.2	326	6	388	26	369	69

William Mansfield
Metamorphic evolution of the Mercara Shear Zone

ples15.D	0.057	0.002	0.0533	0.0009	0.421	0.01	0.025	0.002	76.94	354.7	9.8	334.7	6	496	30	435	72
ples16.D	0.054	0.0017	0.05099	0.0008	0.382	0.01	0.018	0.001	93.44	327.5	8.3	320.5	5	367	21	343	67
ples17.D	0.105	0.004	0.0556	0.0011	0.808	0.03	0.073	0.004	21.02	595	17	348.7	7	1421	75	1659	70
ples18.D	0.089	0.005	0.0557	0.0011	0.685	0.04	0.061	0.004	26.97	523	24	349.2	7	1192	74	1295	96
ples20.D	0.055	0.0017	0.05207	0.0009	0.4	0.01	0.017	0.001	89.13	340.2	9.3	327.1	6	344	22	367	64
ples21.D	0.078	0.002	0.05418	0.001	0.582	0.01	0.047	0.002	30.66	464.2	8.9	340	6	930	45	1109	53
ples22.D	0.055	0.0017	0.0559	0.0011	0.417	0.01	0.016	0.001	95.22	352.6	8.5	350.4	7	321	27	368	66
ples23.D	0.068	0.0049	0.0557	0.001	0.538	0.05	0.036	0.003	45.95	424	25	349.2	6	708	60	760	120
ples24.D	0.065	0.0028	0.05363	0.0009	0.491	0.03	0.031	0.002	46.31	401	16	336.7	6	623	43	727	94
ples25.D	0.066	0.0032	0.0547	0.0012	0.506	0.03	0.026	0.002	47.95	409	18	343.3	7	514	42	716	96
ples26.D	0.094	0.0032	0.0551	0.001	0.725	0.02	0.052	0.003	23.56	550	13	345.8	6	1020	55	1468	63
ples27.D	0.097	0.0039	0.0564	0.001	0.77	0.04	0.066	0.005	23.4	574	20	353.8	6	1282	95	1512	77
ples28.D	0.055	0.002	0.05099	0.001	0.386	0.01	0.016	0.001	92.9	330	10	320.5	6	312	21	345	74
ples29.D	0.055	0.0018	0.05084	0.0009	0.388	0.01	0.017	0.001	83.01	331.5	8.8	319.6	5	332	22	385	70
ples30.D	0.07	0.0029	0.0549	0.0012	0.533	0.02	0.029	0.002	39.53	429	14	344.3	7	566	40	871	84
ples31.D	0.132	0.0068	0.058	0.0012	1.081	0.06	0.109	0.008	18	729	31	363.1	7	2070	140	2017	93
ples32.D	0.106	0.0032	0.0586	0.001	0.868	0.03	0.093	0.004	21.46	631	14	367.2	6	1800	74	1711	54
ples33.D	0.075	0.0023	0.0543	0.001	0.573	0.02	0.041	0.003	32.46	457	12	340.8	6	799	49	1050	65
ples34.D	0.078	0.002	0.05468	0.0009	0.599	0.02	0.041	0.002	30.04	474.5	9.6	343.1	5	817	38	1142	50
ples35.D	0.08	0.0021	0.05403	0.0008	0.6	0.01	0.039	0.002	29.13	475.9	9	339.1	5	766	32	1164	54
ples36.D	0.056	0.0021	0.05089	0.0009	0.398	0.02	0.017	0.001	76.17	338	11	319.9	6	340	22	420	77
I16-64																	
Ples1.D	0.054	0.0022	0.414	0.013	12.58	0.31	0.012	1E-03	95.04	296	12	345	16	241	19	363	84
Ples2.D	0.054	0.002	0.518	0.021	18.36	0.52	0.011	8E-04	95.52	310	10	341	16	220	16	357	80
Ples3.D	0.053	0.002	0.515	0.021	16.91	0.7	0.012	1E-03	114.6	315	11	346	14	246	19	302	81
ples4.D	0.054	0.0024	0.407	0.021	12.31	0.42	0.014	0.002	81.5	318	13	326	14	270	37	400	110
ples5.D	0.053	0.0014	0.0519	0.0018	0.407	0.02	0.013	0.001	109.5	319	10	331.9	9	263	22	303	62
ples6.D	0.054	0.0024	0.452	0.016	14.74	0.4	0.014	0.001	88.65	321	17	328	12	280	26	370	110
ples7.D	0.054	0.0017	0.56	0.018	19.53	0.58	0.012	0.001	92.37	322	12	339	13	247	22	367	72
ples8.D	0.053	0.0016	0.0535	0.0017	0.417	0.02	0.016	9E-04	108.3	330	9.8	333.5	10	318	18	308	70

William Mansfield
Metamorphic evolution of the Mercara Shear Zone

ples9.D	0.053	0.0011	0.411	0.013	13.54	0.45	0.013	9E-04	104.6	330.2	7.6	344	10	260	18	329	46
ples10.D	0.054	0.0017	0.0523	0.002	0.373	0.02	0.016	0.001	91.9	331.7	9.2	329	10	323	23	358	69
ples11.D	0.055	0.0019	0.409	0.02	12.39	0.63	0.013	0.001	86.22	332.5	8.8	338	10	262	25	392	74
ples12.D	0.054	0.0016	0.0517	0.0014	0.388	0.01	0.017	0.001	93.9	332.7	8	324.9	9	341	24	346	67
ples13.D	0.054	0.0018	0.693	0.028	31.01	0.97	0.015	0.002	94.92	333	15	336	15	300	36	354	77
ples14.D	0.055	0.0018	0.764	0.052	25.7	1.4	0.013	9E-04	80.14	334	12	335	13	263	19	418	85
ples15.D	0.054	0.0019	0.552	0.027	19.08	0.87	0.015	9E-04	94.15	334.1	9.7	338	12	300	17	359	75
ples16.D	0.055	0.0019	0.3955	0.0098	11.54	0.21	0.014	0.002	87.56	335	13	338	12	277	33	386	79
ples17.D	0.054	0.0025	0.409	0.017	11.38	0.39	0.015	0.002	94.72	336	11	341	14	295	34	360	100
ples18.D	0.056	0.0025	0.626	0.029	26.9	1.2	0.015	0.001	76.78	336	14	334	17	305	24	435	96
ples19.D	0.054	0.0015	0.0548	0.0017	0.385	0.01	0.017	0.001	91.36	336.9	9.8	328	12	348	26	359	61
ples20.D	0.055	0.0023	0.592	0.027	22.57	0.72	0.016	0.001	89.01	340	13	340	12	313	22	382	87
ples21.D	0.053	0.0014	0.628	0.027	22.84	0.76	0.018	0.002	104.1	340.3	8.2	333	11	352	29	320	60
ples22.D	0.054	0.0016	0.529	0.018	17.89	0.49	0.014	0.001	93.46	340.8	9.4	343	11	285	20	367	79
ples23.D	0.053	0.0022	0.432	0.013	13.45	0.41	0.018	0.001	106.3	341	12	336	13	357	23	316	86
ples24.D	0.054	0.0023	0.531	0.023	19.25	0.9	0.015	0.001	97.75	344	12	347	14	299	26	355	91
ples25.D	0.055	0.0014	0.0539	0.0024	0.445	0.02	0.018	0.002	79.37	344.4	7.9	327	11	361	33	412	58
ples26.D	0.053	0.0016	0.0531	0.0028	0.393	0.02	0.02	0.001	100.3	346.5	9.5	337	11	402	21	336	64
ples27.D	0.054	0.002	1.03	0.55	48	35	0.018	0.002	91.78	348	12	335	11	355	32	365	97
ples28.D	0.053	0.003	0.551	0.024	17.24	0.6	0.019	0.002	111.7	349	17	335	17	380	48	300	110
ples29.D	0.054	0.002	0.0535	0.0024	0.39	0.02	0.021	0.001	93.94	350	12	341	13	418	28	363	92
ples30.D	0.055	0.002	0.486	0.019	16.19	0.69	0.021	0.001	81.91	350	14	326	11	415	27	398	77
ples31.D	0.054	0.0015	0.482	0.022	16.69	0.8	0.022	0.002	91.06	353	11	336	10	446	43	369	60
ples32.D	0.055	0.0018	0.391	0.01	10.67	0.23	0.02	0.001	84.85	354	12	336	14	394	29	396	71
ples33.D	0.054	0.0017	0.55	0.02	19.84	0.53	0.022	0.002	99.1	358	11	339.9	9	435	37	343	72
ples34.D	0.054	0.0016	0.364	0.012	7.61	0.22	0.017	0.001	89.57	361	12	335	10	348	28	374	68
ples35.D	0.055	0.0024	0.404	0.033	13.7	1.2	0.022	0.003	89.69	365	17	348	18	447	59	388	94
ples36.D	0.059	0.0023	0.651	0.018	25.01	0.54	0.023	0.003	62.25	373	14	338	15	458	53	543	84
I16-65																	
ples1.D	0.055	0.0024	0.404	0.033	13.7	1.2	0.022	0.003	89.69	365	17	348	18	447	59	388	94

William Mansfield
Metamorphic evolution of the Mercara Shear Zone

ples2.D	0.054	0.0017	0.55	0.02	19.84	0.53	0.022	0.002	99.1	358	11	339.9	9	435	37	343	72
ples3.D	0.053	0.0022	0.0533	0.0011	0.392	0.02	0.017	0.001	101.9	339	11	336.4	7	357	24	330	82
ples4.D	0.054	0.0021	0.0537	0.001	0.397	0.01	0.017	0.001	81.27	336	11	327.5	7	349	36	403	95
ples5.D	0.057	0.0021	0.05153	0.0009	0.403	0.01	0.018	0.001	90.81	321.1	8.3	315.1	5	345	23	347	75
ples6.D	0.058	0.0026	0.0526	0.0013	0.406	0.02	0.015	0.002	56.05	357	12	321.7	7	428	29	574	91
ples7.D	0.055	0.0023	0.0535	0.0011	0.4	0.02	0.016	0.001	30.06	449	19	321.6	7	732	45	1070	100
ples8.D	0.055	0.0024	0.0521	0.0012	0.396	0.02	0.018	0.002	60.38	365	15	332.1	8	444	35	550	100
ples9.D	0.203	0.0035	0.386	0.011	10.98	0.38	0.097	0.005	107.8	337	12	337.3	6	324	29	313	87
ples10.D	0.054	0.0026	0.0537	0.001	0.401	0.02	0.016	0.002	117.9	333	12	334.8	7	346	23	284	77
ples11.D	0.052	0.0025	0.0538	0.001	0.387	0.02	0.017	0.002	82.93	345	13	331.7	7	359	38	400	87
ples12.D	0.055	0.0029	0.0535	0.0013	0.394	0.02	0.018	0.002	86.37	336	13	330.8	7	346	34	383	98
ples13.D	0.292	0.0034	0.767	0.013	31.07	0.51	0.178	0.004	93.24	338	13	333.8	7	365	30	358	98
ples14.D	0.261	0.0025	0.641	0.0094	23.37	0.43	0.167	0.002	52.82	338	14	301.1	8	390	40	570	110
ples15.D	0.238	0.0032	0.474	0.01	15.64	0.41	0.156	0.005	42.83	396	13	329.8	6	582	35	770	86
ples16.D	0.247	0.0024	0.6301	0.0084	21.72	0.29	0.17	0.003	99.38	337.9	9.8	336.9	6	348	27	339	75
ples17.D	0.21	0.0029	0.4679	0.0088	13.69	0.29	0.14	0.004	44.99	385	11	324.8	5	525	28	722	78
ples18.D	0.2	0.0021	0.5116	0.0061	14.23	0.22	0.136	0.006	128.8	329	13	337.4	6	344	29	262	91
ples19.D	0.054	0.0016	0.364	0.012	7.61	0.22	0.017	0.001	89.57	361	12	335	10	348	28	374	68
ples20.D	0.061	0.0031	0.0511	0.0013	0.428	0.02	0.025	0.002	71.61	344	11	330.1	8	296	29	461	93
ples21.D	0.061	0.003	0.0529	0.0013	0.439	0.02	0.022	0.002	123.2	337	14	343.6	7	360	32	279	97
ples22.D	0.061	0.003	0.0478	0.0012	0.4	0.02	0.02	0.002	57.34	357	15	321.1	8	489	42	560	100
ples23.D	0.055	0.0028	0.0532	0.0011	0.4	0.02	0.018	0.002	94.91	333	12	330.3	7	306	29	348	92
ples24.D	0.066	0.0027	0.0525	0.001	0.482	0.02	0.029	0.002	87.23	334	11	324.5	6	328	26	372	81
ples25.D	0.057	0.0028	0.05192	0.0008	0.407	0.02	0.018	0.001	96.75	328.2	8.8	327	5	363	23	338	76
ples26.D	0.056	0.0025	0.0528	0.0012	0.41	0.02	0.018	0.002	90.7	334	13	335.6	8	359	40	370	100
ples27.D	0.055	0.0026	0.0526	0.0012	0.393	0.02	0.015	0.002	94.86	340	11	335.8	7	317	23	354	82
ples28.D	0.054	0.0022	0.0536	0.0012	0.4	0.02	0.018	0.001	103	328.6	9.6	330.7	6	323	22	321	79
ples29.D	0.064	0.0025	0.05283	0.0009	0.46	0.02	0.027	0.001	72.86	344.9	9.8	325.7	5	330	18	447	75
ples30.D	0.065	0.0024	0.05168	0.0008	0.464	0.02	0.026	0.001	49.89	382	11	331.8	6	539	28	665	80
ples31.D	0.055	0.0022	0.05164	0.001	0.392	0.02	0.016	0.001	95.76	337	10	332.3	7	308	27	347	76

William Mansfield
Metamorphic evolution of the Mercara Shear Zone

ples32.D	0.054	0.0021	0.0537	0.001	0.397	0.01	0.017	0.001	81.27	336	11	327.5	7	349	36	403	95
ples33.D	0.054	0.002	0.0529	0.0011	0.394	0.01	0.015	0.001	202.5	314	11	338.2	7	324	24	167	83
ples34.D	0.056	0.0018	0.05183	0.0008	0.405	0.01	0.016	9E-04	106.4	330.7	8.7	332.9	6	328	20	313	70
ples35.D	0.053	0.0017	0.05301	0.0009	0.387	0.01	0.016	0.001	84.95	343	13	326.2	5	365	25	384	81
ples36.D	0.054	0.0019	0.05205	0.0009	0.384	0.01	0.018	0.001	76.73	341.7	9.9	323.8	5	353	22	422	76
I16-66																	
ples1.D	0.057	0.0021	0.05153	0.0009	0.403	0.01	0.018	0.001	90.81	321.1	8.3	315.1	5	345	23	347	75
ples2.D	0.054	0.0019	0.05205	0.0009	0.384	0.01	0.018	0.001	76.73	341.7	9.9	323.8	5	353	22	422	76
ples3.D	0.057	0.0028	0.05192	0.0008	0.407	0.02	0.018	0.001	96.75	328.2	8.8	327	5	363	23	338	76
ples4.D	0.053	0.0017	0.05301	0.0009	0.387	0.01	0.016	0.001	84.95	343	13	326.2	5	365	25	384	81
ples5.D	0.056	0.0018	0.05183	0.0008	0.405	0.01	0.016	9E-04	106.4	330.7	8.7	332.9	6	328	20	313	70
ples6.D	0.064	0.0025	0.05283	0.0009	0.46	0.02	0.027	0.001	72.86	344.9	9.8	325.7	5	330	18	447	75
ples7.D	0.065	0.0024	0.05168	0.0008	0.464	0.02	0.026	0.001	49.89	382	11	331.8	6	539	28	665	80
ples8.D	0.21	0.0029	0.4679	0.0088	13.69	0.29	0.14	0.004	44.99	385	11	324.8	5	525	28	722	78
ples9.D	0.054	0.002	0.0529	0.0011	0.394	0.01	0.015	0.001	202.5	314	11	338.2	7	324	24	167	83
ples10.D	0.055	0.0022	0.05164	0.001	0.392	0.02	0.016	0.001	95.76	337	10	332.3	7	308	27	347	76
ples11.D	0.066	0.0027	0.0525	0.001	0.482	0.02	0.029	0.002	87.23	334	11	324.5	6	328	26	372	81
ples12.D	0.238	0.0032	0.474	0.01	15.64	0.41	0.156	0.005	42.83	396	13	329.8	6	582	35	770	86
ples13.D	0.061	0.003	0.0529	0.0013	0.439	0.02	0.022	0.002	123.2	337	14	343.6	7	360	32	279	97
ples14.D	0.055	0.0024	0.0521	0.0012	0.396	0.02	0.018	0.002	60.38	365	15	332.1	8	444	35	550	100
ples15.D	0.054	0.0021	0.0537	0.001	0.397	0.01	0.017	0.001	81.27	336	11	327.5	7	349	36	403	95
ples16.D	0.247	0.0024	0.6301	0.0084	21.72	0.29	0.17	0.003	99.38	337.9	9.8	336.9	6	348	27	339	75
ples17.D	0.054	0.0022	0.0536	0.0012	0.4	0.02	0.018	0.001	103	328.6	9.6	330.7	6	323	22	321	79
ples18.D	0.053	0.0022	0.0533	0.0011	0.392	0.02	0.017	0.001	101.9	339	11	336.4	7	357	24	330	82
ples19.D	0.054	0.0026	0.0537	0.001	0.401	0.02	0.016	0.002	117.9	333	12	334.8	7	346	23	284	77
ples20.D	0.203	0.0035	0.386	0.011	10.98	0.38	0.097	0.005	107.8	337	12	337.3	6	324	29	313	87
ples21.D	0.058	0.0026	0.0526	0.0013	0.406	0.02	0.015	0.002	56.05	357	12	321.7	7	428	29	574	91
ples22.D	0.061	0.0031	0.0511	0.0013	0.428	0.02	0.025	0.002	71.61	344	11	330.1	8	296	29	461	93
ples23.D	0.061	0.003	0.0478	0.0012	0.4	0.02	0.02	0.002	57.34	357	15	321.1	8	489	42	560	100
ples24.D	0.261	0.0025	0.641	0.0094	23.37	0.43	0.167	0.002	52.82	338	14	301.1	8	390	40	570	110

ples25.D	0.055	0.0029	0.0535	0.0013	0.394	0.02	0.018	0.002	86.37	336	13	330.8	7	346	34	383	98
ples26.D	0.056	0.0025	0.0528	0.0012	0.41	0.02	0.018	0.002	90.7	334	13	335.6	8	359	40	370	100
ples27.D	0.052	0.0025	0.0538	0.001	0.387	0.02	0.017	0.002	82.93	345	13	331.7	7	359	38	400	87
ples28.D	0.2	0.0021	0.5116	0.0061	14.23	0.22	0.136	0.006	128.8	329	13	337.4	6	344	29	262	91
ples29.D	0.055	0.0023	0.0535	0.0011	0.4	0.02	0.016	0.001	30.06	449	19	321.6	7	732	45	1070	100
ples30.D	0.055	0.0026	0.0526	0.0012	0.393	0.02	0.015	0.002	94.86	340	11	335.8	7	317	23	354	82
ples31.D	0.055	0.0028	0.0532	0.0011	0.4	0.02	0.018	0.002	94.91	333	12	330.3	7	306	29	348	92
ples32.D	0.292	0.0034	0.767	0.013	31.07	0.51	0.178	0.004	93.24	338	13	333.8	7	365	30	358	98

APPENDIX C: ZIRCON ANALYSES

Analysis	Pb ²⁰⁷ /Pb ²⁰⁶	1σ	Pb ²⁰⁶ /U ²³⁸	1σ	Pb ²⁰⁷ /U ²³⁸	1σ	Pb ²⁰⁸ /Th ²³²	1σ	% Conc	Pb ²⁰⁷ /U ²³⁵	1σ	Pb ²⁰⁶ /U ²³⁸	1σ	Pb ²⁰⁸ /Th ²³²	1σ	Pb ²⁰⁷ /Pb ²⁰⁶	1σ
I16-42																	
z1c.D	0.2934	0.0029	0.6813	0.0093	28.45	0.37	0.2389	0.0033	97.40978	3432	13	3347	36	4328	54	3436	16
z1r.D	0.263	0.0031	0.506	0.0078	18.82	0.22	0.2356	0.0061	80.86477	3031	11	2637	33	4270	100	3261	18
z2c.D	0.2548	0.0025	0.5997	0.0082	21.56	0.3	0.208	0.0034	94.17808	3161	14	3025	33	3816	57	3212	16
z2r.D	0.2334	0.0019	0.5545	0.0069	18.26	0.19	0.2164	0.0093	92.45283	3002	10	2842	29	3960	160	3074	13
z3c.D	0.234	0.0028	0.5721	0.0078	18.9	0.32	0.1893	0.007	94.70091	3033	16	2913	32	3490	120	3076	20
z3r.D	0.238	0.0023	0.5894	0.0075	19.71	0.25	0.1897	0.0097	96.165	3074	12	2984	30	3480	170	3103	15
z4c.D	0.2552	0.0029	0.618	0.011	22.23	0.43	0.2119	0.0052	96.26866	3188	19	3096	43	3891	84	3216	17
z4r.D	0.2362	0.0028	0.574	0.0076	18.9	0.29	0.175	0.011	94.44085	3034	15	2922	31	3230	200	3094	18
z5c.D	0.244	0.0024	0.5932	0.0075	20.34	0.26	0.1975	0.0076	95.45021	3104	12	3000	30	3630	130	3143	16
z5r.D	0.2397	0.0021	0.5814	0.0059	19.58	0.19	0.1815	0.0058	94.79936	3069	9.3	2953	24	3360	100	3115	14
z6c.D	0.2639	0.0028	0.6246	0.0076	23.19	0.27	0.2105	0.0072	95.68279	3232	11	3125	30	3850	130	3266	17
z6r.D	0.264	0.0028	0.6446	0.0083	24.28	0.32	0.2232	0.0041	98.04221	3281	12	3205	33	4070	68	3269	17
z7c.D	0.2824	0.0035	0.656	0.01	26.02	0.37	0.2116	0.0086	96.26445	3343	14	3247	40	3880	140	3373	19
z7r.D	0.2741	0.0043	0.6341	0.0093	24.5	0.36	0.196	0.0084	95.12489	3285	14	3161	37	3650	130	3323	25
z8c.D	0.2469	0.0024	0.6173	0.0077	21.44	0.24	0.2133	0.0066	97.91271	3157	11	3096	31	3900	110	3162	15
z8r.D	0.2498	0.0029	0.635	0.011	22.07	0.37	0.185	0.011	99.59119	3183	16	3167	44	3400	190	3180	18

William Mansfield
Metamorphic evolution of the Mercara Shear Zone

z9c.D	0.2588	0.0035	0.624	0.01	23	0.35	0.2192	0.003	96.53894	3224	15	3124	40	4004	50	3236	21
z9r.D	0.2538	0.0037	0.625	0.0095	22.12	0.31	0.211	0.014	97.62722	3186	14	3127	38	3820	240	3203	22
z10c.D	0.2452	0.0024	0.6109	0.0068	21.09	0.24	0.1877	0.0064	97.43346	3141	11	3075	27	3500	100	3156	16
z10r.D	0.2744	0.003	0.6616	0.0084	25.49	0.31	0.2197	0.0063	98.2277	3324	12	3270	32	4000	110	3329	17
z11c.D	0.2442	0.0035	0.643	0.01	22.23	0.34	0.2328	0.0039	101.7505	3191	15	3197	41	4228	63	3142	23
z11r.D	0.2333	0.0037	0.615	0.011	20.06	0.36	0.178	0.013	100.3249	3094	17	3088	45	3280	230	3078	26
z12c.D	0.24	0.0034	0.595	0.011	19.84	0.42	0.175	0.014	96.46983	3079	20	3006	44	3230	240	3116	22
z12r.D	0.2175	0.0017	0.5667	0.0057	17.35	0.18	0.1236	0.005	97.67049	2952	10	2893	23	2347	92	2962	13
z13c.D	0.2511	0.0029	0.6031	0.0079	21.23	0.27	0.1988	0.0097	95.35613	3146	13	3039	32	3640	170	3187	18
z13r.D	0.2284	0.0028	0.577	0.0098	18.47	0.3	0.19	0.01	96.57557	3011	16	2933	40	3490	170	3037	20
z15c.D	0.2813	0.0034	0.648	0.014	25.28	0.49	0.186	0.014	95.45724	3318	19	3215	57	3410	260	3368	19
z15r.D	0.2583	0.0024	0.6252	0.0065	22.69	0.27	0.1887	0.0064	96.75325	3211	12	3129	26	3480	110	3234	15
z16c.D	0.2694	0.0027	0.6496	0.0091	24.53	0.34	0.2102	0.0099	97.6378	3287	14	3224	36	3860	170	3302	15
z16r.D	0.2634	0.0024	0.6375	0.0081	23.56	0.26	0.2109	0.0077	97.42647	3248	11	3180	31	3870	130	3264	14
z17c.D	0.2379	0.003	0.599	0.01	19.78	0.39	0.198	0.014	97.45326	3079	18	3023	42	3620	250	3102	20
z17r.D	0.2345	0.0027	0.5652	0.008	18.65	0.34	0.2054	0.0081	93.69721	3018	17	2884	33	3800	130	3078	18
z18c.D	0.2643	0.003	0.6411	0.008	24.01	0.31	0.2234	0.0032	97.61395	3266	13	3191	32	4074	52	3269	18
z18r.D	0.2243	0.0021	0.5505	0.0083	17.53	0.23	0.253	0.014	93.7583	2962	13	2824	34	4560	220	3012	16
z19c.D	0.2187	0.0022	0.5239	0.0072	16.1	0.22	0.1818	0.0061	91.40836	2881	13	2713	30	3370	110	2968	16
z19r.D	0.2562	0.0034	0.5919	0.008	21.32	0.29	0.1947	0.0072	92.98137	3150	13	2994	32	3580	130	3220	21
z20c.D	0.2708	0.0031	0.6291	0.0089	23.92	0.38	0.2143	0.008	95.03932	3260	15	3142	35	3950	130	3306	18
z20r.D	0.2578	0.0037	0.6268	0.0093	22.58	0.49	0.194	0.01	97.11717	3200	22	3133	37	3600	170	3226	23
z21c.D	0.2862	0.0042	0.669	0.011	26.9	0.39	0.2166	0.0099	97.31801	3378	14	3302	42	3960	170	3393	24
z21r.D	0.2838	0.0027	0.675	0.01	27.02	0.4	0.2194	0.0071	98.22538	3382	14	3321	40	3990	120	3381	15
z22c.D	0.2751	0.0039	0.686	0.013	26.59	0.6	0.2114	0.009	100.9006	3358	22	3361	49	3900	140	3331	23
z22r.D	0.223	0.0029	0.5818	0.0092	18.14	0.26	0.1788	0.0099	98.4985	2994	14	2952	37	3300	170	2997	21
z23c.D	0.2646	0.0032	0.6469	0.0097	24.16	0.52	0.2166	0.0049	98.13627	3267	21	3212	38	3958	82	3273	19
z23r.D	0.222	0.0029	0.5129	0.009	16.28	0.23	0.1781	0.0063	89.01503	2891	14	2666	38	3300	110	2995	22
z24c.D	0.2296	0.006	0.612	0.02	19.23	0.53	0.1888	0.0092	101.1815	3052	26	3083	76	3480	160	3047	39
z24r.D	0.2277	0.0024	0.5859	0.0074	18.8	0.28	0.1817	0.0047	97.89057	3029	14	2970	30	3368	83	3034	17

William Mansfield
Metamorphic evolution of the Mercara Shear Zone

z25c.D	0.2429	0.0031	0.5713	0.0087	19.62	0.23	0.2079	0.0039	93.01213	3072	12	2915	37	3824	63	3134	21
z25r.D	0.241	0.0029	0.566	0.0092	19.13	0.29	0.1949	0.0053	92.5024	3044	15	2887	38	3591	92	3121	19
z26c.D	0.2688	0.0036	0.631	0.012	23.5	0.4	0.1984	0.0097	95.60073	3248	17	3151	47	3680	160	3296	21
z26r.D	0.2505	0.0025	0.6002	0.008	21.11	0.28	0.2016	0.0055	95.0691	3140	13	3027	32	3704	96	3184	15
z27c.D	0.2836	0.0038	0.672	0.012	26.48	0.46	0.198	0.01	98.13499	3360	17	3315	44	3660	170	3378	21
z27r.D	0.2662	0.0033	0.631	0.011	23.72	0.37	0.218	0.0041	95.91712	3255	15	3148	42	3982	67	3282	20
z28c.D	0.2362	0.0023	0.5863	0.0074	19.44	0.23	0.1959	0.0055	96.11776	3061	11	2971	30	3607	97	3091	15
z28r.D	0.2256	0.0021	0.5786	0.0061	18.35	0.19	0.1912	0.0075	97.35187	3006.4	9.8	2941	25	3540	130	3021	15
z29c.D	0.3074	0.0023	0.6912	0.009	29.85	0.35	0.2176	0.0063	96.49273	3479	12	3384	34	3970	110	3507	12
z29r.D	0.2918	0.0034	0.662	0.01	27.11	0.38	0.2218	0.0062	95.50102	3384	14	3269	39	4040	110	3423	18
z30c.D	0.2941	0.0039	0.657	0.011	27.13	0.43	0.209	0.011	94.69851	3383	16	3251	42	3830	180	3433	20
z30r.D	0.2402	0.0037	0.5	0.008	16.84	0.34	0.1612	0.0093	83.73436	2919	20	2610	34	3000	160	3117	24
z31c.D	0.2291	0.0032	0.562	0.0079	18.1	0.35	0.1893	0.0055	94.50296	2988	18	2871	33	3495	96	3038	22
z31r.D	0.2294	0.0035	0.563	0.0092	18.34	0.37	0.1907	0.0052	94.54306	3002	19	2876	38	3535	91	3042	24
z32c.D	0.2018	0.0029	0.5434	0.0084	15.39	0.23	0.1682	0.0064	98.62337	2836	15	2794	35	3130	110	2833	24
z32r.D	0.2044	0.0029	0.573	0.011	16.34	0.34	0.1525	0.0081	101.9237	2891	20	2914	47	2870	140	2859	23
z33c.D	0.2676	0.0037	0.672	0.011	25.27	0.48	0.2044	0.004	100.5473	3313	19	3307	42	3755	68	3289	21
z33r.D	0.2773	0.0036	0.677	0.011	26.29	0.41	0.2015	0.0072	99.43199	3353	15	3326	41	3730	120	3345	20
z34c.D	0.2397	0.0024	0.6028	0.0079	20.23	0.27	0.1859	0.0059	97.46551	3101	13	3038	32	3440	100	3117	16
z34r.D	0.228	0.0031	0.5538	0.0089	17.78	0.37	0.1544	0.0088	93.59947	2970	20	2837	37	2880	160	3031	22
z35c.D	0.2568	0.0024	0.6178	0.0077	22.27	0.3	0.1945	0.0064	96.09181	3192	13	3098	31	3580	110	3224	15
z35r.D	0.2526	0.0025	0.6169	0.0088	22.12	0.3	0.2077	0.0066	96.90528	3187	13	3100	36	3810	110	3199	16
z36c.D	0.2401	0.0033	0.5982	0.0091	20.41	0.32	0.2052	0.0034	96.88803	3108	15	3020	37	3771	57	3117	22
z36r.D	0.2523	0.0029	0.326	0.016	11.54	0.56	0.1862	0.0087	56.28911	2519	55	1799	79	3500	140	3196	18
z37c.D	0.2437	0.0033	0.5846	0.0084	19.98	0.28	0.1845	0.006	94.3949	3087	13	2964	34	3410	110	3140	22
z37r.D	0.2025	0.0024	0.5267	0.008	14.96	0.2	0.168	0.007	95.84799	2809	13	2724	34	3160	120	2842	19
z38c.D	0.3089	0.0038	0.6927	0.0098	29.95	0.46	0.2081	0.0071	96.52422	3482	15	3388	37	3830	120	3510	19
z38r.D	0.2892	0.0054	0.661	0.015	26.82	0.74	0.207	0.011	95.88356	3363	26	3261	59	3760	180	3401	29
z39c.D	0.2355	0.0028	0.5428	0.0081	18.32	0.26	0.2138	0.0077	90.50551	3004	13	2793	34	3910	130	3086	19
z39r.D	0.2338	0.0027	0.6049	0.0068	19.78	0.25	0.1619	0.0073	99.15392	3081	12	3047	27	3060	120	3073	19

William Mansfield
Metamorphic evolution of the Mercara Shear Zone

z40c.D	0.2732	0.0033	0.5532	0.0092	21.66	0.35	0.2011	0.0036	85.31447	3165	15	2835	38	3717	65	3323	20
z40r.D	0.2758	0.003	0.6814	0.0096	26.28	0.41	0.186	0.011	100.2999	3354	15	3345	37	3410	200	3335	17
z41.D	0.2112	0.0028	0.5653	0.0099	16.85	0.31	0.1814	0.0032	99.10684	2923	18	2885	40	3368	55	2911	22
z41a.D	0.218	0.0018	0.5451	0.0066	16.74	0.22	0.1549	0.0047	94.56632	2919	12	2802	27	2918	80	2963	13
z42.D	0.2324	0.0023	0.6683	0.0091	21.63	0.29	0.1647	0.0088	107.5342	3167	13	3297	35	3090	150	3066	16
z43.D	0.2344	0.0027	0.699	0.011	22.98	0.39	0.1791	0.0082	110.8187	3223	17	3411	42	3330	140	3078	19
z44.D	0.2329	0.0024	0.644	0.009	21.17	0.32	0.1757	0.0077	104.3351	3144	15	3201	35	3290	130	3068	16
z45.D	0.2558	0.003	0.67	0.011	24.05	0.44	0.1911	0.0077	102.6119	3264	18	3300	43	3540	130	3216	19
z46.D	0.2904	0.0028	0.702	0.011	28.66	0.46	0.2015	0.0057	100.1755	3439	16	3424	41	3720	93	3418	15
z47.D	0.2504	0.0031	0.642	0.011	22.7	0.54	0.1979	0.0062	100.1883	3203	24	3192	42	3640	110	3186	19
z48.D	0.2409	0.0024	0.616	0.011	20.83	0.49	0.1773	0.0051	99.03939	3122	21	3093	46	3291	90	3123	16
z49.D	0.2732	0.0032	0.6781	0.0097	25.94	0.35	0.1985	0.006	100.4218	3341	13	3333	37	3650	110	3319	18
z50.D	0.2171	0.0023	0.5487	0.0071	16.71	0.19	0.1641	0.0047	95.43302	2918	11	2821	29	3065	85	2956	17
z51.D	0.2426	0.0024	0.646	0.01	21.93	0.35	0.185	0.01	102.3293	3176	16	3207	39	3400	180	3134	16
z52.D	0.3279	0.0031	0.7302	0.0092	33.62	0.42	0.2061	0.0056	97.97447	3597	12	3531	34	3779	97	3604	14
z53.D	0.2516	0.0037	0.62	0.011	21.85	0.3	0.1857	0.0041	97.39649	3175	14	3105	42	3439	70	3188	23
z54.D	0.2788	0.0026	0.695	0.01	27.2	0.39	0.1994	0.0061	101.3123	3389	14	3397	39	3660	110	3353	15
z55.D	0.2365	0.002	0.5667	0.0066	18.81	0.23	0.151	0.004	93.47123	3029	12	2892	27	2837	73	3094	13
z56.D	0.27	0.0027	0.6579	0.0095	24.85	0.37	0.1837	0.0069	98.54678	3299	15	3255	37	3400	120	3303	16
z57.D	0.2649	0.0028	0.6187	0.0091	22.8	0.31	0.1682	0.0099	94.77544	3216	13	3102	36	3150	170	3273	16
z58.D	0.2697	0.0026	0.6736	0.0087	25.4	0.35	0.1867	0.0059	100.4544	3322	14	3316	34	3450	100	3301	15
z59.D	0.1746	0.0041	0.4496	0.0092	10.89	0.22	0.1253	0.0082	92.3493	2508	19	2390	41	2370	150	2588	39
z60.D	0.2325	0.002	0.6223	0.0089	20.24	0.27	0.1754	0.0082	101.5319	3101	13	3115	36	3260	140	3068	13
z61.D	0.2992	0.0044	0.67	0.011	28	0.45	0.1906	0.0085	95.26559	3414	16	3300	43	3540	140	3464	22
z62.D	0.2709	0.003	0.794	0.013	30.12	0.57	0.2007	0.0064	113.668	3484	19	3759	48	3680	110	3307	18
z63.D	0.2354	0.0029	0.699	0.012	22.88	0.44	0.172	0.01	110.5997	3216	19	3412	46	3180	190	3085	20
z64.D	0.2229	0.0019	0.6394	0.0085	20.05	0.27	0.1686	0.006	106.1354	3091	13	3183	34	3150	110	2999	14
z65.D	0.311	0.0042	0.684	0.02	30.1	1.1	0.2166	0.0091	95.16908	3460	44	3349	79	3960	150	3519	22
z66.D	0.1913	0.0031	0.582	0.029	16.1	1.1	0.213	0.025	108.9253	2852	59	2990	130	3770	390	2745	26
z67.D	0.2661	0.0027	0.674	0.011	25.14	0.38	0.1795	0.0052	101.2199	3309	15	3319	40	3329	91	3279	16

William Mansfield
Metamorphic evolution of the Mercara Shear Zone

z68.D	0.2409	0.003	0.6019	0.0086	20.53	0.26	0.1867	0.0041	97.21332	3115	12	3035	34	3456	70	3122	20
z69.D	0.229	0.0022	0.593	0.011	18.92	0.32	0.1535	0.0091	98.68551	3036	17	3003	44	2870	170	3043	15
z70.D	0.2572	0.0026	0.6107	0.0091	21.99	0.35	0.1723	0.006	95.13329	3180	16	3069	36	3252	91	3226	16
z71.D	0.2208	0.0026	0.5035	0.0075	15.45	0.2	0.1401	0.0077	88.03218	2841	13	2626	32	2640	140	2983	18
z72.D	0.2703	0.0033	0.65	0.011	24.6	0.49	0.1884	0.0048	97.79123	3288	20	3232	46	3485	82	3305	19
z73.D	0.2697	0.0038	0.633	0.011	23.65	0.33	0.158	0.012	95.69827	3252	14	3159	44	2950	220	3301	22
z74.D	0.277	0.0028	0.6632	0.0087	25.75	0.36	0.1837	0.005	97.99581	3335	14	3276	34	3402	88	3343	16
z75.D	0.2217	0.0028	0.5699	0.008	17.7	0.25	0.1607	0.0055	97.35521	2970	13	2908	34	3017	94	2987	20
z76.D	0.2378	0.0031	0.644	0.011	21.35	0.26	0.1847	0.0034	103.4505	3153	12	3208	45	3423	58	3101	21
z77.D	0.28	0.0026	0.6432	0.0083	25.17	0.27	0.1726	0.007	95.29762	3315	10	3202	32	3200	130	3360	15
z78.D	0.2364	0.0019	0.5983	0.0083	19.76	0.26	0.179	0.01	97.48225	3077	13	3020	34	3300	180	3098	13
z79.D	0.2813	0.003	0.6724	0.0092	26.37	0.31	0.1833	0.0064	98.36601	3359	12	3311	35	3390	110	3366	16
z80.D	0.2636	0.0029	0.6444	0.0095	23.82	0.39	0.176	0.0078	98.04042	3258	16	3202	37	3310	130	3266	18
z81.D	0.244	0.0023	0.5651	0.0086	19.32	0.26	0.1447	0.0038	91.75947	3056	14	2884	35	2727	70	3143	15
z82.D	0.2547	0.003	0.627	0.01	22.41	0.35	0.1827	0.0065	97.54124	3197	15	3134	40	3380	110	3213	19
z83.D	0.2931	0.0027	0.771	0.012	31.76	0.53	0.2004	0.0056	107.1033	3538	17	3679	44	3684	97	3435	15
z84.D	0.2751	0.0029	0.7706	0.0094	29.79	0.38	0.1982	0.0034	110.4442	3477	13	3680	34	3651	57	3332	16
z85.D	0.2891	0.0046	0.708	0.014	28.66	0.65	0.1891	0.0076	101.1157	3432	22	3444	51	3500	130	3406	25
z86.D	0.2393	0.0022	0.5985	0.0095	20.08	0.35	0.1709	0.0061	96.98137	3092	17	3020	38	3180	110	3114	15
z87.D	0.2208	0.0022	0.6058	0.0092	18.79	0.33	0.1679	0.003	102.0415	3026	17	3049	37	3135	52	2988	15
z88.D	0.2771	0.0028	0.642	0.01	24.88	0.41	0.1883	0.0058	95.42601	3300	16	3192	40	3480	100	3345	16
z89.D	0.2537	0.0034	0.632	0.012	22.05	0.35	0.1585	0.009	98.56295	3189	15	3155	46	2950	160	3201	21
z90.D	0.2822	0.0032	0.6393	0.0094	25.31	0.33	0.1801	0.0055	94.54006	3319	13	3186	38	3355	92	3370	18
z91.D	0.2425	0.0018	0.6043	0.007	20.58	0.23	0.1769	0.0073	97.09821	3117	11	3045	28	3310	120	3136	12
z92.D	0.2454	0.002	0.5664	0.0073	19.5	0.25	0.1415	0.0036	91.65874	3064	13	2890	30	2670	66	3153	13
z93.D	0.2532	0.0036	0.597	0.011	21	0.36	0.1694	0.0063	94.18568	3136	17	3013	44	3150	110	3199	22
z94.D	0.2671	0.004	0.605	0.011	22.72	0.41	0.1829	0.0069	92.74611	3211	17	3043	45	3380	120	3281	24
z95.D	0.2588	0.0026	0.6212	0.0079	22.49	0.29	0.1792	0.0064	96.04938	3202	13	3112	31	3320	110	3240	17
z96.D	0.271	0.0035	0.602	0.0086	22.84	0.3	0.1889	0.0061	91.92377	3218	13	3039	36	3490	110	3306	20
z97.D	0.2248	0.0035	0.597	0.014	19.1	0.4	0.2043	0.0087	100.0664	3044	20	3015	56	3750	150	3013	25

William Mansfield
Metamorphic evolution of the Mercara Shear Zone

z98.D	0.3116	0.0033	0.715	0.012	31.56	0.49	0.1841	0.0038	98.46895	3534	15	3473	45	3413	64	3527	16
z99.D	0.2718	0.0037	0.66	0.01	25.39	0.35	0.1845	0.0042	98.49034	3321	14	3262	41	3420	71	3312	21
z100.D	0.2757	0.003	0.656	0.011	25.07	0.41	0.1626	0.0097	97.3913	3306	16	3248	41	3020	170	3335	17
z101.D	0.2355	0.0034	0.613	0.01	20.21	0.46	0.241	0.014	99.74068	3095	22	3077	41	4310	230	3085	23
z102.D	0.214	0.0035	0.5275	0.0096	15.74	0.28	0.1584	0.0051	93.20819	2859	17	2731	41	2978	87	2930	26
z104.D	0.27	0.0034	0.723	0.015	27.14	0.56	0.1662	0.0097	106.0569	3386	20	3502	55	3110	170	3302	20
z105.D	0.2722	0.0032	0.678	0.01	25.91	0.44	0.1761	0.0055	100.4218	3338	17	3333	38	3269	97	3319	17
z106.D	0.2381	0.0018	0.622	0.011	20.43	0.34	0.1402	0.0084	100.2254	3107	16	3112	42	2630	150	3105	12
z107.D	0.2506	0.0029	0.6079	0.0085	21.33	0.36	0.1604	0.0051	96.04271	3148	17	3058	34	2998	92	3184	19
z109.D	0.2536	0.0027	0.6056	0.0085	21.37	0.27	0.1592	0.0083	95.10446	3153	12	3050	34	2970	150	3207	16
z110.D	0.2726	0.0027	0.64	0.012	24.44	0.49	0.1679	0.0049	95.87101	3283	20	3181	49	3129	88	3318	15
z111.D	0.2364	0.0028	0.5865	0.0087	19.33	0.27	0.1586	0.0052	96.11776	3055	13	2971	35	2968	93	3091	19
z112.D	0.2587	0.0026	0.6332	0.0078	22.96	0.28	0.1658	0.0042	97.74413	3222	12	3163	31	3096	74	3236	16
z113.D	0.2426	0.0029	0.5944	0.0089	20.14	0.27	0.149	0.0042	95.88123	3095	13	3003	36	2802	75	3132	19
z114.D	0.2553	0.0023	0.5899	0.0092	21.14	0.36	0.1786	0.0039	92.84603	3140	17	2985	38	3318	67	3215	14
z115.D	0.2554	0.0035	0.5906	0.0093	20.99	0.31	0.1641	0.0085	92.99502	3134	14	2987	37	3050	150	3212	22
z116.D	0.2863	0.0024	0.6591	0.0088	26.43	0.41	0.1649	0.0054	95.96703	3358	15	3260	34	3076	97	3397	13
z117.D	0.2979	0.0031	0.6652	0.0086	27.68	0.37	0.1704	0.0055	95.02315	3404	13	3284	33	3187	93	3456	16
z118.D	0.2295	0.0026	0.5838	0.0081	18.79	0.27	0.1497	0.0077	97.20946	3029	14	2961	33	2800	140	3046	19
z119.D	0.2689	0.0024	0.6444	0.0082	24.3	0.35	0.1768	0.0043	97.14892	3277	14	3203	32	3285	74	3297	14
z120.D	0.2172	0.0027	0.5401	0.0087	16.41	0.31	0.1368	0.0062	94.07583	2895	18	2779	36	2590	110	2954	20
z121.D	0.2063	0.0028	0.5252	0.0072	15.34	0.19	0.1624	0.0052	94.67456	2835	12	2720	31	3037	90	2873	22
z122.D	0.24	0.0022	0.5881	0.0078	19.71	0.31	0.1512	0.0055	95.54201	3073	15	2979	32	2837	99	3118	15
z123.D	0.2454	0.0017	0.6237	0.0088	21.48	0.33	0.139	0.0037	98.92235	3156	15	3121	35	2626	68	3155	11
z124.D	0.318	0.0045	0.79	0.014	35.36	0.65	0.1853	0.0046	105.4024	3643	18	3746	50	3432	78	3554	22
z125.D	0.2231	0.0027	0.5947	0.0098	18.69	0.45	0.1448	0.005	100.2001	3016	22	3004	40	2725	90	2998	19
z126.D	0.2363	0.0023	0.5953	0.0086	19.64	0.29	0.1463	0.0062	97.25097	3073	14	3007	35	2780	110	3092	16
z127.D	0.3003	0.0027	0.6909	0.0087	28.93	0.34	0.1719	0.0056	97.5209	3448	12	3383	33	3213	95	3469	14
z128.D	0.2575	0.0039	0.584	0.011	20.82	0.32	0.1426	0.0077	91.70279	3127	15	2962	44	2700	130	3230	25
z129.D	0.2187	0.0033	0.4928	0.0089	14.9	0.27	0.118	0.01	86.95652	2806	17	2580	39	2240	190	2967	24

William Mansfield
Metamorphic evolution of the Mercara Shear Zone

z130.D	0.2404	0.0028	0.5788	0.0087	19.49	0.33	0.1498	0.0051	94.29121	3061	16	2940	36	2813	92	3118	18
z131.D	0.2709	0.0032	0.699	0.01	26.42	0.36	0.1856	0.0056	103.3273	3359	14	3416	39	3432	97	3306	18
z132.D	0.2373	0.0019	0.483	0.012	16.21	0.41	0.1288	0.0035	81.65108	2878	24	2532	54	2446	64	3101	14
z133.D	0.3104	0.0025	0.6664	0.0091	29.17	0.49	0.1819	0.0021	93.41096	3457	16	3289	35	3377	37	3521	12
z134.D	0.2583	0.0021	0.587	0.0078	21.27	0.3	0.1565	0.0052	92.08411	3149	13	2978	32	2930	94	3234	13
z135.D	0.2366	0.0015	0.5875	0.0076	19.46	0.26	0.1495	0.0067	96.12403	3062	13	2976	31	2850	110	3096	10
z136.D	0.2587	0.0032	0.5592	0.0084	19.97	0.3	0.1335	0.0087	88.41162	3087	14	2861	35	2520	160	3236	19
z137.D	0.2432	0.002	0.5609	0.0072	19.1	0.26	0.1475	0.0042	91.33482	3043	13	2867	30	2775	76	3139	13
z138.D	0.2761	0.0031	0.6296	0.0073	24.29	0.26	0.1689	0.0027	94.31138	3279	11	3150	28	3153	48	3340	17
z139.D	0.2603	0.0021	0.5899	0.0086	21.5	0.32	0.1389	0.004	91.95933	3157	15	2985	35	2637	68	3246	13
z13r.D	0.2284	0.0028	0.577	0.0098	18.47	0.3	0.19	0.01	96.57557	3011	16	2933	40	3490	170	3037	20
z140.D	0.2531	0.0029	0.561	0.0071	19.84	0.26	0.154	0.0045	89.65302	3080	13	2868	30	2890	81	3199	18
z141.D	0.2338	0.0023	0.5522	0.0069	18.06	0.2	0.1555	0.0068	92.0377	2990	11	2832	29	2940	110	3077	16
z142.D	0.2824	0.0025	0.6371	0.0078	25.11	0.28	0.1636	0.0058	94.12985	3310	11	3175	31	3050	100	3373	14
z143.D	0.3142	0.0038	0.657	0.011	28.79	0.45	0.1664	0.0068	91.83385	3442	15	3250	41	3110	120	3539	19
z144.D	0.2435	0.0016	0.5967	0.0068	20.33	0.26	0.1603	0.0079	95.9567	3104	12	3014	27	3020	130	3141	10
I16-64																	
z1c.D	0.1252	0.0043	0.272	0.015	6.86	0.42	0.0533	0.0018	56.50025	1511	59	1143	58	1050	35	2023	61
z1r.D	0.2816	0.0046	0.0543	0.0024	0.393	0.015	0.201	0.012	93.91691	3324	30	3165	88	3690	210	3370	26
z2c.D	0.2732	0.0052	0.0538	0.002	0.392	0.018	0.1964	0.0089	93.01626	3261	48	3090	120	3620	150	3322	30
z2r.D	0.2549	0.0055	0.0538	0.0017	0.388	0.012	0.1687	0.0055	85.77653	3053	36	2756	79	3149	95	3213	33
z3c.D	0.2583	0.0042	0.0541	0.0015	0.423	0.015	0.1683	0.0055	91.12828	3142	24	2948	59	3143	96	3235	26
z3r.D	0.2186	0.0039	0.0536	0.0022	0.418	0.017	0.124	0.0043	77.7965	2689	30	2309	61	2361	77	2968	29
z4c.D	0.1979	0.0045	0.0536	0.0022	0.4	0.017	0.114	0.012	68.53172	2415	34	1923	63	2180	220	2806	38
z4r.D	0.2161	0.0039	0.053	0.0017	0.398	0.011	0.1526	0.0039	79.69492	2720	25	2351	49	2870	69	2950	29
z5c.D	0.2094	0.0042	0.0523	0.0019	0.394	0.013	0.1596	0.0078	88.06485	2777	37	2553	73	2990	130	2899	32
z5r.D	0.2549	0.0043	0.0547	0.0018	0.399	0.013	0.154	0.0042	89.85688	3102	20	2888	65	2895	74	3214	26
z6c.D	0.2466	0.0047	0.0539	0.0021	0.374	0.016	0.1514	0.0044	92.34419	3078	37	2919	92	2848	78	3161	30
z6r.D	0.2402	0.0054	0.0552	0.0023	0.365	0.015	0.104	0.014	78.25529	2835	37	2440	70	1980	250	3118	36
z7c.D	0.2499	0.0049	0.0543	0.0026	0.357	0.013	0.1049	0.0032	76.36706	2857	46	2430	100	2015	58	3182	31

William Mansfield
Metamorphic evolution of the Mercara Shear Zone

z7r.D	0.1994	0.0033	0.055	0.0026	0.339	0.016	0.0931	0.0024	71.08904	2427	19	2004	50	1799	44	2819	27
z8r.D	0.2125	0.0033	0.0538	0.002	0.39	0.013	0.103	0.0029	84.77592	2707	24	2478	75	1980	54	2923	25
z9c.D	0.2084	0.0037	0.0542	0.0019	0.399	0.018	0.0876	0.0029	80.94085	2608	25	2340	67	1698	54	2891	28
z9r.D	0.2585	0.0037	0.0554	0.0029	0.434	0.024	0.165	0.01	92.74019	3093	26	3002	81	3080	180	3237	23
z10c.D	0.2281	0.0043	0.0533	0.0016	0.427	0.018	0.1573	0.0069	85.67194	2889	26	2601	57	2950	120	3036	31
z10r.D	0.2203	0.0039	0.0531	0.0016	0.384	0.013	0.1316	0.0042	73.29755	2649	28	2185	56	2498	76	2981	28
z11c.D	0.2402	0.003	0.0533	0.0017	0.41	0.017	0.1817	0.0059	84.39603	2955	22	2634	52	3370	100	3121	20
z11r.D	0.2742	0.0051	0.0519	0.0024	0.368	0.018	0.1924	0.0078	91.64663	3210	36	3050	110	3550	130	3328	29
z12c.D	0.2814	0.0043	0.0534	0.0027	0.411	0.024	0.1411	0.0034	95.66637	3294	24	3223	72	2667	60	3369	24
z12r.D	0.2047	0.0041	0.0528	0.0014	0.369	0.014	0.0937	0.0041	77.56029	2541	33	2219	75	1808	76	2861	33
z13c.D	0.2106	0.0041	0.052	0.0018	0.404	0.011	0.0887	0.0033	75.92847	2551	32	2208	78	1717	62	2908	32
z13r.D	0.2386	0.004	0.0544	0.0022	0.413	0.017	0.1132	0.0026	84.14281	2861	25	2616	59	2167	46	3109	26
z15c.D	0.2277	0.0062	0.0537	0.0018	0.407	0.013	0.1016	0.0041	85.45035	2780	38	2590	100	1955	76	3031	45
z15r.D	0.262	0.0075	0.0523	0.0016	0.387	0.013	0.1103	0.0061	92.50154	3071	36	3010	120	2110	110	3254	45
z16c.D	0.2569	0.005	0.0534	0.0022	0.39	0.016	0.1129	0.0022	92.27907	3033	26	2976	99	2161	40	3225	31
z16r.D	0.2506	0.0033	0.651	0.033	26.46	0.89	0.0552	0.0093	79.00847	2798	39	2518	91	1080	180	3187	21
z17c.D	0.2509	0.0035	0.518	0.019	18.43	0.58	0.0935	0.002	84.16431	2858	27	2684	77	1807	38	3189	22
z17r.D	0.2844	0.0062	0.691	0.039	30.4	1.6	0.1138	0.0031	92.49409	3140	36	3130	130	2179	56	3384	34
z18c.D	0.2799	0.0047	0.339	0.018	10.49	0.49	0.2133	0.0062	90.89286	3295	29	3054	78	3910	100	3360	26
z18r.D	0.18	0.0026	0.542	0.023	21.42	0.91	0.1064	0.0038	68.91739	2277	25	1827	56	2042	68	2651	24
z19c.D	0.2157	0.0034	0.555	0.041	18.4	1.4	0.1451	0.0059	78.24907	2704	26	2306	58	2740	100	2947	26
z19r.D	0.2989	0.0056	0.338	0.019	10.67	0.51	0.2146	0.006	93.61825	3416	28	3242	91	3929	99	3463	29
z20c.D	0.2701	0.0042	0.497	0.023	19.19	0.9	0.1695	0.0049	84.96218	3137	21	2808	55	3163	85	3305	24
z20r.D	0.2227	0.0051	0.675	0.026	28.1	1.5	0.1264	0.005	77.41074	2715	53	2320	120	2404	91	2997	37
z21c.D	0.198	0.0041	0.436	0.02	15	0.74	0.1244	0.0029	69.04168	2433	28	1938	61	2369	52	2807	34
z21r.D	0.2204	0.0051	0.404	0.012	12.61	0.38	0.1284	0.0036	66.72258	2550	45	1989	97	2442	64	2981	36
z22c.D	0.2251	0.0041	0.505	0.012	17.39	0.4	0.134	0.0034	68.70027	2613	24	2072	65	2542	61	3016	29
z22r.D	0.1904	0.0028	0.546	0.024	19.71	0.8	0.1424	0.0089	77.47813	2494	20	2126	48	2740	190	2744	25
z23c.D	0.2183	0.0044	0.422	0.016	12.93	0.37	0.1217	0.0036	77.98382	2719	34	2313	59	2320	66	2966	32
z23r.D	0.2578	0.0042	0.376	0.018	11.18	0.57	0.1638	0.0035	97.15347	3218	32	3140	110	3066	62	3232	26

William Mansfield
Metamorphic evolution of the Mercara Shear Zone

z24c.D	0.2387	0.0036	0.346	0.01	9.73	0.24	0.1313	0.0041	87.87781	2982	27	2733	76	2493	74	3110	24
z24r.D	0.2257	0.0029	0.382	0.019	12.25	0.79	0.1275	0.0028	85.00497	2837	21	2568	61	2426	50	3021	21
z25c.D	0.2037	0.0039	0.39	0.013	10.29	0.27	0.1387	0.0054	78.5489	2623	23	2241	58	2623	95	2853	32
z25r.D	0.2189	0.0046	0.643	0.021	25.46	0.63	0.149	0.0049	76.98759	2716	33	2295	84	2806	86	2981	39
z26c.D	0.2317	0.0047	0.608	0.027	22.71	0.83	0.1511	0.0053	85.69095	2907	27	2623	74	2843	93	3061	32
z26r.D	0.2191	0.0046	0.649	0.018	24.7	0.6	0.1314	0.0037	74.83176	2664	27	2224	68	2494	67	2972	34
z27c.D	0.2148	0.0036	0.613	0.027	22	0.93	0.1236	0.0034	79.86395	2699	26	2348	68	2354	61	2940	27
z27r.D	0.2352	0.0041	0.2972	0.0082	7.43	0.2	0.1324	0.003	84.15424	2901	27	2597	82	2512	53	3086	27
z28c.D	0.2056	0.0037	0.405	0.012	11.52	0.31	0.1047	0.0053	79.88846	2613	33	2292	77	2011	98	2869	29
z28r.D	0.2367	0.0045	0.631	0.046	23.8	2	0.1408	0.005	74.34572	2795	46	2301	79	2661	88	3095	30
z29c.D	0.204	0.0031	0.631	0.031	25.2	1.1	0.1114	0.0052	75.21876	2574	23	2149	58	2133	95	2857	25
z29r.D	0.2703	0.0046	0.555	0.015	19.53	0.42	0.1653	0.0048	82.57713	3109	28	2730	76	3090	84	3306	27
z30c.D	0.2156	0.0058	0.539	0.03	22	1.2	0.1189	0.0042	76.6644	2669	46	2257	71	2271	76	2944	42
z30r.D	0.2279	0.0042	0.384	0.013	12.5	0.6	0.1753	0.0061	86.22735	2907	31	2617	92	3300	120	3035	29
z31c.D	0.251	0.01	0.623	0.029	25.5	1	0.182	0.012	88.337	3065	95	2810	180	3380	200	3181	69
z31r.D	0.2014	0.003	0.412	0.016	11.26	0.4	0.101	0.012	70.52186	2479	21	2000	48	1940	230	2836	25
z32c.D	0.2962	0.0052	0.3418	0.0089	9.47	0.29	0.173	0.0053	80.0464	3218	42	2760	110	3223	92	3448	28
z32r.D	0.2074	0.0027	0.488	0.016	15.6	0.48	0.099	0.0041	71.22053	2535	35	2054	58	1908	76	2884	21
z33c.D	0.245	0.0045	0.501	0.014	15.77	0.43	0.163	0.0068	90.92063	3066	29	2864	74	3050	120	3150	29
z33r.D	0.2326	0.0052	0.496	0.024	14.52	0.57	0.1531	0.0043	87.15357	2924	40	2673	90	2878	75	3067	36
z34c.D	0.2535	0.0048	0.597	0.031	19.65	0.74	0.1345	0.0044	83.89513	3006	28	2688	88	2549	78	3204	30
z34r.D	0.2087	0.0035	0.588	0.025	18.87	0.5	0.146	0.0039	77.05598	2647	23	2230	57	2754	69	2894	27
z35c.D	0.2258	0.0035	0.479	0.021	14.81	0.59	0.1416	0.0049	66.89838	2603	42	2021	88	2675	87	3021	25
z35r.D	0.2047	0.0038	0.517	0.018	15.73	0.43	0.0936	0.0055	78.36421	2620	38	2242	88	1810	100	2861	31
z36c.D	0.2637	0.0047	0.626	0.031	21.13	0.81	0.1603	0.0041	83.34864	3082	24	2723	54	3004	72	3267	27
z36r.D	0.1988	0.0055	0.607	0.02	24.51	0.62	0.077	0.0039	66.80896	2386	39	1878	72	1498	74	2811	44
z37c.D	0.2549	0.006	0.328	0.012	8.44	0.23	0.1883	0.0078	77.98879	2967	44	2505	97	3480	130	3212	37
z37r.D	0.2467	0.0062	0.431	0.013	13.38	0.38	0.1561	0.0061	79.68997	2939	28	2519	82	2930	110	3161	39
z38c.D	0.313	0.006	0.655	0.023	27.98	0.78	0.2101	0.0046	95.78381	3521	26	3385	98	3854	77	3534	29
z38r.D	0.269	0.0063	0.546	0.013	21	0.46	0.1729	0.0065	89.17197	3188	38	2940	110	3220	110	3297	37

William Mansfield
Metamorphic evolution of the Mercara Shear Zone

z39c.D	0.2179	0.0049	0.434	0.027	13.62	0.78	0.1633	0.0034	78.02161	2728	33	2311	74	3057	59	2962	35
z39r.D	0.1995	0.0044	0.351	0.013	10.01	0.29	0.0942	0.0083	75.31039	2551	28	2123	78	1820	150	2819	35
z40c.D	0.2369	0.0036	0.635	0.023	25.48	0.79	0.1219	0.0052	66.46223	2666	31	2059	69	2323	93	3098	24
z40r.D	0.2249	0.0041	0.616	0.03	24	1.2	0.1382	0.0046	63.33776	2550	31	1909	45	2615	82	3014	30
z41.D	0.2667	0.0054	0.362	0.02	11.41	0.54	0.1727	0.0045	80.51157	3072	28	2644	80	3219	77	3284	32
z41a.D	0.2443	0.0044	0.38	0.014	12.14	0.31	0.1588	0.0042	83.24857	2969	34	2619	86	2978	74	3146	29
z42.D	0.2693	0.004	0.49	0.014	15.38	0.34	0.1242	0.0079	94.24242	3210	38	3110	100	2360	140	3300	23
z43.D	0.2203	0.0034	0.416	0.013	12.26	0.3	0.1	0.0031	81.28773	2708	26	2424	69	1925	56	2982	25
z44.D	0.1715	0.003	0.428	0.019	13.56	0.48	0.1132	0.0055	62.56809	2125	29	1608	52	2170	100	2570	29
z45.D	0.2156	0.0048	0.503	0.017	16.56	0.45	0.1857	0.0066	80.67912	2752	37	2376	85	3440	110	2945	36
z46.D	0.2482	0.0054	0.412	0.015	12.81	0.36	0.161	0.012	86.49842	3047	46	2742	97	3010	210	3170	34
z47.D	0.2389	0.0055	0.44	0.015	13.3	0.37	0.1691	0.0033	91.02605	3039	44	2830	110	3157	57	3109	37
z48.D	0.2606	0.0063	0.497	0.019	16.32	0.54	0.1738	0.0053	92.085	3205	31	2990	110	3238	91	3247	38
z49.D	0.2313	0.0073	0.428	0.017	12.17	0.44	0.1145	0.0057	71.33508	2712	81	2180	150	2190	100	3056	52
z50.D	0.2737	0.0058	0.43	0.017	14.79	0.7	0.1823	0.0085	89.92481	3240	44	2990	120	3380	150	3325	33
z51.D	0.2409	0.0042	0.396	0.013	11.63	0.29	0.183	0.01	76.72855	2851	27	2397	73	3380	180	3124	28
z52.D	0.2545	0.0042	0.528	0.018	20.42	0.57	0.1336	0.0093	79.76339	2973	32	2562	89	2530	170	3212	26
z53.D	0.2258	0.0086	0.194	0.011	3.48	0.26	0.1038	0.0066	66.04713	2560	87	1990	100	1990	120	3013	63
z54.D	0.2116	0.0034	0.42	0.016	12.96	0.65	0.1539	0.0089	76.92044	2672	35	2243	81	2890	160	2916	26
z55.D	0.2159	0.0063	0.502	0.022	16.57	0.54	0.1235	0.0045	63.80306	2491	36	1879	62	2352	81	2945	48
z56.D	0.2393	0.0037	0.534	0.019	19.32	0.74	0.1453	0.0055	74.69493	2818	36	2326	74	2741	97	3114	25
z57.D	0.1582	0.0043	0.58	0.014	21.11	0.52	0.0868	0.0059	62.15549	1973	51	1511	67	1680	110	2431	47
z58.D	0.2154	0.0037	0.549	0.043	20.1	2	0.1212	0.0051	70.1998	2574	40	2073	92	2312	92	2953	24
z59.D	0.229	0.0047	0.364	0.01	10.43	0.2	0.1319	0.0044	85.37627	2879	31	2598	98	2503	79	3043	33
z60.D	0.2583	0.0045	0.537	0.025	22.93	0.99	0.1475	0.0044	86.70377	3077	35	2804	95	2781	78	3234	27
z61.D	0.2492	0.0047	0.376	0.012	11.19	0.41	0.14	0.0043	84.85993	2988	24	2696	76	2647	76	3177	30
z62.D	0.2781	0.0052	0.369	0.019	12.05	0.53	0.0725	0.0043	83.40299	2913	27	2794	75	1413	82	3350	28
z63.D	0.2473	0.0044	0.417	0.02	12.26	0.48	0.0939	0.0028	88.08847	2787	26	2788	84	1814	52	3165	29
z64.D	0.236	0.0057	0.526	0.013	19.84	0.5	0.0582	0.0035	83.00971	2622	25	2565	70	1143	67	3090	39
z65.D	0.2512	0.0058	0.339	0.015	9.54	0.4	0.0989	0.0026	98.4326	2891	42	3140	150	1906	47	3190	36

William Mansfield
Metamorphic evolution of the Mercara Shear Zone

z66.D	0.2063	0.0045	0.476	0.022	17.69	0.8	0.061	0.0014	69.27607	2184	26	2000	58	1196	27	2887	25
z68.D	0.2618	0.0037	0.692	0.026	31.15	0.82	0.2013	0.004	99.14005	3307	22	3228	70	3706	68	3256	22
z69.D	0.3073	0.0064	0.579	0.027	22.22	0.88	0.2154	0.0054	96.71897	3516	31	3390	110	3942	90	3505	32
z70.D	0.2273	0.0068	0.432	0.016	13.73	0.48	0.135	0.0056	77.30426	2768	49	2340	100	2560	100	3027	49
z71.D	0.2636	0.0036	0.391	0.017	11.37	0.34	0.1524	0.0042	87.9094	3149	31	2872	81	2867	74	3267	21
z72.D	0.2678	0.0053	0.377	0.015	12.86	0.42	0.2006	0.005	85.29322	3164	28	2807	76	3693	84	3291	31
z73.D	0.2543	0.0055	0.3448	0.0093	11.36	0.37	0.1756	0.0068	85.26021	3076	29	2736	97	3270	120	3209	34
z74.D	0.2246	0.0066	0.431	0.013	13.17	0.4	0.1274	0.0051	64.19548	2555	57	1931	80	2422	91	3008	47
z75.D	0.2451	0.0057	0.348	0.013	9.83	0.36	0.1406	0.0039	73.96825	2838	37	2330	110	2657	69	3150	37
z76.D	0.2208	0.0056	0.508	0.019	19.64	0.57	0.1642	0.0083	78.47082	2763	70	2340	120	3070	140	2982	40
z77.D	0.274	0.0047	0.502	0.02	17.68	0.61	0.1732	0.0061	79.65134	3118	47	2650	120	3230	100	3327	27
z78.D	0.194	0.011	0.622	0.026	22.72	0.86	0.109	0.013	63.27273	2280	150	1740	180	2090	240	2750	100
z79.D	0.259	0.0051	0.457	0.016	13.42	0.36	0.1941	0.0068	85.85547	3119	39	2780	120	3580	110	3238	31
z80.D	0.2149	0.0032	0.284	0.01	7.13	0.23	0.1496	0.0034	77.94018	2714	26	2293	66	2816	60	2942	24
z81.D	0.2561	0.0049	0.447	0.019	14.11	0.55	0.1941	0.0049	94.06832	3202	23	3029	79	3585	83	3220	30
z82.D	0.2393	0.0052	0.593	0.031	23.5	1.1	0.1675	0.0079	97.68638	3133	32	3040	90	3130	140	3112	35
z83.D	0.2587	0.005	0.44	0.011	13.6	0.37	0.1529	0.0049	85.04788	3081	31	2753	92	2874	86	3237	31
z84.D	0.2295	0.0051	0.487	0.017	14.48	0.57	0.1248	0.006	80.66316	2825	28	2457	75	2370	110	3046	35
z85.D	0.241	0.0033	0.451	0.017	15.62	0.44	0.1346	0.0035	85.44061	2964	32	2676	78	2552	62	3132	18
z86.D	0.289	0.0056	0.489	0.021	17.57	0.5	0.265	0.02	91.78886	3373	45	3130	120	4740	310	3410	30
z87.D	0.2208	0.0032	0.362	0.021	11.7	1	0.1617	0.0032	80.46901	2796	26	2402	71	3030	56	2985	23
z88.D	0.2069	0.0049	0.417	0.018	12.96	0.49	0.1425	0.0054	76.43379	2635	27	2199	94	2690	94	2877	38
z89.D	0.2149	0.0032	0.339	0.013	10.55	0.35	0.1398	0.0042	96.19307	2945	33	2830	100	2643	74	2942	24
z91.D	0.26	0.0038	0.265	0.013	6.04	0.34	0.1628	0.005	88.16841	3138	27	2869	75	3048	86	3254	28
z92.D	0.1974	0.0026	0.38	0.02	11.68	0.51	0.0978	0.0032	75.57061	2516	23	2119	51	1885	59	2804	22
z93.D	0.2038	0.0031	0.497	0.023	16.1	0.53	0.1693	0.0055	78.07356	2643	32	2229	75	3159	96	2855	25
z94.D	0.2431	0.0038	0.546	0.023	19.8	0.71	0.1753	0.0049	85.5368	3018	28	2685	73	3264	85	3139	25
z95.D	0.2184	0.004	0.566	0.016	20.24	0.4	0.1606	0.0047	83.18166	2810	39	2468	89	3009	83	2967	30
z96.D	0.2321	0.0039	0.574	0.022	19.8	0.79	0.1579	0.0038	84.0783	2913	23	2577	70	2963	67	3065	27
z97.D	0.2308	0.004	0.52	0.018	18	0.45	0.1444	0.0056	87.33639	2969	22	2669	65	2725	98	3056	28

William Mansfield
Metamorphic evolution of the Mercara Shear Zone

z98.D	0.237	0.0059	0.537	0.021	16.65	0.46	0.2024	0.0072	90.76227	3050	60	2810	130	3720	120	3096	39
z99.D	0.2436	0.0054	0.542	0.02	14.6	0.41	0.1902	0.0067	88.3121	3059	39	2773	86	3520	110	3140	36
z100.D	0.2777	0.0063	0.489	0.016	12.25	0.32	0.2044	0.0042	96.20556	3360	33	3220	130	3758	71	3347	35
z101.D	0.2437	0.0045	0.631	0.038	16.32	0.72	0.1602	0.0059	85.5506	3010	30	2688	81	3000	100	3142	30
z102.D	0.2898	0.006	0.461	0.016	15.38	0.61	0.248	0.0078	100.1757	3491	49	3420	170	4470	130	3414	32
z103.D	0.2078	0.0062	0.459	0.024	15.78	0.75	0.1174	0.0055	65.09368	2472	44	1876	85	2240	100	2882	49
z104.D	0.2659	0.0053	0.438	0.023	14.4	0.74	0.1923	0.0086	84.99543	3152	43	2787	97	3550	150	3279	32
z105.D	0.2278	0.0051	0.562	0.02	21.3	0.67	0.1739	0.0083	93.2762	2994	70	2830	170	3240	140	3034	36
z106.D	0.2109	0.0056	0.546	0.018	21.62	0.63	0.1189	0.0082	64.33975	2489	38	1871	88	2270	150	2908	43
z107.D	0.2579	0.0056	0.53	0.023	19.74	0.58	0.129	0.015	80.47044	3045	43	2600	100	2450	270	3231	35
z109.D	0.2791	0.0062	0.35	0.017	11.52	0.7	0.2315	0.0095	98.95678	3415	47	3320	99	4210	150	3355	34
z110.D	0.2292	0.005	0.437	0.024	15.44	0.59	0.1867	0.0052	76.56918	2821	42	2330	90	3458	89	3043	34
z111.D	0.2276	0.0059	0.44	0.027	14.5	1.1	0.203	0.013	120.0924	3326	53	3640	190	3730	210	3031	42
z112.D	0.2199	0.0048	0.511	0.028	20.71	0.97	0.1504	0.0042	74.47094	2714	31	2217	60	2831	73	2977	35
z113.D	0.2321	0.0044	0.314	0.038	9.2	1.4	0.1809	0.0055	82.64274	2910	46	2533	93	3359	94	3065	30
z114.D	0.225	0.0045	0.541	0.028	20.7	0.84	0.1593	0.0041	84.60518	2882	41	2550	83	2987	71	3014	32
z115.D	0.246	0.004	0.365	0.011	9.93	0.21	0.133	0.016	88.66371	3072	40	2800	100	2510	290	3158	26
z116.D	0.2106	0.0038	0.386	0.036	14.2	4.3	0.1266	0.0035	77.99175	2672	27	2268	74	2409	63	2908	29
z117.D	0.1981	0.004	0.428	0.015	13.52	0.38	0.1642	0.0064	73.07692	2530	50	2052	83	3070	110	2808	34
z118.D	0.1886	0.003	0.601	0.02	22.46	0.53	0.119	0.0046	70.17222	2408	23	1915	49	2271	83	2729	26
z119.D	0.2153	0.0048	0.604	0.023	20.74	0.6	0.1284	0.0054	70.8121	2612	57	2084	88	2440	97	2943	36
z120.D	0.1796	0.0032	0.534	0.022	19.85	0.62	0.1172	0.0047	80.16623	2459	24	2122	62	2239	85	2647	30
z121.D	0.272	0.0053	0.465	0.017	15.2	0.44	0.1778	0.0051	96.44042	3324	24	3197	85	3306	88	3315	31
z122.D	0.2484	0.0042	0.515	0.018	17.59	0.58	0.1637	0.0049	96.75386	3178	41	3070	110	3062	86	3173	26
z123.D	0.1714	0.0024	0.469	0.017	13.4	0.34	0.0862	0.0022	65.21401	2162	24	1676	41	1671	42	2570	23
z124.D	0.1968	0.0045	0.438	0.015	12.08	0.32	0.1115	0.0042	78.33393	2564	25	2191	53	2135	76	2797	37
z125.D	0.2499	0.0055	0.464	0.054	19.9	7.3	0.247	0.048	98.7111	3243	71	3140	170	4390	650	3181	35
z126.D	0.2676	0.0055	0.561	0.018	21.03	0.59	0.2005	0.0062	95.46975	3310	43	3140	120	3690	100	3289	32
z127.D	0.2369	0.004	0.389	0.011	10.93	0.27	0.1904	0.0047	91.80116	3067	21	2844	64	3521	80	3098	27
z128.D	0.1692	0.0036	0.414	0.016	12.55	0.42	0.081	0.013	60.55512	2084	51	1549	73	1560	230	2558	42

William Mansfield
Metamorphic evolution of the Mercara Shear Zone

z129.D	0.2786	0.0039	0.517	0.017	18.6	0.53	0.154	0.0073	82.58795	3173	56	2770	130	2890	130	3354	22
z130.D	0.2154	0.005	0.467	0.02	14.99	0.61	0.159	0.0048	71.04995	2635	48	2091	61	2981	84	2943	38
z131.D	0.274	0.0048	0.492	0.016	16.64	0.39	0.2152	0.0072	93.77818	3323	39	3120	110	3940	120	3327	28
z132.D	0.1962	0.0026	0.514	0.016	17.65	0.41	0.1324	0.0036	76.84324	2567	17	2147	45	2512	64	2794	22
z133.D	0.2048	0.0038	0.549	0.031	19.4	1.2	0.1251	0.0041	77.11391	2626	49	2207	90	2381	74	2862	30
z134.D	0.2466	0.0046	0.539	0.021	19.44	0.8	0.1581	0.0042	89.27555	3081	25	2822	84	2965	73	3161	29
z135.D	0.1913	0.0027	0.594	0.02	20.08	0.53	0.0985	0.0024	68.79768	2382	29	1894	43	1899	44	2753	23
z136.D	0.221	0.0031	0.497	0.013	16.25	0.44	0.1297	0.0043	85.47094	2850	29	2559	71	2464	77	2994	27
I16-65																	
z1c.D	0.2837	0.0026	0.6691	0.009	25.39	0.36	0.1621	0.0028	97.69299	3319	14	3303	34	3034	50	3381	14
z1r.D	0.2253	0.0043	0.532	0.018	15.84	0.6	0.135	0.0071	90.99967	2858	38	2740	73	2550	130	3011	30
z2c.D	0.1855	0.0019	0.3566	0.0045	8.96	0.12	0.0973	0.0014	72.72391	2332	12	1965	21	1879	27	2702	17
z2r.D	0.1728	0.0024	0.3336	0.0063	7.81	0.21	0.0813	0.0032	71.86047	2201	24	1854	31	1578	59	2580	23
z3c.D	0.2587	0.0025	0.584	0.0085	20.18	0.36	0.1501	0.0032	91.65379	3098	17	2965	34	2823	56	3235	15
z3r.D	0.212	0.0018	0.5999	0.0067	17.26	0.23	0.1403	0.0046	103.8725	2948	12	3031	26	2647	83	2918	14
z4c.D	0.1462	0.0027	0.2607	0.0055	5.25	0.2	0.0803	0.0034	65.13761	1840	32	1491	28	1557	64	2289	30
z4r.D	0.1918	0.0021	0.4058	0.0048	10.56	0.14	0.1008	0.0029	79.69488	2482	13	2194	22	1939	53	2753	18
z5c.D	0.2524	0.0032	0.6341	0.0097	22.15	0.34	0.1823	0.0048	98.9365	3188	15	3163	39	3381	82	3197	20
z5r.D	0.2422	0.0024	0.5711	0.0073	18.84	0.3	0.1507	0.0035	93.03737	3032	15	2913	31	2834	62	3131	16
z6c.D	0.2172	0.0027	0.4333	0.0061	12.96	0.14	0.1246	0.0017	78.45061	2675	11	2319	27	2373	31	2956	20
z6r.D	0.1994	0.0023	0.3696	0.0047	10.04	0.14	0.1109	0.0029	71.94602	2438	13	2026	22	2123	54	2816	19
z7c.D	0.2044	0.0022	0.4193	0.0055	11.69	0.19	0.1138	0.0022	78.92895	2576	15	2255	25	2176	40	2857	18
z7r.D	0.237	0.003	0.4508	0.006	14.53	0.2	0.12	0.0026	77.4475	2782	13	2397	27	2288	47	3095	20
z8c.D	0.2123	0.0022	0.4108	0.0065	11.94	0.24	0.1121	0.0025	75.91641	2595	19	2216	30	2154	44	2919	17
z8r.D	0.1824	0.002	0.4021	0.0079	10.07	0.27	0.1133	0.0032	81.42322	2428	25	2174	36	2166	59	2670	19
z9c.D	0.2292	0.0034	0.571	0.011	18.26	0.34	0.1553	0.0027	95.56359	3001	18	2908	45	2916	48	3043	24
z10c.D	0.2102	0.0031	0.4207	0.0076	11.91	0.29	0.1021	0.0057	77.91178	2598	22	2261	35	1970	100	2902	24
z10r.D	0.2328	0.003	0.4447	0.0098	14.33	0.46	0.1315	0.0043	77.1615	2750	34	2365	44	2503	76	3065	21
z11c.D	0.1468	0.0033	0.2344	0.0084	4.71	0.29	0.0613	0.0036	58.95425	1740	42	1353	42	1200	69	2295	37
z11r.D	0.2151	0.0023	0.4309	0.0077	12.62	0.29	0.1136	0.0034	78.43537	2648	21	2306	35	2172	62	2940	17

William Mansfield
Metamorphic evolution of the Mercara Shear Zone

z12c.D	0.2312	0.0023	0.5145	0.0069	16.27	0.27	0.1263	0.0026	87.3815	2888	16	2673	29	2402	47	3059	16
z12r.D	0.2245	0.0021	0.5542	0.0095	16.89	0.26	0.1419	0.0031	94.22311	2926	14	2838	39	2679	54	3012	15
z13c.D	0.2234	0.0026	0.4841	0.0067	14.77	0.22	0.1198	0.003	84.64868	2796	14	2542	29	2284	55	3003	19
z13r.D	0.2331	0.003	0.4794	0.0065	15.2	0.2	0.1253	0.0041	82.14984	2828	13	2522	28	2382	74	3070	20
z14c.D	0.1971	0.0017	0.4342	0.005	11.76	0.15	0.0989	0.0039	82.96429	2583	12	2323	22	1910	70	2800	14
z14r.D	0.2212	0.0027	0.4462	0.008	13.59	0.35	0.0934	0.004	79.50435	2712	25	2374	36	1800	73	2986	20
z15c.D	0.2245	0.0022	0.4299	0.0066	13.3	0.2	0.126	0.0034	76.47841	2699	14	2302	30	2405	60	3010	16
z15r.D	0.1981	0.0026	0.4032	0.0059	10.94	0.18	0.1264	0.0042	77.78174	2513	16	2181	27	2401	76	2804	21
z16c.D	0.2639	0.0032	0.567	0.012	20.31	0.45	0.1343	0.0056	88.55219	3105	21	2893	48	2540	100	3267	19
z16r.D	0.2383	0.002	0.5531	0.0067	18.16	0.28	0.1149	0.006	91.30715	2996	15	2836	28	2200	110	3106	13
z17c.D	0.2669	0.0025	0.6228	0.0083	23.04	0.3	0.1748	0.0022	94.91629	3227	13	3118	33	3255	37	3285	15
z17r.D	0.1743	0.0032	0.2869	0.0045	6.88	0.14	0.0713	0.0029	62.7027	2090	17	1624	23	1389	55	2590	31
z18c.D	0.2123	0.0028	0.3999	0.0061	11.76	0.19	0.107	0.0029	74.34053	2581	15	2170	29	2052	54	2919	22
z18r.D	0.2011	0.0021	0.3642	0.0056	10.08	0.18	0.0962	0.003	70.64641	2439	16	2000	27	1861	58	2831	17
z19c.D	0.1556	0.0021	0.2613	0.0043	5.68	0.11	0.0714	0.0029	62.13633	1924	16	1495	22	1391	55	2406	24
z19r.D	0.1759	0.0025	0.2663	0.0042	6.45	0.12	0.0686	0.0021	58.2982	2034	16	1521	21	1339	40	2609	24
z20c.D	0.2246	0.0025	0.5071	0.0074	15.76	0.27	0.1359	0.0034	87.74086	2857	17	2641	32	2572	60	3010	18
z20r.D	0.2218	0.0023	0.4813	0.0077	14.77	0.31	0.1281	0.0035	84.5254	2795	20	2529	34	2442	60	2992	16
z21c.D	0.2594	0.0038	0.5551	0.0092	19.73	0.4	0.1461	0.0039	87.82447	3071	20	2842	38	2760	67	3236	23
z21r.D	0.0746	0.0022	0.1389	0.0022	1.412	0.039	0.0398	0.0019	82.72458	889	16	838	12	788	38	1013	58
z22c.D	0.246	0.0036	0.587	0.011	19.19	0.34	0.1707	0.0069	94.14001	3055	17	2972	43	3170	120	3157	24
z22r.D	0.1997	0.002	0.3781	0.0051	10.28	0.15	0.0622	0.0029	73.33333	2458	13	2068	23	1217	55	2820	16
z23c.D	0.2603	0.002	0.5316	0.0063	18.9	0.29	0.1423	0.0021	84.57037	3034	15	2746	27	2688	37	3247	12
z23r.D	0.2207	0.0023	0.4292	0.006	12.89	0.18	0.1285	0.003	77.12944	2670	13	2300	27	2441	54	2982	17
z24c.D	0.2122	0.0022	0.3905	0.0045	11.39	0.14	0.113	0.0028	72.78958	2553	12	2124	21	2161	52	2918	17
z24r.D	0.1328	0.0031	0.1933	0.004	3.53	0.11	0.0614	0.0024	53.75531	1521	25	1138	22	1203	45	2117	43
z25c.D	0.2498	0.0021	0.496	0.0065	16.95	0.23	0.1332	0.0017	81.54668	2930	13	2594	28	2526	31	3181	13
z25r.D	0.176	0.0032	0.2826	0.0045	6.75	0.12	0.0729	0.0024	61.4883	2078	17	1603	23	1422	45	2607	30
z26c.D	0.2448	0.002	0.6055	0.007	20.32	0.26	0.1622	0.0025	96.82439	3103	13	3049	28	3036	44	3149	13
z26r.D	0.203	0.0023	0.4079	0.0048	11.32	0.15	0.0512	0.0023	77.44202	2547	12	2204	22	1007	44	2846	18

William Mansfield
Metamorphic evolution of the Mercara Shear Zone

z27c.D	0.2672	0.004	0.635	0.0094	23.09	0.33	0.1625	0.004	96.34703	3227	14	3165	37	3039	70	3285	24
z27r.D	0.242	0.0026	0.4908	0.0069	16.02	0.21	0.1278	0.0041	82.14628	2876	13	2572	30	2427	75	3131	17
z28c.D	0.2102	0.0032	0.3897	0.0083	11.27	0.3	0.1136	0.0091	72.94969	2537	25	2117	38	2150	160	2902	24
z28r.D	0.238	0.0028	0.485	0.0062	15.78	0.22	0.1467	0.0052	82.10832	2860	14	2547	27	2758	93	3102	19
z29c.D	0.2495	0.0036	0.485	0.0095	16.63	0.41	0.1388	0.0041	80.15123	2902	24	2544	41	2623	74	3174	23
z29r.D	0.2566	0.0021	0.5906	0.007	20.92	0.29	0.156	0.0025	92.74868	3133	13	2993	29	2928	43	3227	13
z30c.D	0.2005	0.0018	0.3596	0.0044	9.91	0.16	0.0997	0.0019	70.00354	2424	15	1979	21	1920	36	2827	14
z30r.D	0.2103	0.0023	0.3462	0.0048	10.06	0.2	0.0895	0.003	65.96624	2434	18	1915	23	1736	57	2903	18
z31c.D	0.267	0.0063	0.568	0.012	21.17	0.48	0.153	0.0049	88.40979	3142	21	2891	47	2871	86	3270	36
z31r.D	0.2055	0.0027	0.42	0.007	12.16	0.22	0.121	0.0042	78.97311	2613	17	2261	32	2302	77	2863	22
z32c.D	0.2647	0.0026	0.6291	0.0081	23.6	0.33	0.1688	0.0029	96.05746	3250	14	3143	32	3150	50	3272	15
z32r.D	0.2634	0.0027	0.6419	0.009	24.07	0.31	0.1595	0.0037	97.61541	3268	12	3193	35	2987	65	3271	16
z33c.D	0.2573	0.0029	0.5502	0.0096	20.09	0.45	0.1619	0.0039	87.39157	3086	23	2821	40	3029	68	3228	19
z33r.D	0.1669	0.0021	0.2628	0.0033	6.244	0.086	0.0786	0.0021	59.69084	2008	12	1506	17	1527	39	2523	21
z34c.D	0.2371	0.0035	0.5167	0.0098	17.61	0.38	0.1406	0.004	86.65158	2966	21	2681	41	2655	71	3094	24
z34r.D	0.2216	0.0021	0.4308	0.0057	13.64	0.24	0.1119	0.0031	77.183	2722	17	2307	26	2140	57	2989	15
z35c.D	0.2476	0.0032	0.4598	0.0061	16.22	0.21	0.1404	0.0031	77.02276	2886	13	2437	27	2652	56	3164	20
z35r.D	0.2169	0.0049	0.2591	0.0058	8.1	0.24	0.1145	0.0048	50.40816	2228	27	1482	30	2184	87	2940	37
z36c.D	0.2427	0.003	0.4699	0.0058	16.31	0.22	0.1204	0.0025	79.21456	2892	13	2481	25	2296	46	3132	20
z36r.D	0.2297	0.0022	0.4637	0.0046	15.28	0.2	0.1131	0.0038	80.56467	2830	12	2454	20	2170	68	3046	15
z37c.D	0.2995	0.0023	0.6594	0.0076	28.48	0.37	0.1775	0.0032	94.11425	3432	13	3262	30	3300	57	3466	12
z37r.D	0.2636	0.0028	0.5825	0.0077	22.15	0.4	0.164	0.0038	90.50827	3188	18	2956	32	3066	67	3266	17
z38c.D	0.2116	0.0064	0.2935	0.0073	8.82	0.25	0.0816	0.0033	57.06897	2312	27	1655	36	1589	61	2900	51
z38r.D	0.2158	0.0024	0.4284	0.0057	13.38	0.22	0.126	0.0036	78.01154	2702	15	2299	26	2403	63	2947	18
z39c.D	0.2137	0.0031	0.405	0.0054	12.48	0.18	0.1169	0.0025	74.76955	2639	14	2190	25	2232	45	2929	24
z39r.D	0.2619	0.0026	0.58	0.0073	21.98	0.3	0.1572	0.0025	90.59908	3183	13	2949	29	2949	45	3255	15
z40c.D	0.2408	0.0024	0.51	0.0057	17.85	0.21	0.1428	0.0047	85.04164	2981	11	2655	24	2691	84	3122	16
z40r.D	0.2041	0.0028	0.4098	0.0058	12.12	0.2	0.1236	0.0034	77.55961	2609	16	2212	27	2352	62	2852	23
z41.D	0.2175	0.0024	0.4884	0.0066	14.92	0.2	0.1459	0.0018	86.58331	2808	13	2562	28	2752	32	2959	18
z42.D	0.2493	0.0027	0.6095	0.0078	21.16	0.26	0.1649	0.0032	96.4443	3143	12	3065	31	3082	56	3178	17

William Mansfield
Metamorphic evolution of the Mercara Shear Zone

z43.D	0.266	0.0043	0.665	0.018	24.82	0.57	0.1561	0.0043	100.0305	3298	22	3281	71	2930	76	3280	26
z44.D	0.2591	0.002	0.6412	0.0077	23.18	0.31	0.1552	0.0029	98.51806	3231	14	3191	30	2914	51	3239	12
z45.D	0.2147	0.0021	0.4823	0.0057	14.38	0.18	0.126	0.0024	86.34661	2772	12	2536	25	2398	44	2937	16
z46.D	0.2353	0.0025	0.4549	0.0057	14.9	0.21	0.122	0.0023	78.30739	2807	13	2415	25	2326	41	3084	17
z47.D	0.2293	0.0025	0.5459	0.0086	17.43	0.35	0.1459	0.0035	92.14591	2962	18	2804	36	2750	63	3043	17
z48.D	0.1953	0.0022	0.4112	0.0061	11.19	0.18	0.1037	0.0027	79.83465	2535	15	2221	28	1993	49	2782	18
z49.D	0.2649	0.0027	0.6309	0.0079	23.28	0.3	0.1651	0.0034	96.36419	3235	13	3154	32	3086	59	3273	16
z50.D	0.2404	0.0023	0.5445	0.0065	18.3	0.22	0.1457	0.0027	89.81096	3003	12	2803	26	2747	48	3121	15
z51.D	0.2408	0.0027	0.5437	0.0088	18.34	0.33	0.1458	0.0035	89.71154	3004	17	2799	38	2748	63	3120	18
z52.D	0.2272	0.0028	0.5243	0.0073	16.48	0.24	0.1525	0.004	89.60053	2901	14	2714	31	2864	72	3029	19
z53.D	0.221	0.002	0.48	0.0075	14.73	0.3	0.1358	0.0035	84.55611	2790	20	2524	33	2569	63	2985	15
z54.D	0.2214	0.0022	0.4881	0.0077	15.06	0.32	0.146	0.0028	85.58528	2816	20	2559	33	2752	50	2990	16
z55.D	0.2156	0.0032	0.404	0.012	12.22	0.45	0.115	0.0034	74.08163	2598	39	2178	57	2197	63	2940	24
z56.D	0.2787	0.0029	0.6205	0.0089	24.32	0.43	0.1659	0.0024	92.7506	3276	18	3109	36	3100	42	3352	16
z57.D	0.2471	0.0036	0.5445	0.0084	18.6	0.32	0.1383	0.0051	88.54793	3016	16	2799	35	2622	89	3161	23
z58.D	0.2322	0.0029	0.4	0.006	12.9	0.22	0.1261	0.0021	70.77074	2669	16	2167	28	2400	38	3062	20
z59.D	0.2305	0.0029	0.4664	0.0067	14.94	0.2	0.1231	0.0029	80.84618	2808	13	2465	29	2344	54	3049	20
z60.D	0.264	0.0021	0.6178	0.0081	22.6	0.37	0.1612	0.0036	94.74006	3209	15	3098	33	3017	64	3270	12
z61.D	0.1777	0.0017	0.3325	0.0045	8.18	0.1	0.093	0.002	70.35769	2248	12	1849	22	1797	37	2628	16
z62.D	0.2115	0.0022	0.4137	0.0064	11.57	0.21	0.1065	0.0032	76.46655	2569	16	2229	29	2042	59	2915	17
z63.D	0.2563	0.0029	0.689	0.011	23.4	0.39	0.1597	0.0028	104.719	3240	16	3373	43	2992	49	3221	19
z64.D	0.2501	0.0044	0.47	0.0091	15.26	0.34	0.1172	0.0045	77.94533	2826	21	2481	40	2252	78	3183	29
z65.D	0.2235	0.0024	0.4778	0.007	14.02	0.23	0.1258	0.0025	83.84948	2754	15	2518	31	2392	45	3003	18
z66.D	0.2513	0.0026	0.5469	0.0082	18.1	0.31	0.1482	0.0042	88.08404	2989	17	2809	34	2797	72	3189	16
z67.D	0.2457	0.003	0.4862	0.0099	15.71	0.36	0.1368	0.003	80.86929	2852	23	2549	43	2589	54	3152	20
z68.D	0.2274	0.0031	0.4473	0.0073	13.34	0.24	0.1178	0.0029	78.6257	2702	16	2380	32	2249	53	3027	22
z69.D	0.1878	0.0017	0.4593	0.0059	11.48	0.14	0.0995	0.0013	89.52206	2561	12	2435	26	1917	23	2720	15
z70.D	0.1945	0.0019	0.3743	0.0043	9.64	0.11	0.091	0.0025	73.69557	2400	10	2048	20	1759	46	2779	16
z72.D	0.2303	0.002	0.494	0.0069	14.99	0.25	0.1317	0.003	84.72632	2810	16	2585	30	2498	53	3051	14
z73.D	0.2703	0.0032	0.5662	0.0074	20.14	0.27	0.1474	0.0028	87.41301	3098	12	2889	30	2777	50	3305	18

William Mansfield
Metamorphic evolution of the Mercara Shear Zone

z74.D	0.2599	0.0025	0.5899	0.0074	20.05	0.29	0.1487	0.0033	92.07524	3092	14	2986	30	2800	59	3243	15
z75.D	0.2608	0.0028	0.5739	0.0086	19.72	0.34	0.1506	0.0031	89.87381	3077	16	2920	36	2832	55	3249	17
z76.D	0.2267	0.0021	0.4904	0.0062	14.7	0.21	0.1364	0.0026	84.8745	2793	14	2570	27	2583	46	3028	15
z77.D	0.233	0.0023	0.5303	0.007	16.3	0.21	0.1408	0.0032	89.2799	2892	13	2740	29	2659	57	3069	16
z78.D	0.1788	0.0021	0.4173	0.0082	9.77	0.22	0.1022	0.0029	84.90352	2411	20	2244	37	1972	51	2643	22
z79.D	0.2235	0.0031	0.501	0.012	14.5	0.45	0.1109	0.0074	87.00433	2774	30	2611	51	2110	140	3001	22
z80.D	0.2411	0.003	0.4896	0.0085	15.5	0.26	0.1289	0.0036	82.13256	2842	16	2565	37	2447	66	3123	20
z81.D	0.1673	0.0018	0.3496	0.0048	7.76	0.13	0.0919	0.0021	76.29395	2201	15	1931	23	1775	40	2531	19
z82.D	0.2966	0.0032	0.6087	0.0081	24.39	0.36	0.1565	0.0019	88.73117	3281	15	3063	33	2938	34	3452	17
z83.D	0.216	0.0052	0.413	0.011	11.93	0.35	0.1216	0.0051	75.75449	2592	28	2234	53	2316	91	2949	37
z84.D	0.1959	0.0018	0.4138	0.0055	10.94	0.14	0.0881	0.003	79.99283	2517	12	2231	25	1705	55	2789	15
z85.D	0.195	0.0026	0.4577	0.0074	11.99	0.23	0.1191	0.0031	87.26619	2600	18	2426	33	2272	56	2780	23
z86.D	0.2718	0.0027	0.6775	0.0091	24.78	0.31	0.1696	0.0034	100.5433	3296	13	3331	35	3163	59	3313	15
z87.D	0.2093	0.0018	0.4275	0.0052	12.05	0.14	0.1119	0.0021	79.09624	2606	11	2293	23	2143	39	2899	14
z88.D	0.2231	0.0018	0.546	0.0092	16.32	0.35	0.1085	0.0047	93.37329	2887	21	2804	38	2085	85	3003	13
z89.D	0.087	0.0015	0.152	0.0026	1.785	0.043	0.04054	0.00079	67.03458	1035	16	911	14	803	15	1359	34
z90.D	0.2588	0.0026	0.6	0.009	20.91	0.3	0.1631	0.0029	93.51051	3131	15	3026	36	3052	50	3236	16
z91.D	0.2408	0.0024	0.5619	0.007	18.23	0.27	0.146	0.0025	92.02179	3000	14	2872	29	2753	44	3121	16
z92.D	0.2616	0.0023	0.641	0.0095	23.14	0.35	0.1634	0.0025	97.94289	3230	15	3190	38	3058	44	3257	15
z93.D	0.1927	0.0021	0.3387	0.0045	8.88	0.11	0.0903	0.0017	67.98119	2324	11	1879	21	1747	31	2764	17
z94.D	0.2159	0.0022	0.4685	0.0056	13.72	0.18	0.1244	0.0028	84.11944	2727	13	2479	24	2368	50	2947	16
z95.D	0.1989	0.002	0.4186	0.0059	11.27	0.19	0.1071	0.0029	80	2541	16	2252	27	2054	53	2815	17
z96.D	0.2259	0.0028	0.4575	0.0072	13.96	0.19	0.1273	0.0024	80.37786	2744	13	2425	31	2420	43	3017	20
z97.D	0.2205	0.0024	0.4681	0.0075	14.01	0.31	0.1411	0.0034	82.92519	2747	22	2472	33	2664	61	2981	18
z98.D	0.2529	0.0024	0.5144	0.0076	17.68	0.29	0.1393	0.0024	83.5	2967	16	2672	33	2633	43	3200	15
z99.D	0.2449	0.0035	0.498	0.009	16.95	0.29	0.1389	0.0032	82.68742	2929	17	2603	39	2627	57	3148	22
z100.D	0.2622	0.0036	0.5777	0.0091	20.64	0.35	0.1509	0.0034	90.22441	3117	16	2935	37	2848	58	3253	22
z101.D	0.2137	0.0028	0.4322	0.0076	12.34	0.25	0.1096	0.0051	78.96175	2628	19	2312	34	2093	94	2928	21
z102.D	0.2567	0.0028	0.571	0.01	19.98	0.43	0.149	0.0036	90.19243	3081	21	2906	43	2804	64	3222	17
z103.D	0.2695	0.0028	0.6331	0.0087	23.4	0.35	0.1656	0.0029	95.81818	3239	15	3162	34	3094	52	3300	16

William Mansfield
Metamorphic evolution of the Mercara Shear Zone

z104.D	0.165	0.0025	0.2991	0.0066	6.86	0.2	0.0712	0.0024	67.33307	2084	26	1684	33	1389	46	2501	26
z105.D	0.2572	0.0025	0.6299	0.0099	22.25	0.37	0.1626	0.0036	97.33746	3191	16	3144	39	3042	64	3230	16
z106.D	0.2503	0.003	0.5424	0.0068	18.5	0.24	0.115	0.0032	87.62951	3015	12	2791	29	2198	58	3185	19
z107.D	0.2373	0.0024	0.522	0.01	17	0.42	0.1379	0.003	87.12903	2929	24	2701	42	2608	54	3100	16
z108.D	0.1877	0.0017	0.3748	0.0048	9.66	0.13	0.0929	0.0025	75.39537	2400	12	2050	23	1793	46	2719	15
z109.D	0.29	0.0036	0.683	0.0096	27.2	0.43	0.1778	0.0031	98.35873	3388	15	3356	36	3305	54	3412	19
z110.D	0.2268	0.0024	0.5275	0.0096	16.47	0.36	0.1424	0.0036	90.19155	2895	21	2731	40	2688	63	3028	18
z111.D	0.2642	0.0029	0.5818	0.0088	21.2	0.38	0.1687	0.0035	90.27523	3144	18	2952	36	3147	62	3270	18
z112.D	0.2536	0.0031	0.569	0.011	20.02	0.49	0.1498	0.0036	90.50593	3081	24	2898	44	2826	62	3202	19
z113.D	0.259	0.0019	0.6184	0.0082	22.24	0.38	0.1584	0.0033	95.70855	3189	17	3100	33	2968	58	3239	12
z114.D	0.2502	0.0035	0.5781	0.0081	20.03	0.31	0.145	0.0042	92.419	3090	15	2938	33	2730	76	3179	22
z116.D	0.1903	0.0015	0.3993	0.0055	10.6	0.18	0.1114	0.0051	78.86297	2485	16	2164	26	2138	95	2744	14
z117.D	0.1885	0.002	0.434	0.0074	11.34	0.23	0.1373	0.0062	85.13761	2549	18	2320	33	2590	110	2725	17
z118.D	0.2478	0.0026	0.5068	0.0077	17.44	0.36	0.1282	0.0032	83.32807	2951	21	2639	33	2436	58	3167	17
z119.D	0.2327	0.0038	0.421	0.0065	13.53	0.2	0.1102	0.0028	73.82507	2715	14	2262	29	2110	51	3064	26
z120.D	0.2589	0.0025	0.558	0.0068	20.16	0.3	0.1453	0.0029	88.26798	3095	15	2859	29	2740	52	3239	15
z121.D	0.248	0.0032	0.4401	0.007	15.18	0.26	0.1152	0.0024	74.16298	2821	16	2348	31	2201	43	3166	21
z122.D	0.2426	0.0032	0.385	0.0075	13.07	0.29	0.1127	0.0032	66.90073	2678	21	2096	35	2164	57	3133	22
z123.D	0.2386	0.0026	0.404	0.0052	13.44	0.2	0.0953	0.0025	70.37991	2707	14	2186	24	1837	47	3106	17
z125.D	0.2456	0.0024	0.5358	0.0079	18.33	0.32	0.1448	0.0028	87.5198	3002	17	2763	33	2731	50	3157	15
z126.D	0.2722	0.0027	0.6225	0.0086	23.54	0.41	0.1529	0.0051	93.8837	3246	17	3116	34	2882	88	3319	16
z127.D	0.2581	0.0021	0.5644	0.007	20.19	0.28	0.1394	0.0027	89.26693	3100	13	2886	28	2635	50	3233	13
z128.D	0.2354	0.0021	0.4712	0.0057	15.46	0.17	0.1271	0.0021	80.68697	2842	11	2490	25	2418	39	3086	14
z129.D	0.2601	0.0036	0.5441	0.0083	18.84	0.33	0.1369	0.0044	86.1984	3035	17	2798	35	2605	74	3246	22
z130.D	0.238	0.0028	0.4767	0.0084	15.2	0.4	0.1073	0.0062	81.0506	2823	25	2515	38	2050	110	3103	19
z131.D	0.1647	0.0027	0.2661	0.0071	6.01	0.24	0.0691	0.003	60.82598	1956	36	1517	36	1346	57	2494	28
z132.D	0.2575	0.0032	0.562	0.016	19.9	0.64	0.1542	0.0042	88.75116	3071	33	2864	68	2895	73	3227	20
z133.D	0.1889	0.0018	0.4218	0.0054	10.96	0.19	0.1253	0.0033	83.04029	2515	16	2267	25	2384	59	2730	16
z134.D	0.3009	0.0035	0.6704	0.0098	27.41	0.41	0.1718	0.0043	95.1599	3396	14	3303	38	3198	75	3471	18
z135.D	0.2407	0.0021	0.5154	0.0054	17.01	0.17	0.1269	0.0025	85.77835	2934.9	9.5	2678	23	2413	45	3122	14

William Mansfield
Metamorphic evolution of the Mercara Shear Zone

z136.D	0.2562	0.0032	0.5271	0.0099	20.19	0.41	0.1466	0.002	84.66315	3098	19	2727	42	2764	35	3221	20
z137.D	0.2652	0.0027	0.6345	0.0087	23.14	0.25	0.1607	0.0022	96.64122	3231	10	3165	34	3011	39	3275	16
z138.D	0.2294	0.003	0.526	0.01	16.48	0.4	0.1354	0.003	89.26813	2894	24	2720	42	2564	54	3047	21
z139.D	0.1921	0.0024	0.3764	0.007	9.92	0.23	0.1184	0.0031	74.57381	2418	23	2056	33	2259	57	2757	22
z140.D	0.1938	0.0018	0.4177	0.006	11.09	0.22	0.1076	0.003	81.09668	2526	18	2248	27	2063	54	2772	16
z141.D	0.2404	0.0036	0.481	0.012	15.35	0.43	0.1097	0.0083	81.12179	2832	28	2531	51	2100	150	3120	24
z142.D	0.2271	0.0022	0.4812	0.0085	15.08	0.31	0.126	0.0036	83.43234	2816	19	2528	37	2394	64	3030	16
z143.D	0.2196	0.0021	0.4007	0.0058	12.21	0.21	0.1214	0.0017	72.94118	2618	17	2170	27	2315	30	2975	15
z144.D	0.2644	0.0033	0.5353	0.0091	19.88	0.37	0.1437	0.0019	84.43901	3083	19	2762	38	2714	34	3271	19
z145.D	0.1959	0.0016	0.3571	0.0043	9.65	0.13	0.0893	0.0023	70.52707	2401	13	1967	20	1726	43	2789	14
z146.D	0.2732	0.0028	0.657	0.011	25.24	0.4	0.1728	0.003	97.86338	3316	15	3252	42	3221	51	3323	16
z147.D	0.2534	0.0026	0.5779	0.0073	20.17	0.33	0.1417	0.0041	91.63807	3097	16	2937	30	2684	70	3205	16
z148.D	0.2695	0.0026	0.5767	0.0094	21.52	0.48	0.1358	0.0044	88.7341	3156	22	2930	38	2579	76	3302	15
z149.D	0.1832	0.002	0.313	0.0046	7.82	0.14	0.0776	0.0034	65.50952	2207	17	1755	23	1508	64	2679	18
z150.D	0.189	0.0035	0.2921	0.0063	7.58	0.21	0.0627	0.0027	60.60272	2171	24	1649	31	1227	52	2721	30
I16-66																	
z1.D	0.2101	0.0029	0.4679	0.0088	13.69	0.29	0.1402	0.0041	85.20179	2721	20	2470	39	2648	73	2899	23
z2.D	0.1859	0.0026	0.36	0.0067	9.38	0.17	0.1276	0.0028	73.30618	2373	16	1980	31	2433	52	2701	23
z3.D	0.2376	0.0026	0.5695	0.0075	18.83	0.29	0.1705	0.0053	93.64516	3029	15	2903	31	3187	90	3100	17
z4.D	0.2131	0.0028	0.4587	0.0075	13.62	0.26	0.168	0.011	83.13953	2719	18	2431	33	3110	180	2924	21
z5.D	0.2145	0.0042	0.4522	0.0083	13.43	0.32	0.1206	0.0041	82.08547	2700	23	2401	37	2306	72	2925	33
z6.D	0.235	0.0027	0.5428	0.0077	17.84	0.27	0.1585	0.002	90.53485	2978	14	2793	32	2972	35	3085	19
z7.D	0.2507	0.0029	0.6176	0.0085	21.51	0.28	0.1702	0.0039	97.26759	3158	13	3097	34	3172	69	3184	18
z8.D	0.1962	0.0031	0.3916	0.0066	10.66	0.19	0.0897	0.0051	76.38191	2491	16	2128	31	1728	95	2786	26
z9.D	0.2242	0.0039	0.4099	0.0072	12.78	0.24	0.1329	0.0029	73.68421	2659	18	2212	33	2520	52	3002	28
z10.D	0.2028	0.0025	0.4143	0.008	11.75	0.29	0.1115	0.0053	78.21817	2574	23	2230	37	2127	97	2851	21
z11.D	0.2518	0.0036	0.6149	0.009	21.42	0.29	0.1692	0.0044	96.77015	3156	13	3086	36	3155	78	3189	22
z12.D	0.2472	0.0026	0.5957	0.0088	20.49	0.29	0.1739	0.0046	95.07109	3111	14	3009	36	3234	81	3165	17
z13.D	0.2582	0.0035	0.57	0.01	20.38	0.35	0.1584	0.0048	89.87616	3107	17	2903	41	2966	85	3230	22
z14.D	0.2402	0.0029	0.5209	0.0072	17.39	0.26	0.196	0.0088	86.64955	2953	14	2700	30	3610	150	3116	19

William Mansfield
Metamorphic evolution of the Mercara Shear Zone

z17.D	0.2595	0.0032	0.6402	0.0089	23.01	0.26	0.1828	0.0046	98.24237	3225	11	3186	35	3388	80	3243	19
z18.D	0.2289	0.0028	0.5284	0.0085	16.91	0.28	0.1565	0.0083	89.86842	2928	15	2732	36	2940	150	3040	19
z19.D	0.2712	0.004	0.62	0.0098	23.58	0.49	0.1748	0.0032	93.92382	3246	21	3107	39	3254	54	3308	23
z20.D	0.2121	0.0023	0.4423	0.0053	13.04	0.16	0.1418	0.0074	80.81535	2681	12	2359	24	2660	130	2919	18
z21.D	0.2456	0.0056	0.598	0.013	20.31	0.41	0.1695	0.005	96.08155	3099	20	3016	51	3179	86	3139	36
z22.D	0.2096	0.0027	0.4123	0.0068	11.95	0.22	0.1389	0.0069	76.76663	2595	17	2227	32	2620	120	2901	21
z23.D	0.2073	0.0042	0.428	0.0082	12.37	0.28	0.1164	0.0043	79.63864	2627	21	2292	37	2219	78	2878	33
z24.D	0.2381	0.0032	0.474	0.01	15.64	0.41	0.1555	0.0052	80.46422	2845	26	2496	44	2916	92	3102	22
z25.D	0.2858	0.0027	0.6517	0.0087	26	0.33	0.1876	0.0045	95.11334	3343	13	3231	34	3484	74	3397	15
z26.D	0.2542	0.0031	0.5568	0.0075	19.77	0.25	0.1674	0.0043	88.96509	3077	12	2854	32	3123	76	3208	19
z27.D	0.2288	0.0033	0.5127	0.0095	16.45	0.3	0.1502	0.004	87.69737	2900	18	2666	41	2826	69	3040	24
z28.D	0.2496	0.0039	0.603	0.011	20.73	0.5	0.176	0.0096	95.72193	3119	21	3043	46	3310	180	3179	25
z29.D	0.2014	0.0026	0.4512	0.008	12.65	0.24	0.1377	0.006	84.40141	2648	18	2397	36	2610	110	2840	22
z30.D	0.2156	0.0025	0.4729	0.0067	14.26	0.26	0.1625	0.006	84.71467	2763	17	2494	29	3030	100	2944	19
z31r.D	0.3045	0.0058	0.706	0.014	29.79	0.58	0.1855	0.0059	98.53617	3475	19	3433	52	3430	100	3484	30
z32c.D	0.1951	0.003	0.397	0.0061	10.77	0.18	0.1154	0.0049	77.44604	2501	15	2153	28	2222	86	2780	26
z33c.D	0.2222	0.0034	0.3822	0.0072	11.83	0.24	0.1379	0.0034	69.699	2588	19	2084	33	2608	60	2990	25
z34r.D	0.1964	0.0023	0.3871	0.0054	10.59	0.18	0.1174	0.0048	75.50143	2487	16	2108	25	2238	85	2792	20
z35.D	0.3008	0.004	0.655	0.012	27.29	0.42	0.1752	0.0071	93.46198	3391	15	3245	46	3250	130	3472	21
z36.D	0.2387	0.0016	0.5234	0.0056	17.39	0.16	0.129	0.0021	87.17454	2955.1	9	2712	24	2442	43	3111	10
z37.D	0.2187	0.0015	0.4127	0.0059	12.59	0.2	0.1008	0.0015	74.94106	2645	15	2225	27	1941	27	2969	11
z38.D	0.1936	0.0023	0.3475	0.0053	9.35	0.14	0.1518	0.0096	69.40029	2370	13	1921	25	2830	160	2768	19
z39.D	0.2532	0.0033	0.567	0.012	20.04	0.51	0.1508	0.0059	90.5	3084	24	2896	49	2830	110	3200	21
z40.D	0.2713	0.0032	0.643	0.011	24.42	0.37	0.1783	0.0037	96.76639	3281	15	3202	42	3312	64	3309	18
z41.D	0.2826	0.0041	0.659	0.012	25.79	0.45	0.1786	0.0064	96.55991	3335	18	3256	48	3340	100	3372	23
z42.D	0.2852	0.0033	0.6461	0.0095	25.75	0.37	0.1819	0.0032	94.74461	3335	14	3209	37	3374	55	3387	18
z43.D	0.2468	0.0024	0.6301	0.0084	21.72	0.29	0.1702	0.0033	99.52547	3168	13	3146	34	3174	58	3161	15
z44.D	0.2174	0.0025	0.4897	0.0069	14.87	0.22	0.1656	0.0056	86.81096	2803	14	2567	30	3089	96	2957	19
z47.D	0.2027	0.0025	0.401	0.0063	11.26	0.18	0.1294	0.0058	76.36938	2541	15	2175	28	2450	110	2848	20
z48.D	0.2621	0.003	0.6327	0.0091	23.03	0.3	0.1697	0.0036	96.95853	3225	13	3156	36	3165	64	3255	18

William Mansfield
Metamorphic evolution of the Mercara Shear Zone

z50.D	0.2666	0.0047	0.645	0.012	23.69	0.41	0.1653	0.0075	97.65172	3252	17	3202	48	3100	130	3279	28
z51c.D	0.2274	0.0028	0.5313	0.0088	16.86	0.32	0.1538	0.0047	90.57039	2920	19	2747	38	2884	82	3033	19
z52r.D	0.2258	0.0055	0.504	0.012	15.71	0.39	0.1276	0.0093	87.47092	2852	24	2632	52	2410	170	3009	40
z53.D	0.2368	0.0032	0.5212	0.0089	17.14	0.32	0.1442	0.0051	87.26568	2938	18	2700	38	2714	91	3094	22
z54c.D	0.2362	0.0034	0.5345	0.0088	17.62	0.36	0.1426	0.0064	89.27762	2961	20	2756	37	2680	110	3087	23
z55r.D	0.189	0.0019	0.375	0.004	9.86	0.12	0.1107	0.0042	75.10981	2419	11	2052	19	2117	77	2732	16
z56.D	0.2454	0.0029	0.5435	0.0071	18.53	0.27	0.1416	0.0036	88.7619	3016	14	2796	30	2674	65	3150	18
z57.D	0.1866	0.0015	0.3826	0.0051	9.94	0.15	0.1096	0.0036	77.01107	2425	14	2087	24	2098	66	2710	13
z58.D	0.2376	0.0027	0.5739	0.007	19.02	0.27	0.1641	0.0041	94.16505	3041	14	2921	29	3067	72	3102	19
z59.D	0.2723	0.004	0.657	0.011	24.89	0.34	0.1736	0.0031	98.12858	3301	13	3251	41	3234	54	3313	23
z60.D	0.2194	0.0024	0.5127	0.0073	15.64	0.24	0.155	0.008	89.67373	2853	15	2666	31	2910	140	2973	18
z61r.D	0.2518	0.0032	0.6108	0.0095	21.28	0.38	0.1572	0.0049	96.20809	3146	18	3070	38	2945	87	3191	20
z62c.D	0.2387	0.0028	0.551	0.01	18.26	0.39	0.1341	0.0052	90.95299	2996	19	2825	42	2548	91	3106	19
z63.D	0.2603	0.0038	0.619	0.008	22.46	0.32	0.1647	0.0025	95.71252	3203	13	3103	32	3081	44	3242	23
z64.D	0.2224	0.0023	0.452	0.011	14.05	0.4	0.103	0.0045	80.10017	2739	26	2399	46	1985	81	2995	17
z65.D	0.2446	0.0046	0.593	0.012	19.95	0.37	0.1615	0.0067	95.50526	3085	17	2996	48	3010	120	3137	30
z66.D	0.2033	0.0035	0.386	0.011	10.98	0.38	0.0966	0.005	73.68421	2507	34	2100	51	1857	92	2850	29
z67r.D	0.2471	0.0032	0.642	0.011	22.19	0.35	0.1648	0.0023	100.7891	3191	15	3193	43	3088	42	3168	20
z68c.D	0.2383	0.003	0.552	0.011	18.34	0.44	0.1424	0.0047	90.89739	2998	24	2826	46	2698	80	3109	21
z69.D	0.2291	0.0022	0.5065	0.007	16.16	0.25	0.1444	0.0046	86.75214	2884	15	2639	30	2719	83	3042	16
z70.D	0.2679	0.0039	0.532	0.0092	19.66	0.35	0.1488	0.0051	83.52083	3073	18	2747	39	2815	87	3289	23
z71c.D	0.2703	0.0044	0.5718	0.0091	21.33	0.38	0.1439	0.0058	88.15869	3152	16	2911	37	2720	100	3302	26
z72r.D	0.2284	0.0032	0.4631	0.0065	14.76	0.29	0.1255	0.0026	80.67172	2793	19	2450	29	2387	48	3037	23
z73r.D	0.2302	0.0024	0.4775	0.0058	15.28	0.19	0.1243	0.0035	82.55166	2830	12	2517	26	2364	64	3049	17
z74c.D	0.2043	0.0035	0.343	0.01	9.8	0.34	0.1066	0.0033	66.52632	2394	34	1896	49	2044	61	2850	28
z75c.D	0.1672	0.0051	0.2554	0.0057	5.9	0.17	0.0531	0.0025	58.58343	1950	26	1464	29	1044	48	2499	52
z76r.D	0.2601	0.0027	0.6209	0.0082	22.37	0.24	0.158	0.0037	95.8693	3198	10	3110	32	2962	65	3244	16
z77c.D	0.2146	0.0036	0.4682	0.0083	13.97	0.3	0.1195	0.0045	84.67577	2740	20	2481	38	2275	82	2930	27
z78r.D	0.2445	0.0025	0.4931	0.0065	16.74	0.29	0.1319	0.0043	82.07247	2920	16	2582	28	2499	78	3146	16
z79.D	0.2123	0.0035	0.4131	0.0063	12.16	0.2	0.1038	0.0042	76.41607	2612	15	2226	29	1991	76	2913	26

William Mansfield
Metamorphic evolution of the Mercara Shear Zone

z80c.D	0.1859	0.0032	0.2983	0.0042	7.7	0.14	0.081	0.0039	62.4166	2191	17	1684	22	1568	73	2698	28
z81r.D	0.2452	0.0022	0.5503	0.0065	18.74	0.21	0.1414	0.0041	89.5688	3026	11	2825	27	2669	75	3154	14
z82c.D	0.1787	0.0024	0.3619	0.0048	8.97	0.11	0.0905	0.0041	75.46454	2333	12	1990	23	1746	76	2637	22
z83r.D	0.1811	0.0034	0.3892	0.0063	9.81	0.2	0.1045	0.0037	79.75876	2410	19	2116	29	2013	67	2653	31
z84r.D	0.1775	0.0024	0.3546	0.0047	8.74	0.12	0.0723	0.0034	74.53298	2308	12	1955	22	1406	65	2623	22
z85c.D	0.242	0.0029	0.5509	0.0078	18.51	0.23	0.1552	0.0039	90.34527	3014	12	2826	32	2912	70	3128	19
z86c.D	0.2239	0.0024	0.4802	0.0064	14.93	0.24	0.1478	0.0049	83.94816	2807	15	2526	28	2781	88	3009	18
z87r.D	0.261	0.0025	0.641	0.0094	23.37	0.43	0.1674	0.0024	98.06273	3239	18	3189	37	3127	41	3252	15
z88.D	0.2286	0.0034	0.5197	0.0077	16.45	0.24	0.1425	0.0031	88.82663	2901	14	2695	32	2690	54	3034	24
z89c.D	0.231	0.0031	0.5244	0.0084	16.81	0.27	0.1332	0.0036	88.75449	2920	16	2715	36	2524	66	3059	22
z90r.D	0.2432	0.0037	0.529	0.01	17.79	0.4	0.1342	0.0075	87.14514	2971	22	2732	44	2550	130	3135	24
z92c.D	0.2523	0.0029	0.6123	0.0079	21.44	0.29	0.1491	0.0052	96.27543	3157	13	3076	31	2800	93	3195	18
z93r.D	0.2034	0.0019	0.3087	0.0059	8.67	0.17	0.047	0.0023	60.69425	2297	18	1731	29	926	45	2852	15
z94c.D	0.2206	0.0023	0.475	0.0097	14.58	0.35	0.1296	0.0054	83.83635	2778	23	2500	43	2454	98	2982	17
z95r.D	0.218	0.0031	0.4515	0.0074	13.78	0.22	0.1175	0.0041	80.94435	2732	15	2400	33	2243	74	2965	22
z96.D	0.2037	0.0021	0.3899	0.0054	11.03	0.16	0.1083	0.0034	74.29072	2523	14	2121	25	2075	63	2855	17
z97.D	0.2293	0.0031	0.504	0.01	15.97	0.36	0.1268	0.0083	86.36662	2870	21	2629	43	2400	150	3044	21
z98c.D	0.212	0.0029	0.46	0.0071	13.54	0.25	0.1004	0.0047	83.59643	2714	18	2436	31	1926	86	2914	22
z99r.D	0.2259	0.0023	0.4799	0.0061	15.05	0.18	0.1255	0.0039	83.60927	2816	12	2525	27	2397	67	3020	16
z100.D	0.2219	0.0063	0.467	0.013	14.34	0.43	0.1357	0.0062	82.90138	2756	29	2463	55	2560	110	2971	45
z101.D	0.2132	0.0028	0.5062	0.0087	15	0.3	0.1292	0.0023	90.32148	2811	19	2641	36	2455	42	2924	21
z102c.D	0.2015	0.0027	0.4307	0.0057	12.01	0.16	0.1008	0.0035	81.46186	2604	12	2307	25	1954	61	2832	22
z103r.D	0.2932	0.0027	0.6028	0.0074	24.64	0.27	0.1656	0.0033	88.54895	3294	11	3039	30	3095	58	3432	14
z105c.D	0.235	0.003	0.4689	0.007	15.26	0.24	0.1326	0.0077	80.34382	2829	15	2477	31	2500	140	3083	20
z106r.D	0.2379	0.0021	0.5512	0.0063	18.21	0.22	0.1409	0.0028	91.23429	3000	11	2831	26	2662	50	3103	14
z109.D	0.2219	0.0022	0.4763	0.006	14.64	0.17	0.1121	0.0035	83.85695	2790	11	2509	26	2144	65	2992	15
z110.D	0.2289	0.0023	0.5066	0.0058	16.11	0.18	0.1383	0.0028	86.84643	2882	11	2641	25	2615	51	3041	16
z111c.D	0.2339	0.0026	0.5329	0.0076	17.3	0.26	0.1379	0.0041	89.40526	2950	15	2751	32	2607	74	3077	18
z112r.D	0.2	0.0021	0.5116	0.0061	14.23	0.22	0.1362	0.0064	94.29483	2761	15	2661	26	2570	110	2822	17
z113.D	0.2651	0.004	0.731	0.011	27.02	0.48	0.1778	0.0037	108.0428	3379	17	3533	42	3304	62	3270	24

William Mansfield
Metamorphic evolution of the Mercara Shear Zone

z114c.D	0.2303	0.0023	0.5366	0.0075	17.17	0.27	0.1223	0.0049	90.7899	2940	15	2770	31	2336	86	3051	16
z115r.D	0.2471	0.0033	0.6758	0.009	23.38	0.3	0.1624	0.0018	105.1866	3241	12	3326	34	3041	31	3162	21
z116.D	0.2118	0.0025	0.4062	0.0083	11.92	0.25	0.1028	0.0063	75.19699	2593	20	2195	38	1970	120	2919	20
z117.D	0.2835	0.0033	0.664	0.011	26.14	0.44	0.158	0.0054	97.21811	3348	17	3285	44	2959	97	3379	18
z118.D	0.2269	0.0034	0.541	0.011	17.06	0.39	0.1448	0.0067	91.82058	2932	22	2784	45	2720	120	3032	25
z119r.D	0.1606	0.0031	0.2801	0.0067	6.26	0.19	0.0732	0.0028	64.81633	2002	27	1588	33	1425	53	2450	34
z120c.D	0.2484	0.0026	0.5899	0.0086	20.39	0.32	0.1537	0.0029	94.16404	3107	15	2985	35	2888	50	3170	16
z122.D	0.2228	0.0025	0.5224	0.0073	16.19	0.21	0.16	0.0027	90.32366	2886	13	2707	31	2999	46	2997	18
z123.D	0.2801	0.0046	0.629	0.01	24.3	0.39	0.1528	0.0078	93.42458	3280	15	3140	41	2880	130	3361	25
z124c.D	0.2712	0.003	0.6247	0.0089	23.54	0.31	0.1608	0.0051	94.43941	3246	13	3125	36	3019	87	3309	17
z125r.D	0.2839	0.0037	0.637	0.011	24.95	0.41	0.1468	0.0061	93.93491	3303	16	3175	42	2780	100	3380	21
z126c.D	0.2123	0.0025	0.4683	0.0067	13.84	0.19	0.1198	0.0076	84.7841	2737	13	2474	30	2290	140	2918	19
z127r.D	0.2381	0.0032	0.4966	0.0081	16.37	0.24	0.126	0.0054	83.84392	2898	14	2600	34	2400	100	3101	21
z128r.D	0.2809	0.0048	0.632	0.013	24.5	0.52	0.1484	0.0037	93.75186	3286	20	3151	51	2793	66	3361	27
z129c.D	0.2478	0.0033	0.585	0.01	20.26	0.37	0.1521	0.0029	93.61971	3098	18	2964	42	2859	51	3166	21
z130.D	0.2658	0.0031	0.5939	0.0094	21.99	0.36	0.1544	0.0034	91.52181	3179	16	3001	38	2907	58	3279	19
z131r.D	0.2689	0.0034	0.6094	0.0096	22.8	0.36	0.1348	0.0066	93.13904	3215	16	3068	39	2560	120	3294	20
z132c.D	0.2932	0.0031	0.6376	0.0089	26.06	0.34	0.1619	0.0032	92.54079	3346	13	3176	35	3031	56	3432	17
z133r.D	0.3012	0.0028	0.709	0.01	29.72	0.37	0.1756	0.0043	99.39568	3475	12	3454	38	3265	75	3475	14
z134c.D	0.2915	0.0034	0.767	0.013	31.07	0.51	0.1775	0.0038	107.0406	3516	16	3664	47	3298	67	3423	18
z135c.D	0.2135	0.0022	0.5183	0.0067	15.38	0.24	0.1417	0.005	91.83743	2835	15	2689	29	2671	90	2928	17
z136r.D	0.1975	0.0024	0.4471	0.0064	12.27	0.18	0.1221	0.0062	85	2623	14	2380	29	2320	110	2800	20
z137r.D	0.1986	0.0025	0.3933	0.0061	10.86	0.17	0.1049	0.0029	76.0413	2507	15	2136	28	2013	53	2809	20
z138c.D	0.2537	0.0036	0.604	0.011	21.14	0.38	0.1492	0.0055	94.94224	3143	17	3041	45	2804	99	3203	23
z141c.D	0.1961	0.0032	0.4218	0.0071	11.45	0.22	0.1119	0.0039	81.36445	2559	18	2266	32	2149	69	2785	27
z142r.D	0.2329	0.0026	0.586	0.0071	19.12	0.24	0.1499	0.0024	96.61789	3046	12	2971	29	2821	43	3075	19
z143r.D	0.1906	0.0031	0.4176	0.0074	11.12	0.23	0.1181	0.0029	81.91761	2528	19	2247	34	2254	52	2743	26
z144c.D	0.2135	0.0025	0.502	0.0076	14.89	0.23	0.1283	0.0051	89.41618	2804	15	2619	33	2432	93	2929	19
z145c.D	0.2042	0.0032	0.4671	0.0081	13.28	0.26	0.1058	0.004	86.47038	2695	18	2467	35	2037	71	2853	26
z146r.D	0.2307	0.003	0.5599	0.0099	18.05	0.3	0.1455	0.0038	93.97314	2991	16	2869	39	2743	66	3053	21

William Mansfield
Metamorphic evolution of the Mercara Shear Zone

z147r.D	0.2096	0.0033	0.4411	0.0095	12.75	0.27	0.1203	0.0062	81.18744	2657	20	2352	43	2290	110	2897	26
z148c.D	0.2619	0.0068	0.637	0.014	22.91	0.45	0.1526	0.0056	97.83884	3218	20	3169	55	2870	100	3239	41
z149c.D	0.2118	0.0025	0.4829	0.008	14.25	0.27	0.183	0.016	87.16981	2760	18	2541	36	3330	260	2915	19
z150r.D	0.2595	0.0037	0.625	0.01	22.55	0.37	0.1547	0.0039	96.53894	3203	16	3124	40	2903	70	3236	23
z151c.D	0.2137	0.0082	0.408	0.013	11.86	0.43	0.0827	0.0091	75.80979	2579	34	2200	61	1580	170	2902	66
z152r.D	0.2117	0.0019	0.4579	0.0058	13.46	0.18	0.1182	0.0037	83.26475	2709	13	2428	26	2254	68	2916	14
z153.D	0.2003	0.0025	0.412	0.0062	11.47	0.18	0.1174	0.0046	78.67517	2558	15	2221	28	2248	82	2823	21
z154.D	0.2553	0.0025	0.611	0.0097	21.69	0.39	0.1438	0.0035	95.48849	3164	18	3069	39	2711	63	3214	15
z155r.D	0.2551	0.003	0.665	0.011	23.48	0.32	0.1613	0.0045	102.1475	3244	13	3282	41	3018	79	3213	19
z156c.D	0.2505	0.0046	0.5983	0.0095	20.79	0.36	0.1345	0.0034	94.9733	3123	17	3023	39	2548	62	3183	29
z157.D	0.2133	0.0025	0.4641	0.0074	13.75	0.24	0.1104	0.0059	83.86876	2727	17	2454	32	2110	110	2926	19
z158.D	0.1952	0.0025	0.4082	0.0066	11.1	0.19	0.1013	0.0034	79.31034	2527	16	2208	31	1946	63	2784	21
z159.D	0.2637	0.0036	0.619	0.011	22.72	0.38	0.151	0.0046	94.94485	3210	16	3099	43	2849	78	3264	22
z160.D	0.2442	0.0038	0.5732	0.0095	19.46	0.29	0.1486	0.0037	92.83668	3061	15	2916	39	2795	65	3141	25

APPENDIX D: MONAZITE STANDARDS

Analysis	Pb ²⁰⁷ /Pb ²⁰⁶	1σ	Pb ²⁰⁶ /U ²³⁸	1σ	Pb ²⁰⁷ /U ²³⁸	1σ	% Conc	Pb ²⁰⁷ /U ²³⁵	1σ	Pb ²⁰⁶ /U ²³⁸	1σ	Pb ²⁰⁷ /Pb ²⁰⁶	1σ
I16-42													
MADEL - 1.d	0.0576	0.0024	0.0763	0.0021	0.606	0.024	104.8673	477	15	474	12	452	86
MADEL - 10.d	0.0572	0.003	0.0762	0.0021	0.601	0.03	112.619	473	20	473	12	420	100
MADEL - 2.d	0.0554	0.0027	0.0761	0.0023	0.578	0.027	126.2032	458	17	472	14	374	99
MADEL - 3.d	0.057	0.0031	0.0762	0.0019	0.599	0.033	112.619	469	21	473	12	420	110
MADEL - 4.d	0.0573	0.0032	0.0762	0.0021	0.602	0.035	110.4651	469	22	475	13	430	110
MADEL - 5.d	0.0572	0.0031	0.0762	0.0021	0.601	0.031	115.3659	471	20	473	12	410	100
MADEL - 6.d	0.0572	0.0027	0.0762	0.002	0.601	0.03	110.7728	471	19	473	12	427	94
MADEL - 7.d	0.0572	0.003	0.0763	0.0021	0.602	0.031	103.2609	472	20	475	13	460	110

William Mansfield
Metamorphic evolution of the Mercara Shear Zone

MADEL - 8.d	0.0572	0.003	0.0763	0.0022	0.601	0.031	112.619	476	21	473	13	420	100
MADEL - 9.d	0.0572	0.0027	0.0762	0.0024	0.601	0.03	107.5	471	19	473	14	440	100
MADEL-11 - 1.d	0.0572	0.0031	0.0762	0.0022	0.601	0.035	112.619	473	23	473	13	420	110
MADEL-11 - 10.d	0.0571	0.0029	0.0762	0.002	0.601	0.032	105.1111	474	20	473	12	450	100
MADEL-11 - 2.d	0.0571	0.0032	0.0764	0.0026	0.602	0.036	110.2326	472	22	474	16	430	100
MADEL-11 - 3.d	0.0572	0.0034	0.0762	0.0019	0.601	0.035	110	473	23	473	11	430	120
MADEL-11 - 4.d	0.0573	0.0035	0.0762	0.0021	0.602	0.038	115.3659	474	24	473	12	410	110
MADEL-11 - 5.d	0.0572	0.0032	0.0763	0.002	0.601	0.033	110	471	21	473	12	430	110
MADEL-11 - 6.d	0.0572	0.0033	0.0762	0.0016	0.601	0.033	105.1778	477	21	473.3	9.7	450	110
MADEL-11 - 7.d	0.0572	0.0028	0.0763	0.0017	0.602	0.032	102.9783	472	20	473.7	9.9	460	100
MADEL-11 - 8.d	0.056	0.0031	0.0762	0.0018	0.586	0.031	124.4737	462	20	473	11	380	110
MADEL-11 - 9.d	0.0579	0.0063	0.0763	0.0023	0.609	0.072	163.7931	456	41	475	14	290	180
222 - 1.d	0.054	0.0034	0.0668	0.0019	0.497	0.029	130.3125	405	20	417	11	320	120
222 - 2.d	0.0542	0.0034	0.0678	0.0018	0.51	0.031	136.4516	411	21	423	11	310	120
222 - 3.d	0.0556	0.0032	0.0657	0.0018	0.516	0.031	110.8108	417	21	410	11	370	120
222 - 4.d	0.057	0.0037	0.0665	0.002	0.529	0.033	106.4103	422	22	415	12	390	130
222 - 5.d	0.0562	0.0032	0.0709	0.0025	0.533	0.033	116.0526	429	22	441	15	380	120
222 - 6.d	0.054	0.0029	0.0684	0.0019	0.508	0.028	129.0909	414	19	426	12	330	110
222 - 7.d	0.0422	0.0025	0.0679	0.0019	0.398	0.026	-352.5	334	19	423	11	-120	100
222 - 8.d	0.0521	0.0029	0.0666	0.0019	0.476	0.028	166	390	19	415	11	250	110
Ambat - 1.d	0.0561	0.0035	0.0784	0.0024	0.606	0.038	131.3514	470	24	486	14	370	120
Ambat - 2.d	0.0582	0.0037	0.0765	0.002	0.616	0.04	107.9545	476	25	475	12	440	130
Ambat - 3.d	0.0587	0.0036	0.0768	0.0023	0.616	0.036	103.6957	484	23	477	14	460	120
Ambat - 4.d	0.0562	0.0035	0.0772	0.0021	0.602	0.036	129.4595	470	22	479	13	370	120
AMBAT - 5.d	0.0548	0.0031	0.0778	0.0022	0.59	0.036	138	467	22	483	13	350	110
AMBAT - 6.d	0.0534	0.0027	0.0777	0.0025	0.573	0.029	146.0606	455	18	482	15	330	100
AMBAT - 7.d	0.0363	0.0024	0.0768	0.0023	0.371	0.021	-136.08	321	16	479	14	-352	96

William Mansfield
Metamorphic evolution of the Mercara Shear Zone

AMBAT - 8.d	0.0403	0.0027	0.0752	0.0021	0.406	0.024	-222.381	344	18	467	13	-210	100
MT GARNET - 5.d	0.0485	0.0056	0.0444	0.0016	0.31	0.036	254.2727	265	28	279.7	9.9	110	210
MT GARNET - 6.d	0.0519	0.0064	0.045	0.0018	0.316	0.037	189.3333	274	29	284	11	150	210
MT GARNET - 7.d	0.0291	0.0037	0.0445	0.0018	0.171	0.019	-46.8333	160	17	281	11	-600	150
MT GARNET - 8.d	0.0351	0.0036	0.0414	0.0014	0.197	0.02	-64.0732	179	17	262.7	9.3	-410	140
MtGarnet - 1.d	0.0513	0.007	0.0469	0.0021	0.332	0.046	491.6667	273	34	295	13	60	230
MtGarnet - 2.d	0.054	0.0069	0.0477	0.0021	0.358	0.044	136.3636	300	33	300	13	220	220
MtGarnet - 3.d	0.0556	0.0067	0.0456	0.0021	0.341	0.038	119.5833	285	29	287	13	240	210
MtGarnet - 4.d	0.0623	0.0079	0.0463	0.0026	0.381	0.045	72.75	314	33	291	16	400	230
I16-64													
MADEL - 1.d	0.06	0.032	-7.09E-13	7.10E-14	0	1	-3.3E-09	0	1	-4.5E-09	4.60E-10	140	820
MADEL - 3.d	0.073	0.017	8.70E-08	2.60E-08	2.28E-08	4.90E-09	5.71E-05	0.0000232	4.9E-06	0.00056	0.00017	980	440
MADEL - 4.d	0.067	0.026	-7.50E-26	1.20E-26	5.50E-30	3.10E-30	0	0	1	0	1	770	830
MADEL - 5.d	0.0371	0.0066	0.0951	0.0095	0.361	0.062	-194.333	302	44	583	55	-300	260
MADEL - 6.d	0.035	0.026	0.069	0.036	0.59	0.67	-107.5	450	440	430	220	-400	1000
MADEL - 10.d	0.057	0.037	0.076	0.025	0.6	0.25	156.6667	470	150	470	150	300	1200
222 - 3.d	0.0217	0.0015	-1.5E-06	2.5E-07	0.000005	0.000001	0.001028	0.0051	0.0011	-0.0096	0.0016	-934	56
222 - 4.d	0.0214	0.0013	-1.5E-06	2.5E-07	5.6E-06	1.2E-06	0.001049	0.0057	0.0012	-0.0099	0.0016	-944	49
222 - 1.d	0.0383	0.0023	-1.4E-06	2.4E-07	6.2E-06	1.3E-06	0.003536	0.0062	0.0013	-0.0093	0.0015	-263	94
222 - 2.d	0.0382	0.0024	-1.7E-06	2.7E-07	6.2E-06	1.3E-06	0.00363	0.0063	0.0013	-0.0106	0.0018	-292	93
Ambat - 3.d	0.023	0.0015	0.0748	0.0026	0.371	0.024	-52.0763	315	18	464	16	-891	58
Ambat - 4.d	0.022	0.0016	0.0728	0.0027	0.346	0.024	-49.1839	301	19	452	16	-919	62
Ambat - 1.d	0.0455	0.0031	-1.7E-06	2.7E-07	9.4E-06	1.9E-06	-0.109	0.0095	0.002	-0.0109	0.0018	10	120
Ambat - 2.d	0.0422	0.003	-1.6E-06	2.7E-07	7.6E-06	1.6E-06	0.007923	0.0077	0.0016	-0.0103	0.0017	-130	110
MtGarnet - 3.d	0.0227	0.0034	0.0446	0.0024	0.213	0.03	-31.573	188	24	281	15	-890	130
MtGarnet - 4.d	0.022	0.0035	0.0431	0.0024	0.206	0.033	-30.7955	180	26	271	15	-880	140
MtGarnet - 1.d	0.0574	0.0092	-2.80E-19	4.30E-20	9.40E-22	2.40E-22	0	0	1	0	1	210	260

William Mansfield
Metamorphic evolution of the Mercara Shear Zone

MtGarnet - 2.d	0.0428	0.0063	-5.28E-13	8.60E-14	4.10E-14	1.10E-14	1.79E-09	4.20E-11	1.10E-11	-3.4E-09	5.50E-10	-190	210
I16-65													
MADEL - 1.d	0.0572	0.0036	0.0762	0.0022	0.601	0.039	113.0952	476	26	475	13	420	130
MADEL - 2.d	0.0572	0.0042	0.0763	0.0022	0.602	0.042	121.5385	469	27	474	13	390	140
MADEL - 11.d	0.0574	0.0045	0.0762	0.0026	0.603	0.048	131.9444	462	31	475	16	360	150
MADEL - 12.d	0.0567	0.0044	0.0763	0.0024	0.597	0.049	139.1176	462	30	473	15	340	150
MADEL - 13.d	0.0576	0.004	0.0763	0.0025	0.605	0.041	115.3659	472	25	473	15	410	130
MADEL - 14.d	0.057	0.0043	0.0762	0.0023	0.6	0.046	127.8378	462	29	473	14	370	140
MADEL - 15.d	0.0572	0.004	0.0762	0.0023	0.601	0.041	125	471	27	475	14	380	130
MADEL - 3.d	0.0573	0.0049	0.0763	0.0025	0.601	0.049	135.1429	464	31	473	15	350	160
MADEL - 4.d	0.0572	0.0038	0.0762	0.0022	0.601	0.041	113.0952	467	25	475	14	420	130
MADEL - 5.d	0.0572	0.004	0.0762	0.0022	0.601	0.043	124.4737	464	27	473	13	380	140
MADEL - 6.d	0.0572	0.0042	0.0763	0.0026	0.601	0.044	115.3659	475	29	473	16	410	140
MADEL - 7.d	0.0572	0.0043	0.0762	0.0025	0.601	0.043	127.8378	464	27	473	15	370	140
MADEL - 8.d	0.0572	0.0039	0.0762	0.0023	0.602	0.042	118.25	469	26	473	14	400	130
MADEL - 9.d	0.0571	0.0041	0.0763	0.0024	0.601	0.044	118.25	464	28	473	14	400	140
MADEL - 10.d	0.0572	0.0042	0.0762	0.0022	0.601	0.043	124.4737	468	28	473	13	380	140
222 - 3.d	0.0575	0.0033	0.0648	0.0016	0.52	0.029	87.95652	421	20	404.6	9.6	460	120
222 - 4.d	0.0574	0.0039	0.0667	0.0018	0.526	0.036	106.6667	424	23	416	11	390	130
222 - 5.d	0.0565	0.0036	0.0679	0.0018	0.517	0.033	117.5	420	22	423	11	360	120
222 - 6.d	0.0552	0.0032	0.0685	0.0019	0.527	0.031	118.3333	425	21	426	12	360	120
222 - 1.d	0.0553	0.0032	0.0679	0.0017	0.522	0.032	117.5	421	21	423	10	360	110
222 - 2.d	0.059	0.0038	0.0652	0.0016	0.517	0.032	88.47826	421	22	407	9.8	460	120
Ambat - 1.d	0.0606	0.0037	0.076	0.0024	0.624	0.039	92.7451	482	25	473	15	510	130
Ambat - 2.d	0.0576	0.0034	0.0775	0.0026	0.603	0.036	117.3171	470	23	481	15	410	120
Ambat - 3.d	0.0579	0.0035	0.0756	0.002	0.607	0.038	111.9048	471	24	470	12	420	120
Ambat - 4.d	0.0574	0.0035	0.0757	0.0025	0.598	0.037	117.5	466	23	470	15	400	120

William Mansfield
Metamorphic evolution of the Mercara Shear Zone

Ambat - 5.d	0.0549	0.0035	0.0778	0.0023	0.583	0.04	150.625	458	25	482	14	320	120
Ambat - 6.d	0.0546	0.0033	0.0775	0.0021	0.578	0.035	150.3125	454	23	481	13	320	120
MtGarnet - 5.d	0.0548	0.0068	0.0506	0.0025	0.361	0.045	144.5455	301	34	318	15	220	220
MtGarnet - 6.d	0.0538	0.0071	0.045	0.0023	0.311	0.041	166.4706	272	33	283	14	170	230
MtGarnet - 3.d	0.053	0.0071	0.0472	0.0022	0.334	0.043	185.625	280	33	297	14	160	230
MtGarnet - 4.d	0.0599	0.0078	0.046	0.0023	0.365	0.045	85	300	34	289	14	340	240
MtGarnet - 1.d	0.0553	0.007	0.0465	0.0021	0.332	0.039	139.5238	278	28	293	13	210	210
MtGarnet - 2.d	0.0592	0.0079	0.0445	0.0021	0.345	0.043	96.55172	286	33	280	13	290	240
I16-66													
MADEL - 1.d	0.0572	0.0029	0.0762	0.0021	0.601	0.029	112.619	472	18	473	13	420	100
MADEL - 2.d	0.0573	0.003	0.0762	0.0024	0.603	0.03	105.1111	472	19	473	14	450	110
MADEL - 3.d	0.0569	0.0036	0.0762	0.0021	0.598	0.035	118.25	469	23	473	12	400	120
MADEL - 4.d	0.0573	0.0033	0.0763	0.0025	0.602	0.032	112.619	471	20	473	15	420	110
MADEL - 5.d	0.0572	0.0032	0.0762	0.0021	0.601	0.033	113.0952	470	21	475	13	420	110
MADEL - 6.d	0.0572	0.0033	0.0763	0.0024	0.602	0.03	110	474	19	473	14	430	120
MADEL - 7.d	0.0578	0.0033	0.0762	0.0024	0.602	0.033	112.619	473	21	473	15	420	110
MADEL - 8.d	0.0569	0.0033	0.0763	0.0022	0.599	0.034	118.75	470	22	475	14	400	110
MADEL - 9.d	0.0573	0.0035	0.0762	0.0023	0.602	0.033	118.25	471	21	473	14	400	110
MADEL - 10.d	0.0572	0.0033	0.0762	0.002	0.601	0.033	112.619	472	21	473	12	420	120
MADEL - 11.d	0.0573	0.003	0.0763	0.0021	0.602	0.031	112.619	474	20	473	13	420	100
MADEL - 12.d	0.0571	0.0032	0.0762	0.0021	0.6	0.032	112.619	470	20	473	12	420	110
MADEL - 13.d	0.0572	0.003	0.0762	0.0021	0.601	0.03	110	471	19	473	13	430	110
MADEL - 14.d	0.0572	0.0031	0.0763	0.002	0.602	0.032	115.6098	474	20	474	12	410	110
MADEL - 15.d	0.0572	0.003	0.0762	0.0021	0.601	0.032	110	470	20	473	13	430	110
222 - 5.d	0.0589	0.0037	0.0657	0.0017	0.53	0.031	91.11111	424	21	410	11	450	120
222 - 6.d	0.0564	0.0042	0.0656	0.002	0.5	0.036	120.2941	401	24	409	12	340	140
222 - 3.d	0.0585	0.003	0.0658	0.0019	0.547	0.032	85.41667	435	21	410	12	480	110

William Mansfield
Metamorphic evolution of the Mercara Shear Zone

222 - 4.d	0.0528	0.0033	0.0678	0.0019	0.497	0.03	156.6667	407	21	423	12	270	120
222 - 1.d	0.0548	0.0031	0.0674	0.002	0.513	0.031	123.5294	413	20	420	12	340	110
222 - 2.d	0.0542	0.0036	0.0656	0.0018	0.488	0.03	136.3333	396	20	409	11	300	130
Ambat - 5.d	0.0555	0.0032	0.0782	0.0023	0.596	0.034	134.7222	466	21	485	14	360	110
Ambat - 6.d	0.0559	0.0036	0.0777	0.0022	0.592	0.037	133.8889	465	24	482	13	360	120
Ambat - 3.d	0.0551	0.0037	0.0758	0.0022	0.601	0.04	127.2973	469	25	471	13	370	130
Ambat - 4.d	0.0553	0.0037	0.0786	0.0022	0.605	0.038	147.5758	474	23	487	13	330	130
Ambat - 1.d	0.0571	0.0037	0.0756	0.0027	0.589	0.035	117.25	464	23	469	16	400	130
Ambat - 2.d	0.0573	0.0038	0.0762	0.0022	0.606	0.038	121.5385	471	24	474	13	390	130
MtGarnet - 5.d	0.0543	0.008	0.0461	0.0026	0.335	0.047	195.3333	276	35	293	16	150	250
MtGarnet - 6.d	0.0525	0.0073	0.0457	0.0023	0.327	0.043	205	273	33	287	14	140	240
MtGarnet - 1.d	0.0534	0.0068	0.0454	0.0026	0.343	0.038	138.5714	288	29	291	17	210	220
MtGarnet - 2.d	0.0558	0.0061	0.045	0.0023	0.358	0.044	95.33333	301	33	286	15	300	210
MtGarnet - 3.d	0.0618	0.0078	0.0452	0.0021	0.395	0.047	61.95652	323	34	285	13	460	230
MtGarnet - 4.d	0.0549	0.007	0.0461	0.0023	0.365	0.046	111.5385	303	34	290	14	260	220

APPENDIX E: MONAZITE ANALYSES

Analysis	Pb ²⁰⁷ /Pb ²⁰⁶	1σ	Pb ²⁰⁶ /U ²³⁸	1σ	Pb ²⁰⁷ /U ²³⁸	1σ	% Conc	Pb ²⁰⁷ /U ²³⁵	1σ	Pb ²⁰⁶ /U ²³⁸	1σ	Pb ²⁰⁷ /Pb ²⁰⁶	1σ
I16-42													
1 - Mon	0.2089	0.0042	0.436	0.013	12.96	0.55	80.51229	2660	40	2326	56	2889	32
2 - Mon	0.2256	0.0035	0.5546	0.0078	17.69	0.27	94.26393	2971	15	2843	32	3016	25
3 - Mon	0.2144	0.0044	0.4945	0.0092	14.97	0.38	88.29352	2807	24	2587	39	2930	33
4 - Mon	0.2341	0.0033	0.5581	0.0094	18.25	0.45	92.66948	2999	24	2857	39	3083	21
5 - Mon	0.2412	0.0041	0.58	0.0084	19.6	0.34	94.22832	3070	17	2955	37	3136	23
6 - Mon	0.2276	0.0054	0.582	0.01	18.54	0.46	97.58837	3014	24	2954	43	3027	39

William Mansfield
Metamorphic evolution of the Mercara Shear Zone

7 - Mon	0.2111	0.0063	0.554	0.012	16.37	0.42	97.76094	2894	24	2838	49	2903	47
8 - Mon	0.232	0.0053	0.592	0.012	19.22	0.5	97.87443	3053	24	2993	48	3058	37
9 - Mon	0.2227	0.0051	0.543	0.011	17	0.37	93.28209	2931	21	2791	46	2992	36
10 - Mon	0.2235	0.0074	0.564	0.017	17.56	0.64	96.1577	2958	35	2878	70	2993	54
11 - Mon	0.2064	0.0039	0.537	0.013	15.62	0.42	96.1779	2853	24	2768	53	2878	33
12 - Mon	0.1888	0.0046	0.4945	0.0093	13.09	0.34	95.14706	2680	25	2588	40	2720	40
13 - Mon	0.2018	0.0064	0.491	0.015	13.78	0.61	90.7231	2730	41	2572	64	2835	50
14 - Mon	0.2397	0.0057	0.651	0.018	21.75	0.72	103.6644	3166	32	3225	71	3111	37
15 - Mon	0.1137	0.0061	0.2132	0.007	3.35	0.21	68.40659	1480	47	1245	37	1820	100
16 - Mon	0.2281	0.0054	0.553	0.015	17.7	0.53	93.21922	2967	29	2832	63	3038	39
17 - Mon	0.086	0.013	0.136	0.011	1.68	0.3	67.29508	960	110	821	62	1220	340
18 - Mon	0.193	0.011	0.443	0.018	11.93	0.57	84.95862	2592	46	2361	80	2779	81
19 - Mon	0.2333	0.0065	0.588	0.016	19.47	0.5	97.61672	3061	24	2990	69	3063	45
20 - Mon	0.208	0.011	0.493	0.022	14.15	0.89	89.61084	2752	62	2579	95	2878	89
21 - Mon	0.205	0.016	0.462	0.027	12.9	1	85.61404	2658	79	2440	120	2850	140
22 - Mon	0.2304	0.0069	0.586	0.012	19.24	0.5	97.60026	3049	25	2969	50	3042	48
23 - Mon	0.1793	0.0054	0.3456	0.0091	8.65	0.28	72.50664	2298	29	1912	44	2637	52
24 - Mon	0.229	0.012	0.529	0.024	16.35	0.72	89.92095	2895	43	2730	100	3036	90
25 - Mon	0.2128	0.0057	0.5058	0.0096	15.14	0.48	90.37012	2818	30	2637	41	2918	43
26 - Mon	0.211	0.014	0.544	0.03	15.5	1	96.55172	2839	66	2800	120	2900	110
27 - Mon	0.2179	0.0025	0.5358	0.0073	16.5	0.24	93.28383	2904	14	2764	31	2963	19
28 - Mon	0.2349	0.0028	0.542	0.0068	17.99	0.26	90.49935	2987	14	2791	28	3084	19
29 - Mon	0.2321	0.0053	0.621	0.019	20.23	0.74	101.5676	3096	36	3110	77	3062	37
30 - Mon	0.236	0.0038	0.564	0.011	18.61	0.34	93.20168	3019	18	2879	46	3089	25
31 - Mon	0.2181	0.0051	0.543	0.011	16.57	0.43	94.07008	2906	26	2792	45	2968	35
32 - Mon	0.2318	0.0079	0.516	0.025	16.38	0.77	87.72504	2891	45	2680	100	3055	54
33 - Mon	0.1833	0.0049	0.449	0.011	11.51	0.37	89.78676	2559	31	2400	48	2673	44

William Mansfield
Metamorphic evolution of the Mercara Shear Zone

34 - Mon	0.141	0.011	0.267	0.014	5.11	0.48	69.27273	1822	77	1524	73	2200	140
35 - Mon	0.1482	0.0062	0.2295	0.0053	4.76	0.22	57.89474	1767	38	1331	28	2299	71
36 - Mon	0.2171	0.0044	0.49	0.011	14.94	0.34	86.89468	2808	22	2566	46	2953	33
37 - Mon	0.2074	0.0052	0.481	0.01	13.97	0.39	87.83455	2744	26	2527	46	2877	42
38 - Mon	0.2294	0.0059	0.523	0.012	16.67	0.37	89.19987	2912	21	2709	51	3037	42
39 - Mon	0.2263	0.0086	0.498	0.015	15.23	0.67	86.33952	2823	44	2604	64	3016	62
40 - Mon	0.1151	0.0055	0.1788	0.0053	2.83	0.14	57.14286	1357	37	1060	29	1855	90
41 - Mon	0.2343	0.0043	0.54	0.013	17.69	0.49	90.4065	2966	26	2780	56	3075	30
42 - Mon	0.1853	0.0068	0.45	0.014	11.47	0.62	88.92193	2551	50	2392	64	2690	59
43 - Mon	0.1821	0.005	0.3899	0.0087	10	0.29	79.73024	2429	27	2128	38	2669	48
I16-64													
1 - Mon	0.0406	0.0061	0.121	0.0075	0.95	0.13	386.8421	660	68	735	43	190	240
I16-65													
1 - Mon	0.06	0.011	0.112	0.0072	0.97	0.16	175.1282	656	83	683	42	390	330
2 - Mon	0.0971	0.0074	0.1486	0.0073	1.9	0.13	62.23776	1065	48	890	41	1430	150
3 - Mon	0.2008	0.0075	0.335	0.014	8.98	0.43	66.07397	2322	46	1858	67	2812	63
4 - Mon	0.2043	0.0079	0.344	0.013	9.17	0.35	66.94826	2347	36	1902	61	2841	64
5 - Mon	0.0615	0.0042	0.1197	0.004	1.017	0.072	132.3636	693	36	728	23	550	150
6 - Mon	0.066	0.011	0.112	0.011	0.9	0.16	98	641	82	686	63	700	380
7 - Mon	0.0621	0.0069	0.1066	0.0053	0.97	0.1	123.0189	668	55	652	31	530	220
8 - Mon	0.0638	0.0079	0.1135	0.0062	1.05	0.12	130.3774	699	63	691	36	530	240
9 - Mon	0.2342	0.0051	0.478	0.013	15.36	0.4	81.6851	2829	25	2511	56	3074	35
10 - Mon	0.224	0.015	0.38	0.023	10.83	0.51	69.69697	2498	46	2070	110	2970	100
11 - Mon	0.063	0.02	0.1169	0.0092	1.04	0.28	165.5814	690	140	712	53	430	560
12 - Mon	0.0676	0.0038	0.1213	0.0043	1.122	0.091	92.125	748	40	737	25	800	120
13 - Mon	0.1809	0.0052	0.2541	0.0072	6.33	0.21	55.12675	2009	30	1457	37	2643	47
14 - Mon	0.241	0.013	0.546	0.035	17.1	1.3	91.72836	2925	72	2850	170	3107	95

William Mansfield
Metamorphic evolution of the Mercara Shear Zone

I16-66

1 - Mon	0.167	0.01	0.246	0.015	5.69	0.52	56.70683	1899	84	1412	75	2490	100
2 - Mon	0.1474	0.0077	0.2114	0.0094	4.28	0.29	53.83609	1678	55	1235	50	2294	91
3 - Mon	0.2294	0.0046	0.546	0.019	17.39	0.48	92.11823	2954	28	2805	82	3045	32
4 - Mon	0.153	0.013	0.211	0.017	4.68	0.72	53.16017	1700	130	1228	90	2310	170
5 - Mon	0.1405	0.0066	0.207	0.0094	4.03	0.29	54.11081	1626	62	1211	50	2238	75
6 - Mon	0.061	0.0046	0.1291	0.0062	1.08	0.089	132.5424	737	45	782	35	590	170
7 - Mon	0.0591	0.0073	0.1209	0.007	0.97	0.12	150	681	62	735	40	490	250
8 - Mon	0.071	0.014	0.1252	0.0077	1.19	0.21	98.7013	777	99	760	44	770	390
9 - Mon	0.0609	0.0092	0.12	0.012	0.99	0.15	133.0909	688	74	732	67	550	300
10 - Mon	0.0614	0.0052	0.1255	0.0047	1.076	0.085	136.0714	731	42	762	27	560	180
11 - Mon	0.0687	0.0059	0.1397	0.0091	1.31	0.11	103.9506	841	50	842	52	810	180
12 - Mon	0.0839	0.0059	0.1428	0.0056	1.7	0.13	67.71654	1010	53	860	32	1270	150
13 - Mon	0.2177	0.0067	0.486	0.016	14.78	0.54	86.22673	2795	35	2548	68	2955	50
14 - Mon	0.0657	0.0056	0.128	0.0047	1.158	0.093	107.7778	773	43	776	27	720	180
15 - Mon	0.0669	0.0095	0.1299	0.007	1.25	0.19	106.3514	800	86	787	40	740	320
16 - Mon	0.1319	0.0098	0.2036	0.0072	3.74	0.25	57.12919	1572	53	1194	38	2090	130
17 - Mon	0.0701	0.0086	0.126	0.008	1.2	0.13	93.17073	789	62	764	46	820	260
18 - Mon	0.094	0.026	0.114	0.013	1.42	0.32	52.57576	880	140	694	76	1320	570
19 - Mon	0.0682	0.0067	0.1283	0.005	1.21	0.11	98.48101	799	48	778	29	790	200
20 - Mon	0.0625	0.0084	0.1319	0.0086	1.16	0.13	137.4138	772	66	797	49	580	270
21 - Mon	0.063	0.0034	0.1254	0.0041	1.106	0.06	108.7143	753	29	761	24	700	100
22 - Mon	0.0669	0.0049	0.1348	0.0044	1.27	0.082	110	822	37	814	25	740	150
23 - Mon	0.0668	0.006	0.121	0.0072	1.12	0.12	94.35897	755	57	736	41	780	200
24 - Mon	0.0657	0.0095	0.123	0.011	1.11	0.19	107.8261	739	86	744	62	690	320
25 - Mon	0.191	0.0073	0.303	0.012	8.08	0.42	62.15328	2232	47	1703	61	2740	65
26 - Mon	0.2206	0.0044	0.492	0.01	15.48	0.36	86.54362	2841	22	2579	44	2980	32

27 - Mon	0.06	0.0035	0.1257	0.0039	1.084	0.082	129.322	739	40	763	23	590	140
----------	------	--------	--------	--------	-------	-------	---------	-----	----	-----	----	-----	-----

APPENDIX F: EXTENDED U-PB GEOCHRONOLOGY METHODS

Analytical methods for U-Pb isotope dating for zircons and monazites followed the methods outlined by (J. e. a. Payne, 2010). For zircon analysis rocks were cut to a ~10cm diameter then crushed, milled and sieved. Collecting the 79-300 μ m portions, further separation was completed using standard panning techniques, a strong hand magnet and LST heavy mineral processes. From the final portion zircons were then handpicked and mounted on epoxy resin disks. Zircons were imaged on a FEI Quanta 600 Scanning Electron Microscope with attached Gatan Cathodoluminescence detector in laboratories at Adelaide Microscopy, University of Adelaide, Australia.

Monazites were analysed in-situ via thin sections, first imaged on a Quanta 600 SEM – MLA. The images highlights monazites by scanning the thin section finding the correct elemental composition for monazites, then selecting those grains for analysis. The data from the SEM – MLA is then used in the New Wave 213nm Nd-YAG in a He ablation atmosphere coupled with an Agilent 7500cx ICP-MS. The sample is then orientated used pre-defined co-ordinates, analysis then begins on the MLA defined monazite locations. Ablation was performed with a spot size of 9 μ m and a frequency of 4Hz. Total acquisition time for each analysis was 100 seconds, 30 seconds of background measurement, 10 seconds of closed shutter stabilisation and 40 seconds of ablation time. Measured isotopes of ^{204}Pb , ^{206}Pb , ^{207}Pb , and ^{238}U each had a dwell time of 10, 15, 30 and 15ms respectively.

Post analysis data correction techniques for elemental fractionation and mass bias follow those of (J. L. Payne et al., 2008), using “Iolite 2.6” a 1% uncertainty is assigned to the primary monazite standard MADel. (TIMS) Normalisation data: $^{207}\text{Pb}/^{206}\text{Pb} = 491 \pm 2.7$ Ma, $^{206}\text{Pb}/^{238}\text{U} = 518.37 \pm 0.99$ Ma, $^{207}\text{Pb}/^{235}\text{U} = 513.13 \pm 0.19$ Ma, (J. L. Payne et al., 2008). A 1% uncertainty was assigned to the primary zircon standard GJ-1. (TIMS) normalizing ages of $^{207}\text{Pb}/^{206}\text{Pb} = 608.3$ Ma, $^{206}\text{Pb}/^{238}\text{U} = 600.7$ Ma and $^{207}\text{Pb}/^{235}\text{U} = 602.2$ Ma (Jackson et al., 2004). Instrumental drifts was accounted for by linear correct techniques and standard bracketing every 10 analysis for monazite and 20 for zircon.

In-house monazite standard “222” provided weighted average ages of $^{207}\text{Pb}/^{206}\text{Pb} = 451.2 \pm 4.0$ Ma (MSWD = 0.80), $^{206}\text{Pb}/^{238}\text{U} = 448.8 \pm 0.5$ Ma (MSWD = 1.7), and $^{207}\text{Pb}/^{235}\text{U} = 452.7 \pm 1.2$ Ma (MSWD = 1.9) $n = 28$, and MADel were $^{207}\text{Pb}/^{206}\text{Pb} = 425 \pm 23$ (MSWD = 1.5), $^{206}\text{Pb}/^{238}\text{U} = 473.4 \pm 2.7$ (MSWD = 0.40), $^{207}\text{Pb}/^{235}\text{U} = 471.0 \pm 4.5$ (MSWD = 1.1), ($n=20$).

In-house zircon standard “PLES” provided weighted average ages of $^{207}\text{Pb}/^{206}\text{Pb} = 341.2 \pm 3.0$ Ma (MSWD = 1.4), $^{206}\text{Pb}/^{238}\text{U} = 336.8 \pm 1.1$ Ma (MSWD = 0.8), and $^{207}\text{Pb}/^{235}\text{U} = 334.7 \pm 2.5$ Ma (MSWD = 1.7) $n = 145$. GJ-1 were $^{207}\text{Pb}/^{206}\text{Pb} = 615.2 \pm 4.0$ Ma (MSWD = 1.2), $^{206}\text{Pb}/^{238}\text{U} = 603 \pm 3.4$ Ma (MSWD = 0.4), and $^{207}\text{Pb}/^{235}\text{U} = 608.7 \pm 1.5$ Ma (MSWD = 1.8), $n = 353$.

APPENDIX G: EXTENDED PHASE EQUILIBRIA MODELLING METHODS

Forward modelled phase diagrams were calculated for 2 metapelite samples (I16-42 and I16-65). Using the program THERMOCALC (Powell & Holland, 1988) (Holland & Powell, 2011). In the model chemical system, MnNCKFMASHTOaxOam (MnO–Na₂O–CaO–K₂O–FeO–MgO–Al₂O₃–SiO₂–H₂O–TiO₂–O), acknowledging that ‘O’ is a proxy for Fe₂O₃, using the latest internally consistent thermodynamic data set Ds6. (Holland & Powell, 2011). Activity-composition (a-x) models used came from (Powell et al., 2014; R. W. White et al., 2014). Calculations in *THERMOCALC* are based on user specified stable mineral assemblages that then have their coordinates and area calculated exhaustively by line and point. Where lines and points represent the zero abundance of a single or two phases respectively. Starting a pseudosection relies on the calculation of a Gibbs energy minimisation at a set *P-T* condition to produce an initial stable assemblage. The pseudosection is then calculated around that initial starting assemblage by trial and error calculations in order to determine which phases appear or disappear according to pressure, temperature or composition. Throughout the calculation process the focal point of the calculations moves within the pseudosections P-T-X space (X = composition) requiring an update of the “starting guesses” (values for *THERMOCALC* to run its iterative least-squares calculation). Resulting in the user actively calculating every line and point to create a single diagram. P-Mo and P-M_{h₂o} diagrams are used to more accurately constrain the abundances of H₂O and Fe₂O₃ (oxidation state) as the whole rock geochemical analysis produces uncertain results (Kelsey & Hand, 2015). Chosen amounts of H₂O and Fe₂O₃ are selected for the *P-T* modelling of samples as they correspond to the calculated stable assemblage of the interpreted peak metamorphic assemblage observed in the rocks.